Title
Of Islands, Ensembles, and Eigenstates

Author
Wildenhain, Elizabeth Rose

Publication Date
2022

Peer reviewed|Thesis/dissertation

Of Islands, Ensembles, and Eigenstates

by

Elizabeth Rose Wildenhain

A dissertation submitted in partial satisfaction of the

requirements for the degree of

Doctor of Philosophy

in

Physics

in the

Graduate Division

of the

University of California, Berkeley

Committee in charge:

Professor Raphael Bousso, Chair
Professor Wesley Holliday
Professor Yasunori Nomura

Fall 2022

Of Islands, Ensembles, and Eigenstates

Abstract

Of Islands, Ensembles, and Eigenstates

by

Elizabeth Rose Wildenhain

Doctor of Philosophy in Physics

University of California, Berkeley

Professor Raphael Bousso, Chair

This work furthers the program of understanding the black hole information paradox, the firewall paradox, and the relevance of concepts from quantum information to quantum gravity. A gravitational calculation was recently shown to yield the Page curve for the entropy of Hawking radiation. In this work, we generalize the Ryu-Takayanagi (Quantum Extremal Surface) prescription for von Neumann entropies to various settings relevant for this calculation. We examine a puzzle in the calculation, which we call the state paradox: that the calculation makes use of Hawking's result that the radiation entropy becomes large at late times. The paradox is resolved if the gravitational path integral computes averaged quantities in a suitable ensemble of unitary theories. We apply the insights from these calculations to cosmology by searching for entanglement islands in cosmologies with spatial curvature containing thermal radiation purified by a reference spacetime. We show arbitrarily small positive curvature guarantees that the entire universe is an island. Proper subsets of the time-symmetric slice of a closed or open universe can be islands, but only if the cosmological constant is negative and sufficiently large in magnitude. We extend this analysis to cosmologies containing a general fluid, finding that flat universes with time-symmetric slices always have islands on that slice. We find islands in the Simple Harmonic Universe model, which has no classical singularity at the background level. We then argue that the Page curve calculations do not resolve the firewall paradox. We exhibit a sharpened version of the paradox which consists of the Hayden-Preskill thought experiment in which the message thrown into the black hole is itself a smaller black hole. We argue that accounting for decoherence resolves the paradox. Finally, we conclude with an argument that quantum complexity theory can quantify the difficulty of distinguishing eigenstates obeying the Eigenstate Thermalization Hypothesis (ETH).

To my family

You have been there at every step of my educational journey. I cannot thank you enough for your endless encouragement and enthusiasm.

Contents

Acknowledgments

First and foremost, I would like to thank my advisor Raphael Bousso for his support, contributions to this work, and role on my committee. I would also like to thank Ning Bao for his contributions and for being an endless source of invaluable advice. Ning Bao, Ido Ben-Dayan, Raphael Bousso, Merav Hadad, Jason Pollack, and David Wakeham all provided significant contributions to this work. I extend my gratitude to Yasunori Nomura for acting on my committee. Thanks are also owed to Wesley Holliday for his role on my committee and his enthusiasm for discussion. I was for many semesters supported by the Berkeley Connect Fellowship, and I would like to thank the directors Erica Bree Rosenblum and Michele Rabkin for organizing this program and giving me personal advice. I also extend my gratitude to the physics Berkeley Connect director Matt Pyle and to the assistant director Haichen Wang, whom I would additionally like to thank for acting on my qualifying exam committee. Finally, thanks are owed to C. Akers, A. Almheiri, A. Bouland, V. Chandrasekaran, A. Chatwin-Davies, A. Karch, A. Levine, H. Marrochio, C. Murdia, T. Rudelius, A. Shahbazi-Moghaddam, Y. Nomura, G. Penington, and the attendees of the GeoFlow January 2021 Collaboration Meeting for helpful discussion, comments, and correspondence. This work was supported in part by the Berkeley Center for Theoretical Physics; by the Department of Energy, Office of Science, Office of High Energy Physics under QuantISED Award DE-SC0019380 and under contract DE-AC02-05CH11231; and by the National Science Foundation under Award Number 2112880.

Chapter 1

Introduction

Defining a consistent theory of quantum gravity is a long-standing quest in theoretical physics. Quantum mechanics, quantum field theory, and general relativity have proven amazingly powerful in their respective regimes. Putting these theories together, however, has not proven easy. Systems in which both gravitational and quantum mechanical effects are relevant are rife with problems.

A prime example of such a system is the black hole. Thought experiments with black holes have provided a fruitful source of puzzles about what happens when quantum mechanics and gravity come together. One such long-standing puzzle is the black hole information paradox [156]. Hawking famously calculated that black holes should evaporate through the emission of Hawking radiation, emitted in the form of entangled pairs: one falls into the black hole, the other escapes the horizon [100, 98]. A puzzle arises when one assumes that the rules of quantum mechanics apply to the entire process of black hole formation and evaporation. It is consistent with the setup of the thought experiment that the black hole formed from the collapse of matter in a pure state. The result of Hawking's calculation, however, does not depend on whether the matter that formed the black hole was in a pure state or a mixed state—the Hawking out-state is always thermal and therefore a mixed state. By the principle of unitarity, however, quantum information should be preserved in a scattering process that returns all energy to a distant observer. A pure in-state should evolve to a pure out-state. Because Hawking's calculation of black hole radiation implies that the energy is returned but not the information, it conflicts with the unitarity of quantum mechanics.

A useful quantity for investigating the flow of information in black hole evaporation is the von Neumann entropy,

$$S_{VN} = -\mathrm{tr}\rho \log \rho \ , \tag{1.1}$$

where ρ is the density matrix of the state. The von Neumann entropy is zero iff ρ is a pure state and positive otherwise. More specifically, the quantity useful for this problem is the entanglement entropy, which is the von Neumann entropy of a subsystem of a bipartite system. For a bipartite system with density matrix ρ_{AB}, the entanglement entropy for subsystem A is defined as

$$S_A \equiv -\mathrm{tr}\rho_A \log \rho_A \ , \tag{1.2}$$

where ρ_A is the reduced density matrix of subsystem A, defined via

$$\langle a'|\rho_A|a\rangle \equiv \sum_b \langle a'b|\rho_{AB}|ab\rangle \ . \tag{1.3}$$

For a pure total state on AB, $S_A = S_B$, and, intuitively, the entanglement entropy quantifies the amount of entanglement between the subsystems.

Hawking's calculation and unitary evaporation predict different curves for the entanglement entropy of the emitted Hawking radiation (or the black hole) during the evaporation process. According to Hawking, the black hole continues to emit thermal radiation for its whole lifetime, so the radiation entropy grows monotonically before reaching a plateau once (if) the black hole evaporates completely. In contrast, assuming the black hole was formed from matter in a pure state, unitarity requires that the radiation entropy falls back down to zero once the black hole has completely evaporated. More precisely, the entropy $S(t)$ must be the smaller of the coarse-grained radiation entropy and the Bekenstein-Hawking entropy of the remaining black hole at the time t. The time at which the entropy of the radiation begins to decrease is called the "Page time," and the curve expected from unitarity is called the "Page Curve" after the author who originally proposed it [149].

Although the prevailing view is that black hole evaporation should ultimately have a unitary description, the principle evidence in favor of unitary evaporation was for a long time indirect. The AdS/CFT correspondence, which is a conjectured mathematical duality between quantum gravity in asymptotically anti-de Sitter space (AdS_{d+1}) and a non-gravitational conformal field theory (CFT_d) [134], suggests that there should be a dual CFT description of any gravitational process in AdS. Such a CFT description would naturally follow the rules of quantum mechanics, meaning a unitary description of black hole evaporation in AdS should exist. It was not until recently that a purely bulk calculation was found to support unitary black hole evaporation [151, 16]. This challenges Hawking's conclusion directly, rather than through an asserted duality.

The new analysis does not identify an error in Refs. [100, 98]; in fact, it uses Hawking's calculation. But it asks a different question, which leads to a different conclusion. Hawking asked about the quantum state of the black hole radiation and found it to be a thermal state, $\rho_{\mathrm{Haw}}(t)$. Its von Neumann entropy,

$$S = -\operatorname{tr} \rho_{\mathrm{Haw}} \log \rho_{\mathrm{Haw}} \ , \tag{1.4}$$

rises monotonically as more radiation is produced. When the black hole is fully evaporated, S will be of order $\mathcal{A}_0/4G$, where $\mathcal{A}_0$ is the initial black hole area.

By contrast, Refs. [151, 16] ask only about the entropy of the radiation, not its state. The entropy S is computed not via Eq. (1.4), but as the analytic continuation of the n-th Renyi entropy to $n = 1$. In the presence of gravity, this method is compactly encoded [129] in the Ryu-Takayanagi (RT) prescription, also called more recently the Quantum Extremal Surface (QES) prescription [169, 168, 108, 78, 74].

The QES prescription was originally derived as an AdS/CFT technique for computing entropies of boundary CFT regions in terms of quantities in the bulk AdS spacetime [75, 78,

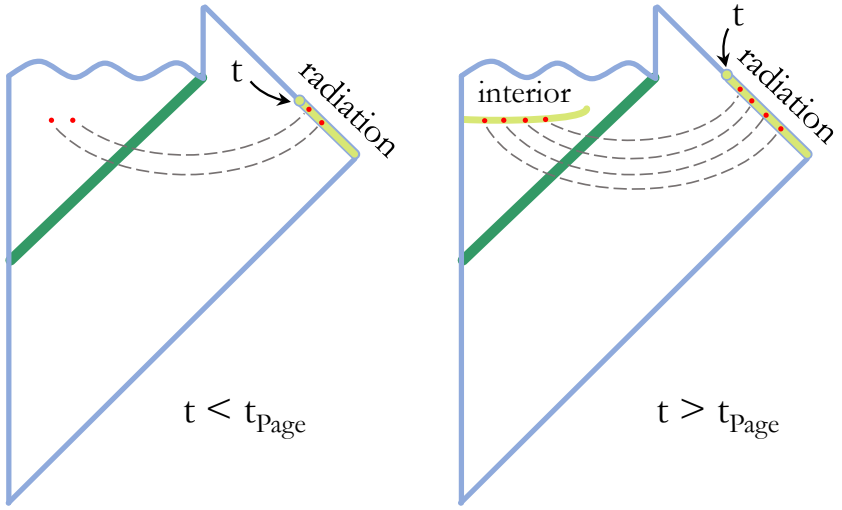

Figure 1.1: Penrose diagrams for an evaporating black hole. The light green region is the entanglement wedge of the radiation that has arrived at infinity before (left) and after (right) the Page time.

108, 169, 168]. It has since been derived as an application of the gravitation path integral in a saddlepoint approximation. We will define the prescription precisely in Chapter 2, but roughly it states that entropy of a region R in a boundary CFT is given by the generalized entropy of a bulk region called its *entanglement wedge*. The generalized entropy for a partial Cauchy surface $X \subset \Sigma_M$ is defined as

$$S_{\text{gen}}(X) = \frac{\text{Area}[\partial X]}{4G_N\hbar} + S(X) \ , \tag{1.5}$$

where $S(X)$ is the von Neumann entropy of the density operator of the quantum field theory state reduced to X. The entanglement wedge is defined by various homology and minimality conditions, which we will detail in Chapter 2.

Refs. [151, 16] applied this prescription to an evaporating black hole coupled to an auxiliary system with absorbing boundary conditions to collect the radiation. Schematically, they find that

$$S(\text{radiation}) = S_{\text{gen}}[\text{EW}(\text{radiation})] \ , \tag{1.6}$$

where EW refers to the entanglement wedge. In this calculation, the spacetime and its matter fields are computed using Hawking's approach, semiclassical gravity. But by using Eq. (1.6) instead of Eq. (1.4), one finds that $S(\text{radiation})$ follows the Page curve, as demanded by unitary evolution. It rises until the Page time, t_{Page}, when the black hole and radiation entropies are equal. Then $S(\text{radiation})$ falls, ultimately vanishing when the evaporation is complete.

Before the Page time, Refs. [151, 16] find that EW(radiation) is the radiation itself (Figure 1.1, left Penrose diagram). The QES (RT) prescription adds nothing new; the entropy rises because it does so in Hawking's calculation. After the Page time (right Penrose diagram), a minimality condition in the definition of the entanglement wedge implies[1] that EW(radiation) contains both the radiation and a disconnected region, which is essentially the black hole interior:

$$\text{EW(radiation)} = \text{radiation} + \text{black hole interior} \qquad (t > t_{\text{Page}}) \ . \tag{1.7}$$

Such a disconnected region has been dubbed an *entanglement island*.

In Hawking's analysis, the interior together with the Hawking radiation are in a pure state. Hence here the von Neumann entropy $S(\text{EW})$ vanishes, and only the area of the boundary of the island contributes. This boundary is approximately the black hole horizon, so

$$S_{\text{gen}}[\text{EW(radiation)}] = \frac{\mathcal{A}(\text{horizon})}{4G} \qquad (t > t_{\text{Page}}) \ . \tag{1.8}$$

The horizon area decreases as the black hole evaporates, yielding the falling part of the Page curve.

This calculation of the Page curve by Refs. [151, 16] represents major progress in our understanding of quantum gravity. It is a semiclassical calculation from which a non-trivial feature of quantum gravity can be derived. The calculation is not, however, without complications and puzzles of its own. The first is its use of the QES (RT) prescription in a variety of unusual settings. Refs. [151, 16] applied the QES prescription to compute the entropy of a bulk region in a nongravitating auxiliary spacetime, rather than a region in a CFT. They furthermore relied upon the assumption of entanglement wedge complementarity, that the entanglement wedge of a region R's complement is the complement of R's entanglement wedge, to derive the Page curve for the radiation. Later works [18, 167, 55, 12, 182, 21, 56] considered another unusual setting in which the matter in the spacetime with the black hole and the auxiliary system is also presumed holographic, meaning that it has its own bulk dual one dimension higher. This setting, which involves two different "layers" of holography, we refer to as double holography. Because these settings are unusual, Chapter 2 of this work is devoted to examining how the QES (RT) prescription should apply in these cases.

Another puzzle is that the Page curve calculations of Refs. [151, 16] make use of Hawking's conclusion that the entropy of the radiation rises monotonically for all time, only to conclude that that the entropy of the radiation instead follows the Page curve. We refer to this seeming contradiction as the *state paradox*. In Chapter 3, we we shall exhibit the state paradox in a variety of settings. The appearance of this paradox makes it difficult to say what physical conclusions can be drawn from the intermediate steps of the Page curve calculations. We thus seek a resolution, and we argue that the paradox is in all these cases resolved by what we

[1] When the minimality condition results in an island, it has been called the "island rule" [18]. However, this is not a new rule nor a modification of RT. The existence of islands after the Page time already follows from the RT prescription in the final form given to it by Engelhardt and Wall [74].

call *gravity-ensemble duality*. This proposal is, roughly, that there exists a duality between the gravitational path integral and an ensemble of theories on the boundary.

Having argued for a resolution of this tension, it is appropriate to examine further the results of the Page curve calculations, that we may learn as much as possible from them. Perhaps the key insight of Refs. [151, 16] is the observation that a region disconnected from the reference region contributes to the entanglement wedge of the radiation after the Page time, producing the falling part of the Page curve. As mentioned above, such a disconnected region is called an *entanglement island*, and the particular relevant application of the QES prescription is known as the *island rule*.

A later work [95] began to investigate whether this key insight could reveal anything about quantum gravity in a setting in which it is poorly understood: cosmology. As a first step, Ref. [95] investigated when a region in a cosmological spacetime can be an island for some reference region in a non-gravitating auxiliary spacetime. Ref. [95] derived three necessary conditions for a region to be an island and applied them to flat Friedman-Robertson-Walker (FRW) universes entangled with an auxiliary system in a thermofield-double-like state. There are, however, many cosmological models more general than flat FRW. In Chapter 4 we therefore extend this analysis to FRW universes with nonzero spatial curvature. Then in Chapter 5 we dispense with the assumption that the contents of the universe is radiation and consider FRW universes containing a general fluid with a general equation of state w.

Although we are hopeful that applying the lessons of the Page curve calculation to cosmology will bear more fruit, there are some questions the calculations have not yet answered. As we shall argue in Chapter 6, one such puzzle is the firewall paradox. This paradox states that even if black hole evaporation is unitary, effective field theory or General Relativity must break down substantially at or outside the horizon at late times [14]. At the beginning of Chapter 6, we argue that the Page curve calculations, even with gravity/ensemble duality, do not resolve the firewall paradox. We then describe a thought experiment that presents a sharp version of the firewall paradox for an asymptotic observer which involves a version of the Hayden-Preskill recovery protocol [103] in which the message is itself a smaller black hole. We propose that correctly accounting for decoherence, which is the observation that quantum systems interacting with an environment leaks information into that environment [195, 196, 87, 113], resolves the paradox.

Decoherence and the quantum circuits of the Hayden-Preskill protocol are only a few of many ways in which concepts from quantum information have proven relevant for black hole physics. Tensor networks [187, 96, 104, 157], quantum error correction [10, 92, 102, 8, 69, 77, 71, 94, 7], complexity [183, 186, 178, 165, 51, 40, 185], and other entropy measures [6, 7, 192] have all made appearances throughout the literature. In the spirit of this program, we present a quantum information perspective on another feature of black holes: their connection to the Eigenstate Thermalization Hypothesis (ETH) [177, 68, 64, 67]. ETH is a conjecture about when an ensemble of energy eigenstates behaves like the microcanonical ensemble. This conjecture relates to black holes through the expectation that holographic CFTs satisfy ETH [27]. In Chapter 7, we shall argue for a connection between ETH and the quantum search algorithm known as Grover search [88]. Intuitively, we demonstrate that

this connection allows one to quantify the difficulty of distinguishing eigenstates obeying ETH.

Chapter 2

Various Generalizations of the RT Prescription

The derivation of the Page curve for an evaporating black hole performed in Refs. [151, 16] and a related calculation of the Page curve directly for the radiation [18] involve applying the Ryu-Takayanagi (Quantum Extremal Surface) prescription to a number of unusual settings. As described in the previous chapter, the QES prescription was originally derived as an AdS/CFT technique for computing entropies of boundary CFT regions in terms of quantities in the bulk AdS spacetime [75, 78, 108, 169, 168]. We will present the full standard Ryu-Takayanagi (RT) prescription below.

Refs. [151, 16] did not explicitly clarify how the Ryu-Takayanagi (RT) prescription generalizes to the unusual settings they consider. They furthermore assumed the prescription satisfies (reasonable) properties, such as entanglement wedge complementarity. As these settings are atypical, it would be preferable to derive these generalizations more carefully and show what properties we can from physical considerations. This is the goal of the current chapter.

The first unusual case we consider is that of an AdS spacetime coupled to an auxiliary, nongravitating spacetime. In the calculations of Refs. [151, 16], such a coupling is required to ensure that the black hole evaporates, as otherwise the Hawking radiation will reflect off the AdS boundary and fall back into the black hole (unless it is very small). The second unusual setting is what we call a "doubly-holographic" model: the matter in the AdS spacetime is assumed to be holographic and thus has its own higher-dimensional bulk dual. The final setting is the one relevant to the calculation of Ref. [18] and combines the previous two cases: double holography with an auxiliary system. In each case, we shall generalize the RT prescription and make note of its salient features.

Notation and Conventions We use the following notation in this chapter. A subscript on a geometric object generally indicates not *its* dimension, but the dimension of the (physical) spacetime in which the object is naturally defined. For example, M_d will denote a d-dimensional spacetime, R_d a $d-1$ dimensional spatial region in M_d, and γ_d a $d-2$ di-

mensional extremal surface in M_d. It is often useful to rescale conformally a manifold M_d so that a boundary can be added to it; the result is called an unphysical manifold or Penrose diagram, $\tilde{M}_d \supset \partial\tilde{M}_d$. Note that the boundary of the physical manifold, $\partial M_d \subset \partial\tilde{M}_d$, need not be empty; it consists of braneworlds or end-of-the-world (EOW) branes.

In this chapter, $\langle x \rangle$ always denotes the ensemble average of x in the sense of Eq. (3.4). Angular brackets never denote a quantum expectation value.

The term *Boundary Conformal Field Theory* (BCFT) refers to the fact that such a theory lives on a manifold *with* Boundary, not to the fact that it lives on the conformal boundary *of* some AdS spacetime. We will capitalize "Boundary" whenever it is used in the sense of a BCFT. For example, "boundary entropy" might refer to the von Neumann entropy of a CFT region on the conformal boundary $M_{d-1} = \partial\tilde{M}_d$, whereas "Boundary entropy" is a specific BCFT parameter defined by Cardy [53].

Throughout this chapter we assume $d > 2$ for convenience. The case $d = 2$ would frequently require a special treatment; see for example Eq. (2.15). This would clutter the presentation. However, the qualitative aspects of our analysis apply in $d = 2$, and hence to the many recent works that studied entanglement islands in JT gravity and other two-dimensional models, such as Refs. [16, 18]. Related to this choice, in examples involving braneworlds we only consider induced gravity on the brane (i.e., the localized graviton due to embedding of the brane in AdS [158]). We never add an additional gravitational action on the brane, because in $d > 2$ this is not necessary.

General Setup

We shall now describe the general setup relevant for all three settings. Consider a $d-1$ dimensional[1] holographic conformal field theory CFT_{d-1} with central charge c_{d-1}, living on a manifold M_{d-1}; see Figure 2.1. Its bulk dual will be an asymptotically AdS_d spacetime M_d,[2] such that the unphysical spacetime (or Penrose diagram) conformally related to M_d [190] is

$$\tilde{M}_d = M_d \cup M_{d-1} \ ; \tag{2.1}$$

thus M_{d-1} is the conformal boundary of M_d. The AdS_d curvature length L_d is related to the central charge by

$$\frac{L_d^{d-2}}{G_d} \sim c_{d-1} \ , \tag{2.2}$$

where $G_d = \ell_d^{d-2}$ is Newton's constant in the d-dimensional bulk.

We shall denote a standard holographic duality of this type as follows:

$$M_{d-1} \longrightarrow M_d \ , \tag{2.3}$$

[1] For consistency with the later sections on double holography, we deviate here from the usual convention of using d for the boundary spacetime dimension.

[2] In general this spacetime can contain additional factors, e.g. $\mathrm{AdS}_d \times \mathbf{S}^{d'}$, so it need not actually be d-dimensional. In order to keep the discussion simple, we will assume that it is; generalizations are straightforward.

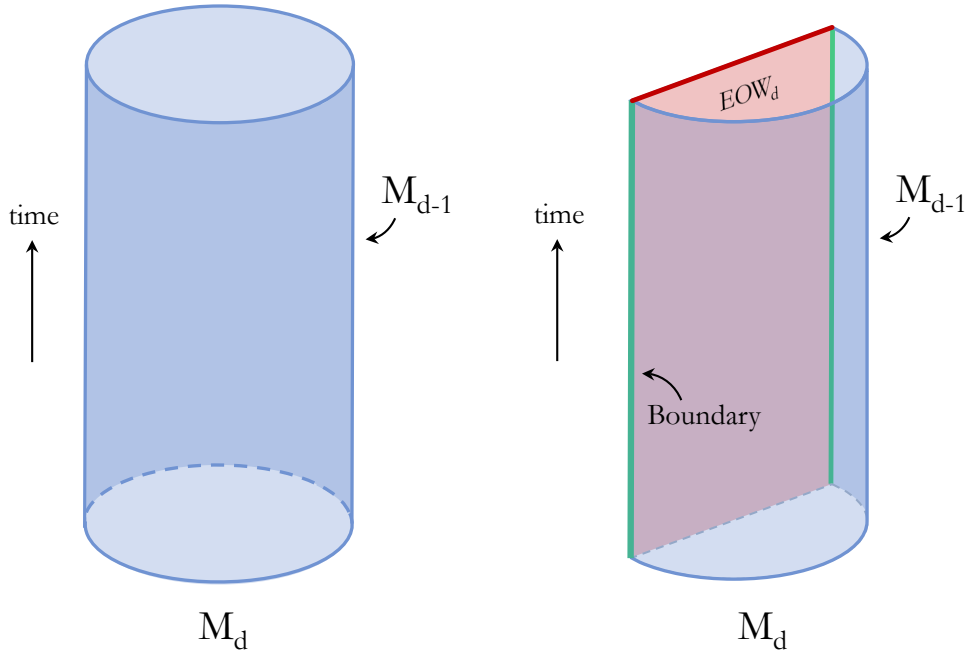

Figure 2.1: Examples of holographic duality. *Left:* The solid bulk M_d is dual to a holographic CFT_{d-1} on M_{d-1} (blue boundary). *Right:* In this example, M_{d-1} is a manifold with boundary, so the boundary theory is a BCFT_{d-1} and M_d contains an end of the world brane EOW_d. (Despite the appearance of a BCFT this is a "singly holographic" example. In Sections 2.2 and 3.3 we will consider a doubly holographic setting where the EOW_d is a braneworld that localizes gravity and contains a holographic CFT_d.)

where the arrow reminds us that in general, this duality is not truly an equivalence. Rather, the lower dimensional field theory without gravity can be viewed as the nonperturbative completion of the bulk theory.

Note that M_{d-1} may itself have a boundary, as in Figure 2.1. The spacetime M_d may also be a manifold with boundary [190], commonly referred to as an "end of the world brane" or EOW:

$$\text{EOW}_d \equiv \partial M_d \ . \tag{2.4}$$

In particular, if M_{d-1} is a manifold with boundary, then the CFT_{d-1} is a "Boundary conformal field theory" (BCFT),[3] and the bulk M_d will contain an $\text{EOW}_d \neq \varnothing$ anchored on the Boundary ∂M_{d-1} [188, 79]. An EOW can also exist in settings where the Lorentzian CFT_{d-1} has no Boundary [125, 61]. They must be included in the gravitational path integral.

[3]See the notation section at the end of the introduction.

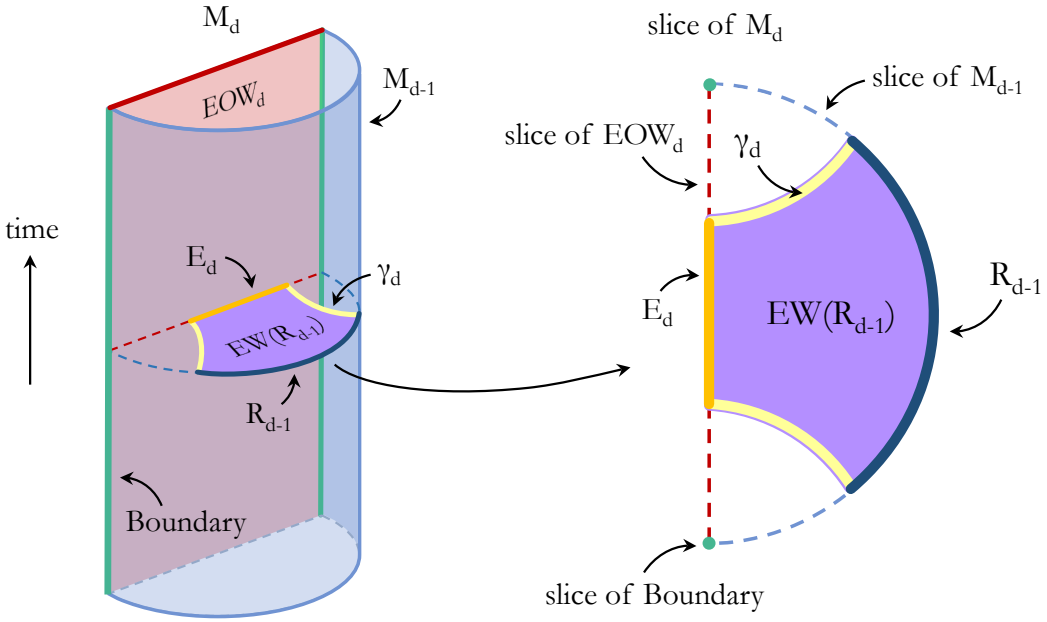

Figure 2.2: RT prescription, applied in the setting shown on the right of Figure 2.1. The entropy of the boundary region R_{d-1} is given by the generalized entropy of its entanglement wedge $\mathrm{EW}(R_{d-1})$. γ_d is the quantum extremal surface.

Standard Ryu-Takayanagi Prescription

We now formulate the standard holographic prescription for computing the von Neumann entropy of a boundary region from bulk quantities. This was first proposed by Ryu and Takayanagi [169, 168] for stationary states. It was generalized to the time-dependent case by Hubeny, Rangamani, and Takayanagi [108], and to the BCFT case by Takayanagi and collaborators [188, 79]. A quantum-corrected prescription was first proposed by Faulkner, Lewkowycz and Maldacena [78]. It was extended to all orders by Engelhardt and Wall [75], whose elegant formulation highlights the central role of generalized entropy. This final formulation is essential for the existence of islands,[4] and it is the only one we will review here. We will refer to it as the RT prescription for short, with apologies to all others involved in its development. We aim to make it clear throughout this work that islands are part and parcel of this prescription. They do not constitute a new ingredient, but a long-overlooked consequence. The recent recognition of their existence [151, 16] has been profoundly impactful.

Let $R_{d-1} \subset M_{d-1}$ be an achronal region (see Figure 2.2).[5] We can think of R_{d-1} as a

[4]Because the empty surface always has less classical area than the boundary of an island, area minimization cannot lead to an island. It is vital that the generalized entropy is minimized.

[5]An achronal region is a submanifold of codimension 1 (in the spacetime) which contains no two points

subregion at some instant of time, to which the CFT_{d-1} state may be restricted. The von Neumann entropy $S(R_{d-1})$ of the restricted CFT_{d-1} state is given by the generalized entropy of its entanglement wedge,

$$S(R_{d-1}) = S_{\mathrm{gen}}[\mathrm{EW}(R_{d-1})] \ . \tag{2.5}$$

The generalized entropy $S_{\mathrm{gen}}(X_d)$ [31] of an arbitrary achronal region $X_d \subset M_d$ is the sum of its gravitational entropy and the von Neumann entropy S of the quantum fields in the region X_d:

$$S_{\mathrm{gen}}(X_d) = \frac{\mathcal{A}(\partial X_d)}{4G_d} + S(X_d) \ . \tag{2.6}$$

Here $\mathcal{A}(\partial X_d)$ is the area of the boundary of X_d in M_d, and G_d is Newton's constant in M_d.

The *entanglement wedge* $\mathrm{EW}(R_{d-1})$ is an achronal region X_d[6] in M_d, that satisfies the following conditions:

1. *Homology*: $\partial X_d = \gamma_d \cup R_{d-1} \cup E_d$, where $\gamma_d \subset M_d - \mathrm{EOW}_d$, and $E_d \subset \mathrm{EOW}_d$.[7] See Figure 2.2.

2. *Stationarity*: $S_{\mathrm{gen}}(X_d)$ is stationary under variations of γ_d.

3. *Minimality*: X_d is has the smallest S_{gen} among all regions with the above properties.

A surface γ_d satisfying the homology constraint (1) and the stationarity condition (2) is called *quantum extremal*[8] with respect to R_{d-1}. If the minimality condition (3) is also satisfied, then γ_d is called the *RT surface* of R_{d-1}. Note that γ_d may be the empty set. Also, γ_d may contain disconnected components that end neither on R_{d-1} nor on E.

2.1 Ryu-Takayanagi Prescription with Auxiliary Systems

The first unusual setting we shall consider is the one relevant in Refs. [151, 16]: that of an AdS spacetime coupled to an auxiliary system. The previous efforts to extend the prescription required additional assumptions, such as entanglement wedge complementarity (defined below) [16]. We present a novel argument that this extension is fully determined by physical considerations. EW complementarity is a consequence rather than an assumption of our argument.

---

connected by a timelike curve.

[6] One can also define $\mathrm{EW}(R)$ to be the (d-dimensional) domain of dependence of this region. Since all Cauchy slices of the domain of dependence have the same generalized entropy, we will use these definitions interchangeably.

[7] Strictly, this is a statement about the image of X_d in the unphysical spacetime $\tilde{M}_d$.

[8] This is conventional. "Quantum stationary" would be more appropriate terminology, as the generalized entropy can be both increased and decreased at second order by suitable deformations.

Consider a bipartite system consisting of a holographic CFT_{d-1} in a region $R_{d-1} \subset M_{d-1}$ and an auxiliary system AUX, in some joint state. Suppose that there exists an RT-like prescription for computing the von Neumann entropy of this state. We shall take "RT-like" to mean that the prescription is of the form

$$S(R_{d-1} \cup \mathrm{AUX}) = S_{\mathrm{gen}}[\mathrm{EW}(R_{d-1} \cup \mathrm{AUX})] \ . \tag{2.7}$$

We now determine the detailed formulation of the prescription from general considerations.

For any bipartite system consisting of a gravitating region X_d and an auxiliary system AUX, we define the generalized entropy as

$$S_{\mathrm{gen}}(X_d \cup \mathrm{AUX}) = \frac{\mathcal{A}(\partial X_d)}{4G_d} + S(X_d \cup \mathrm{AUX}) \ . \tag{2.8}$$

Given these definitions, the nontrivial content of the prescription we seek lies in how we define the entanglement wedge $\mathrm{EW}(R_{d-1} \cup \mathrm{AUX})$.

Entanglement wedge nesting, the property that the entanglement wedge cannot shrink if the boundary algebra is enlarged [191], implies that

$$\mathrm{EW}(R_{d-1} \cup \mathrm{AUX}) \supset \mathrm{EW}(R_{d-1}) \ . \tag{2.9}$$

We next recall that the relative entropy between two boundary states, $S(\rho|\sigma)$, is the same as the relative entropy between the dual bulk states in the entanglement wedge [111]. This implies that bulk operators in the entanglement wedge (but not outside) can be implemented on the boundary [10, 111, 70]. In particular, small deformations of the boundary state do not change the entanglement wedge. Taking $R_{d-1} \cup \mathrm{AUX}$ as the boundary, consider a small deformation of the state in AUX. This can change the boundary relative entropy (in $R_{d-1} \cup \mathrm{AUX}$), but it cannot change the bulk relative entropy in $\mathrm{EW}(R_{d-1} \cup \mathrm{AUX})$, unless we require that

$$\mathrm{EW}(R_{d-1} \cup \mathrm{AUX}) \supset \mathrm{AUX}. \tag{2.10}$$

Therefore, AUX plays an interesting dual role: it appears both on the bulk and on the boundary side.

This does not yet fully determine the prescription. For example, Eqs. (2.9) and (2.10) would be consistent with the mistaken proposal that $\mathrm{EW}(R_{d-1} \cup \mathrm{AUX})$ is given by $\mathrm{EW}(R_{d-1}) \cup \mathrm{AUX}$. To see that this fails, we note that quantum information can be freely exchanged between AUX and R_{d-1} by appropriate couplings. But consider the setting of Section 3.1. Recall that at the Page time, $EW(R_{d-1})$ has a phase transition: it now includes not only the portion connected to R_{d-1}, but also an island inside the black hole. Just after the Page time, let us couple the region R_{d-1} to an AUX system that is initially in some pure reference state, and transfer some of the quantum information of the Hawking radiation into AUX. Then the phase transition is reversed; $EW(R_{d-1})$ loses the island. However, bulk operators in the island could be implemented on $R_{d-1} \cup \mathrm{AUX}$ before the transfer, so this must still be true afterwards. Therefore, $\mathrm{EW}(R_{d-1} \cup \mathrm{AUX})$ cannot have changed.

This shows (at physics-level rigor) that an appropriate definition of the entanglement wedge must treat the bulk and AUX jointly, not separately, when minimizing the generalized entropy. Hence we define

$$\mathrm{EW}(R_{d-1} \cup \mathrm{AUX}) \equiv X_d \cup \mathrm{AUX} \ , \tag{2.11}$$

where the spacetime region $X_d \subset M_d$ is chosen such that

1. $\partial X_d = \gamma_d \cup R_{d-1} \cup E_d$, where $\gamma_d \subset M_d - \mathrm{EOW}_d$ and $E_d \subset \mathrm{EOW}_d$.
2. $S_{\mathrm{gen}}(X_d \cup \mathrm{AUX})$ is stationary under variations of γ_d.
3. $X_d \cup \mathrm{AUX}$ has the smallest S_{gen} among all regions X_d with the above properties.

We have included the possibility that M_d has an EOW brane for generality, although none appears in the setup studied above. Note that the last term in Eq. (2.8) would vanish in a case where X_d and AUX separately have large von Neumann entropy but purify each other. Note also that AUX in the above formulas could represent one of several auxiliary systems, or equivalently, an arbitrary subalgebra of an auxiliary system.

The generalized RT prescription formulated above upholds entanglement wedge complementarity. Consider a pure quantum state for the complete system $M_{d-1} \cup$ AUX. On the boundary, purity implies $S_{d-1}(R_{d-1} \cup \mathrm{AUX}) = S_{d-1}(\bar{R}_{d-1})$, where $\bar{R}_{d-1}$ is complement of R_{d-1} in M_{d-1}. Purity also implies $\gamma_d(M_{d-1} \cup \mathrm{AUX}) = \varnothing$. Hence $\mathrm{EW}(M_{d-1} \cup \mathrm{AUX}) = M_d \cup \mathrm{AUX}$. The global bulk von Neumann entropy must also vanish: $S(M \cup \mathrm{AUX}) = 0$. This in turn implies that any two subsystems of $M \cup \mathrm{AUX}$ must have equal von Neumann entropy. Therefore $\gamma_d(\bar{R}_{d-1}) = \gamma_d(R_{d-1} \cup \mathrm{AUX})$, and hence

$$\mathrm{EW}(\bar{R}_{d-1}) = \overline{\mathrm{EW}(R_{d-1} \cup \mathrm{AUX})} \ . \tag{2.12}$$

In the special case where AUX is a nongravitating system described by quantum field theory and $R_{d-1} = \varnothing$, Eq. (2.7) reduces to the "island formula" of Ref. [18], where it was derived using doubly holographic systems. The formula was already used implicitly by Penington [151]. We have argued here that it emerges as a direct consequence of the standard RT prescription, when auxiliary systems are involved.

2.2 Double Holography without a Bath

Beginning with Ref. [18], a number of interesting papers have explored the RT prescription for evaporating black holes in a "doubly holographic" setting [167, 55, 12, 182, 21, 56]. In these works, the Hawking radiation is mainly carried by excitations of a holographic CFT_d that escape to a (holographic) auxiliary system. This setting is somewhat complicated by the simultaneous appearance of an extra layer of holography and of the auxiliary system. In this chapter, we will therefore separate these two ingredients: we will first introduce double holography without an auxiliary system in this section. We will derive an appropriate "RT-squared" prescription for computing the von Neumann entropy of the top level CFT_{d-1} from its $d+1$ dimensional doubly holographic bulk dual.

General Setup

We consider a holographic CFT_{d-1} on a spacetime M_{d-1}, dual to an asymptotically AdS_d spacetime M_d:

$$M_{d-1} \longrightarrow M_d \ . \tag{2.13}$$

We now suppose that the matter sector of the d-dimensional bulk M_d contains a holographic CFT_d coupled to gravity. This implies that M_d is a Randall-Sundrum braneworld [158, 116]. The holographic duality can then be iterated:

$$M_d \longrightarrow M_{d+1} \ . \tag{2.14}$$

The CFT_d on M_d can be traded for a bulk dual M_{d+1} (see Figure 2.3), with Newton's constant G_{d+1} determined by

$$\frac{G_{d+1}}{L_{d+1}} = \frac{G_d}{d-2} \ . \tag{2.15}$$

Near vacuum regions of the braneworld M_d, M_{d+1} will be locally AdS_{d+1}, with curvature length

$$\frac{L_{d+1}^{d-1}}{G_{d+1}} \sim c_d \ . \tag{2.16}$$

M_{d+1} will be a manifold with boundary, and we define

$$\mathrm{EOW}_{d+1} = \partial M_{d+1} \ . \tag{2.17}$$

By definition, the braneworld M_d is a subset of EOW_{d+1}. The complement $\mathrm{EOW}_{d+1} - M_d$ is the boundary of the entanglement wedge of the entire AdS_d brane. Therefore it is located at the minimal-area stationary surface anchored on the AdS_d brane's boundary. It implements boundary conditions on the AdS_{d+1} bulk that are dual the reflecting boundary conditions at the boundary of the AdS_d brane.

The central charge c_d can be thought of as a number of species. In the presence of gravity, large c_d increases the effective Planck length—the cutoff length scale at which the semiclassical analysis breaks down on M_d—from $G_d^{1/(d-2)}$ to $(G_d c_d)^{1/(d-2)} \sim L_{d+1}$. We assume that $G_{d+1}^{1/(d-1)} \ll L_{d+1} \ll L_d$, or equivalently,

$$1 \ll c_d \ll \frac{L_d^{d-2}}{G_d} \ . \tag{2.18}$$

This ensures that d-dimensional semiclassical gravity is a valid description both in the AdS_{d+1} bulk (the curvature radius is much greater than the Planck scale) and on the AdS_d brane (the curvature radius is much greater than the cutoff scale L_{d+1}).

Usually in holography, there are two descriptions of the same system. The CFT_{d-1} furnishes an exact description. The bulk gives an equivalent description, perturbatively in G_d, in the regime where semiclassical gravity (or perturbative string theory) can be applied. In the setting we consider now, there are three levels:

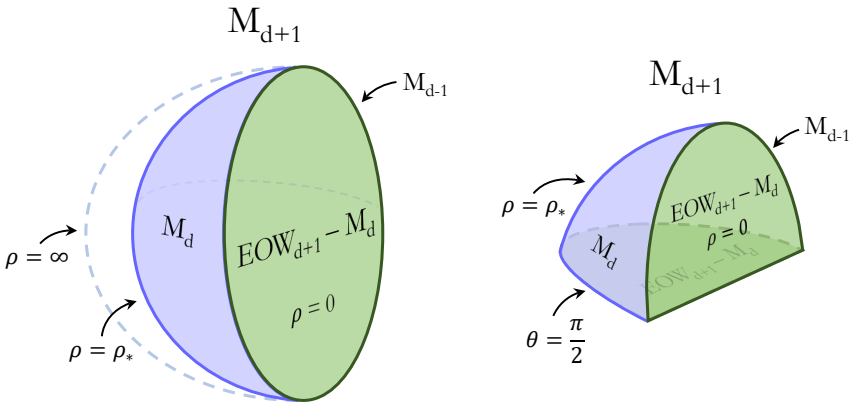

Figure 2.3: Double holography without a bath. M_d (purple surface) is the bulk dual of a holographic CFT_{d-1} (left) or BCFT_{d-1} (right) on M_{d-1} (dark green rim). So far this is identical to (a time slice of) the setups shown in Figure 2.1. But we now assume that M_d contains a holographic CFT_d. This gives rise to a doubly-holographic bulk dual M_{d+1} (the solid interior). From the $d+1$ bulk perspective, M_d is a Karch-Randall braneworld.

1. *Top Level:* The CFT_{d-1} on M_{d-1} is the only exact description.

2. *Holographic Bulk Dual:* The asymptotically AdS_d bulk M_d with a CFT_d coupled to gravity is an approximate d-dimensional description. Note that this description is *alternate* to the CFT_{d-1}, so there is no CFT_{d-1} at this level.

3. *Doubly Holographic Bulk Dual:* The third description, also approximate, is M_{d+1}. There is no CFT_d on the braneworld, at this level; however any other matter fields and dynamical gravity will still be present on M_d.

We will refer to the relation between the top and bottom level as double holography and denote it with a double arrow:

$$M_{d-1} \Longrightarrow M_{d+1} \ . \tag{2.19}$$

Two examples are shown in Figure 2.3.

The first example is a holographic CFT_{d-1} on $M_{d-1} = \mathbf{S}^{d-2} \times \mathbf{R}$. In the vacuum state, this is dual to global AdS_d. We now take the AdS_d to contain a holographic CFT_d with the above parameters. Then the CFT_{d-1} has a doubly holographic dual which is locally AdS_{d+1}:

$$ds^2_{d+1} = L^2_{d+1}\left[d\rho^2 + \cosh^2\rho\,(-\cosh^2 r dt^2 + dr^2 + \sinh^2 r\, d\Omega^2_{d-2})\right] \ , \tag{2.20}$$
$$0 \le \rho \le \operatorname{arccosh}\frac{L_d}{L_{d+1}} \ .$$

Here $d\Omega_{d-2}^2 = d\theta^2 + \sin^2\theta\, d\Omega_{d-3}^2$ is the metric on the unit $d-2$ sphere. In these coordinates, the AdS_d brane M_d sits at ρ_* with $\cosh\rho_* = L_d/L_{d+1}$; a second EOW brane resides at $\rho = 0$. See Figure 2.3.

The second example of Figure 2.3 is half of the previous example. We start with a BCFT_{d-1} on $M_{d-1} = \mathbf{B}^{d-2} \times \mathbf{R}$, where $\mathbf{B}^{d-2}$ is a $d-2$ dimensional hemisphere. For the simplest BCFT with reflecting boundary conditions at the equator, the vacuum state is doubly holographically dual to M_{d+1}, the restriction of Eq. (2.20) to the hemisphere $\theta \leq \pi/2$. There is now an additional EOW_{d+1} at $\theta = \pi/2$. The single holographic dual M_d is half of an AdS_d braneworld (still at $\cosh\rho = L_d/L_{d+1}$), with an EOW_d at $\theta = \pi/2$.

One-Step Ryu-Takayanagi Prescription for Double Holography

The von Neumann entropy S_{d-1} of the CFT_{d-1} restricted to an achronal region $R_{d-1} \subset M_{d-1}$ is given by Eq. (2.5), which we repeat here for convenience:

$$S(R_{d-1}) = S_{\mathrm{gen}}[\mathrm{EW}(R_{d-1})]\ , \tag{2.21}$$

where $\mathrm{EW}(R_{d-1}) \subset M_d$ is the entanglement wedge. In the doubly holographic setting of this section, M_d is a braneworld.

A Ryu-Takayanagi prescription also applies to braneworlds [73, 142, 123]. Let $R_d \subset M_d$ be an achronal region on the braneworld. Then

$$S_{\mathrm{gen}}(R_d) = S_{\mathrm{gen}}[\mathrm{EW}(R_d)]\ . \tag{2.22}$$

More generally, R_d may span both a braneworld region and a region (with no gravity) on $\partial\tilde{M}_{d+1}$, the conformal boundary of M_{d+1}; or it may consist of disconnected components in both types of regions. For $R_d \subset \partial\tilde{M}_{d+1}$, the generalized entropy on the left hand side is defined as the ordinary von Neumann entropy, with an unregulated UV divergence at ∂R_d. Thus Eq. (2.22) reduces to the usual RT prescription when R_d is entirely on the true boundary.

The entanglement wedge $\mathrm{EW}(R_d)$ is defined like that of the standard RT prescription, with $d \to d+1$: it is an achronal region $X_{d+1} \subset M_{d+1}$, such that

1. In the unphysical spacetime, $\partial X_{d+1} = \gamma_{d+1} \cup R_d \cup E_{d+1}$. Here $\gamma_{d+1} \subset M_{d+1} - \mathrm{EOW}_{d+1}$, and $E_{d+1} \subset \mathrm{EOW}_{d+1} - R_d$. Note that any portion of R_d that lies on a braneworld is a subset of EOW_{d+1}.

2. $S_{\mathrm{gen}}(X_{d+1})$ is stationary under variations of γ_{d+1}.

3. X_{d+1} is has the smallest S_{gen} among all regions with the above properties.

Comparing to Eq. (2.21), an important modification in Eq. (2.22) is that the prescription now computes the *generalized* entropy of the region R_d, rather than purely a CFT_d von Neumann entropy.

The above rules can be combined iteratively, by choosing $R_d = \mathrm{EW}(R_{d-1})$. This allows us to compute any CFT_{d-1} (1st level) entropy using the $d+1$ bulk (the 3rd level). Substituting Eq. (2.22) into Eq. (2.21) we find

$$S(R_{d-1}) = S_{\mathrm{gen}}[\mathrm{EW}(\mathrm{EW}(R_{d-1}))] \ . \tag{2.23}$$

This is a two-step prescription: one first finds the stationary surface γ_d on the AdS_d brane, and then one finds the stationary surface γ_{d+1} anchored on γ_d. However, we will now show that this is equivalent to simply minimizing the generalized entropy over surfaces that are allowed to be anchored anywhere on the AdS_d brane (and anywhere on the EOW brane), subject to the homology rules described above.

To see this, suppose that the latter procedure yielded a surface γ_{d+1} whose boundary σ on the AdS_d brane was not the minimal QES, γ_d. Then there are two possibilities: (i) σ does not have stationary generalized entropy with respect to small deformations on the brane or (ii) σ is stationary but has larger generalized entropy than γ_d. Case (i) together with the RT rule for braneworlds implies that the generalized entropy of γ_{d+1} (in the $d+1$ bulk) is not stationary under small deformations of γ_{d+1} that reduce to small deformations of σ. Case (ii) implies that the $d+1$ bulk stationary surface anchored on γ_d has smaller generalized entropy than γ_{d+1}. Either of these implications contradicts the definition of γ_{d+1}.

Thus we can formulate a **one-step Ryu-Takayanagi prescription** for the von Neumann entropy of a region R_{d-1} of a doubly-holographic CFT_{d-1}:

$$S(R_{d-1}) = S_{\mathrm{gen}}[\mathrm{EW}^2(R_{d-1})] \ , \tag{2.24}$$

where $\mathrm{EW}^2(R_{d-1})$ denotes the *doubly-holographic entanglement wedge* of R_{d-1}. This is defined as an achronal region $X_{d+1} \subset M_{d+1}$ such that

1. In the unphysical spacetime, $\partial X_{d+1} = R_{d-1} \cup \gamma_{d+1} \cup E_{d+1}$. Here $\gamma_{d+1} \subset M_{d+1} - \mathrm{EOW}_{d+1}$ and $E_{d+1} \subset \mathrm{EOW}_{d+1}$.

2. $S_{\mathrm{gen}}(X_{d+1})$ is stationary under variations of γ_{d+1}.

3. X_{d+1} has the smallest S_{gen} among all regions with the above properties.

A very simple example is shown in Figure 2.4. Consider the CFT_{d-1} in the vacuum state, and let R be half of the $d-1$ sphere in standard global coordinates. Then the QES γ_d is a $d-1$ dimensional hyperbolic plane cutting a Cauchy surface of the AdS_d brane in half: $\cosh\rho = L_d/L_{d+1}$; $\theta = \pi/2$. (In this example the quantum corrections play no role, so this is also a classical stationary surface.) The QES γ_{d+1} is similarly part of a hyperbolic plane cutting the Cauchy surface of the AdS_{d+1} bulk in half: $\theta = \pi/2$. Of course, it only includes the portion between the AdS_d brane and the EOW brane: $1 < \cosh\rho < L_d/L_{d+1}$. Figure 2.4 also shows other examples.

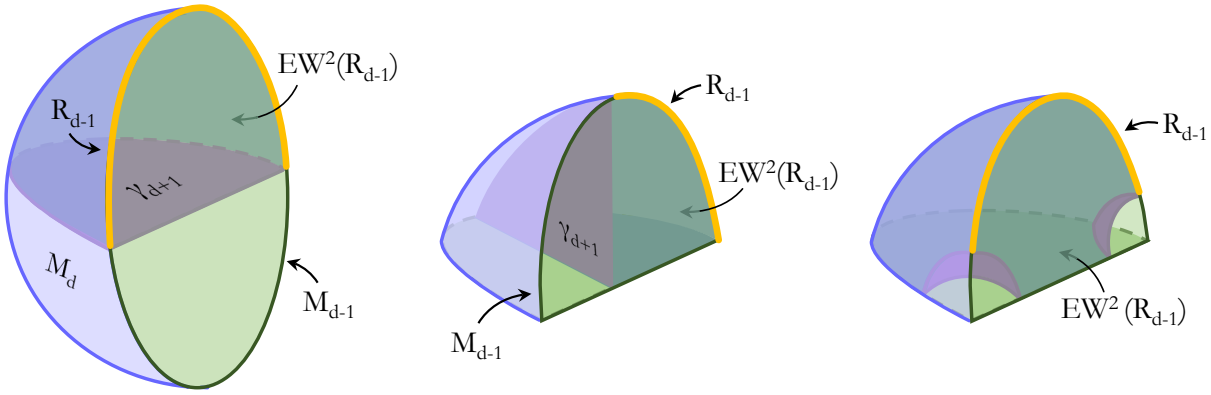

Figure 2.4: Examples of the doubly holographic entanglement wedge $\mathrm{EW}^2(R_{d-1})$ for a (B)CFT$_{d-1}$ region R_{d-1}. As before, the light purple surface M_d is the bulk dual of a holographic CFT$_{d-1}$ (left) or BCFT$_{d-1}$ (middle, right) on M_{d-1} (dark green rim). In each case, the doubly holographic entanglement wedge is bounded in part by the surface γ_{d+1}, shown in dark purple.

Quantum vs. Classical RT in Double Holography

In the case where the generalized entropies of γ_d and γ_{d+1} are both dominated by the area terms, consistency of Eqs. (2.22) and (2.23) requires

$$\frac{\mathcal{A}(\gamma_d)}{4G_d} = \frac{\mathcal{A}(\gamma_{d+1})}{4G_{d+1}} \; ; \tag{2.25}$$

By Eq. (2.15), this implies a very simple relation between the areas of the QESs:

$$\mathcal{A}(\gamma_{d+1}) = \mathcal{A}(\gamma_d)\, \frac{2L_{d+1}}{d-2} \; . \tag{2.26}$$

It is easy to check that this relation is obeyed in the above examples. More generally, consistency requires that γ_{d+1} must have a phase transition if and only if γ_d does, as the region R is varied. For example, if R consists of two antipodal round disks of equal size in the CFT$_{d-1}$, then γ_d undergoes a well-known phase transition as the disk radius is varied. γ_{d+1} must also have a phase transition at the same critical radius. At first this behavior may seem surprising, because one expects the QESs in the $d+1$ bulk to have a richer structure than those on the AdS$_d$ brane. However, in this context we are only considering $d+1$ QESs anchored on very special surfaces on the AdS$_d$ brane—those that are themselves QESs—so there is no contradiction.

A more interesting case arises when the CFT$_d$ is far from its vacuum state, so that the von Neumann entropy of braneworld regions is large. In this case S_{gen} on M_d may have large

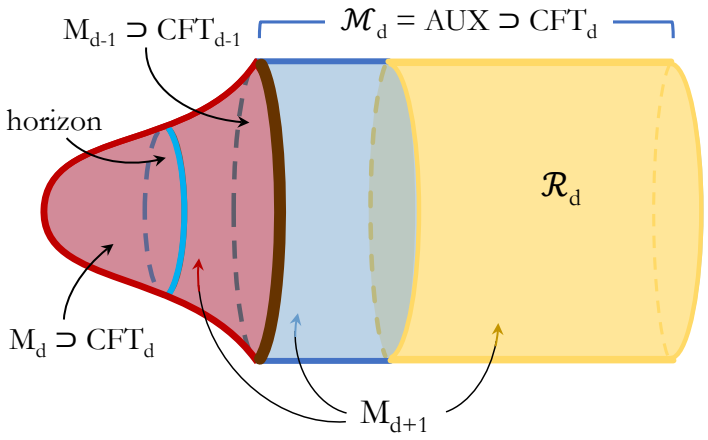

Figure 2.5: A doubly holographic CFT_{d-1} on M_{d-1} is coupled to holographic bath: a CFT_d on $\mathcal{M}_d$. The first holographic dual is $M_d \cup \mathcal{M}_d$, where M_d contains the same CFT_d coupled to gravity. The second holographic dual is M_{d+1} (solid interior). We consider a state which, in the first dual, corresponds to an evaporating black hole in M_d with radiation escaping to $\mathcal{M}_d$. The von Neumann entropy of the subregion $\mathcal{R}_d \subset \mathcal{M}_d$ can be computed using the single or double RT prescription.

quantum contributions (i.e., contributions from the von Neumann entropy term), while S_{gen} of the corresponding entanglement wedge in M_{d+1} is dominated by the classical term (the area term). In such a case, one can replace S_{gen} by $\mathcal{A}(\gamma_{d+1})/4G_{d+1}$ in Eqs. (2.22)–(2.24), but not by $\mathcal{A}(\gamma_d)/4G_d$ in Eq. (2.21).

2.3 Double Holography with a Holographic Bath

This section can be thought of as an extension of the previous settings, in two different ways. Continuing from the previous section, we keep the doubly holographic setup but we add a bath. That is, we couple the CFT_{d-1} (or equivalently, the AdS_d brane) to an auxiliary system AUX. We take AUX to be the same holographic CFT_d that lives on the AdS_d brane, but not coupled to gravity. Thus AUX can be thought of as a CFT_d living on a true asymptotic boundary of an asymptotically AdS_{d+1} bulk dual.

From the perspective of Section 2.1, we keep the bath but make the setting doubly holographic. That is, we now specialize to the case where both the dominant matter content in the gravitating AdS_d spacetime, and also the external bath AUX is a holographic CFT_d, with an asymptotically AdS_{d+1} bulk dual.

General Setup

As before, we consider a holographic CFT_{d-1} with central charge c_{d-1} on a manifold M_{d-1}, dual to a bulk M_d. We now choose this CFT_{d-1} such that the matter content of M_d includes a particular CFT_d coupled to gravity. As in Section 2.1, we couple the CFT_{d-1} to an auxiliary system AUX (see Figure 2.5). We now insist that AUX is specifically a CFT_d on a manifold $\mathcal{M}_d$ such that $M_{d-1} = \partial\mathcal{M}_d$, and we take this to be the same CFT_d that also appears in the bulk dual M_d.

The coupled boundary system (CFT_{d-1} on M_{d-1} and CFT_d on $\mathcal{M}_d$) defines a BCFT_d on $\mathcal{M}_d$. Importantly, there is no dynamical gravity on $\mathcal{M}_d$. Applying the general discussion of Section 3.2 to the CFT_{d-1} and AUX (i.e., to the BCFT_d), we find that this system is holographically dual to a d-dimensional bulk system:

$$M_{d-1} \cup \mathcal{M}_d \quad \longrightarrow \quad M_d \cup \mathcal{M}_d \ . \tag{2.27}$$

Here M_d has dynamical gravity. AUX $= \mathcal{M}_d$ plays a dual role as bulk and boundary system.

Next, we add the ingredient of double holography, as in Section 2.2. Suppose that the CFT_d on $M_d \cup \mathcal{M}_d$ is holographic, with parameters as described in Section 2.2. Let M_{d+1} be its $d+1$ dimensional bulk dual:

$$M_d \cup \mathcal{M}_d \quad \longrightarrow \quad M_{d+1} \ . \tag{2.28}$$

As usual, let $\tilde{M}_{d+1}$ be the associated unphysical spacetime (Penrose diagram), and let $\mathrm{EOW}_{d+1} = \partial M_{d+1}$. Then $\mathcal{M}_d = \partial\tilde{M}_{d+1}$ and $M_d \subset \mathrm{EOW}_{d+1}$. The above two dualities combine to establish the doubly holographic duality

$$M_{d-1} \cup \mathcal{M}_d \quad \Longrightarrow \quad M_{d+1} \ . \tag{2.29}$$

For example, with $M_{d-1} = \mathbf{S}^{d-2} \times \mathbf{R}$ at the equator of the hemishere $\mathcal{M}_d = \mathbf{B}^{d-1} \times \mathbf{R}$, one obtains the Karch-Randall (KR) model [116]. This was first discussed in detail as a doubly-holographic model in Ref. [45]. The first bulk dual is $M_d \cup \mathcal{M}_d$, where M_d is an AdS_d braneworld known as a KR brane. It forms the boundary of the doubly holographic dual M_{d+1}, a global AdS_{d+1} spacetime that terminates on the KR brane. In the vacuum state, the metric of M_{d+1} is given by Eq. (2.20), with the range of ρ extended to

$$-\infty < \rho \leq \operatorname{arccosh} \frac{L_d}{L_{d+1}} \ ; \tag{2.30}$$

The braneworld M_d is located at the upper end of this range, and the asymptotic boundary $\mathcal{M}_d$ is at the lower end. M_{d-1} is at $\rho = 0$, $r \to \infty$.

Alternatively, let $M_{d-1} = \mathbf{R}^{d-2} \times \mathbf{R}$ be the boundary of the half-space $\mathcal{M}_d = \mathbf{B}^{d-1} \times \mathbf{R}$. This gives the Poincare patch of an AdS_d braneworld as the first bulk dual, M_d; it gives the Poincare patch of AdS_{d+1} as the second bulk dual M_{d+1}.

Both of these models were studied further by Takayanagi and collaborators [188, 79], who gave a one-step RT prescription for the duality in Eq. (2.29). We will now derive this prescription from a different perspective, by combining the results of the previous sections.

One-Step Ryu-Takayanagi prescription for Double Holography

The one-step RT prescription for the doubly holographic duality (2.29) can be derived iteratively by combining the RT prescriptions for the single holographic dualities (2.27) and (2.28). For the first step this was given in Eqs. (2.7)-(2.11). Setting AUX $\to \mathcal{R}_d$, Eq. (2.7) becomes:

$$S(R_{d-1} \cup \mathcal{R}_d) = S_{\text{gen}}[\text{EW}(R_{d-1} \cup \mathcal{R}_d)] \ , \tag{2.31}$$

where $R_{d-1} \subset M_{d-1}$ and $\mathcal{R}_d \subset \mathcal{M}_d - M_{d-1}$ are arbitrary subregions of the boundary system. The other equations and the definition of EW are as in Section 3.2. The fact that the auxiliary system is a field theory plays no role in this step.

The second step computes the generalized entropy on the RHS of Eq. (2.31) holographically. Setting $R_d \to \text{EW}(R_{d-1} \cup \mathcal{R}_d)$ in Eq. (2.22), we obtain

$$S_{\text{gen}}(\text{EW}(R_{d-1} \cup \mathcal{R}_d)) = S_{\text{gen}}[\text{EW}(\text{EW}(R_{d-1} \cup \mathcal{R}_d))] \ . \tag{2.32}$$

Thus we obtain

$$S(R_{d-1} \cup \mathcal{R}_d) = S_{\text{gen}}[\text{EW}(\text{EW}(R_{d-1} \cup \mathcal{R}_d))] \ . \tag{2.33}$$

By arguments exactly analogous to those following Eq. (2.23), this iterative result can be condensed into a **one-step RT prescription**:

$$S(R_{d-1} \cup \mathcal{R}_d) = S_{\text{gen}}[\text{EW}^2(R_{d-1} \cup \mathcal{R}_d)] \ . \tag{2.34}$$

The doubly-holographic entanglement wedge $\text{EW}^2(R_{d-1} \cup \mathcal{R}_d)$ is defined as an achronal region $X_{d+1} \subset M_{d+1}$ such that

1. In the unphysical spacetime, $\partial X_{d+1} = R_{d-1} \cup \mathcal{R}_d \cup \gamma_{d+1} \cup E_{d+1}$, where $\gamma_{d+1} \subset M_{d+1} - \text{EOW}_{d+1}$ and $E_{d+1} \subset \text{EOW}_{d+1}$.
2. $S_{\text{gen}}(X_{d+1})$ is stationary under variations of γ_{d+1}.
3. X_{d+1} is has the smallest S_{gen} among all regions with the above properties.

We note that this agrees with the RT prescription for a BCFT_d given by Takayanagi [188, 79], which has been extensively used in recent analyses of entanglement islands, such as Refs. [18, 167, 55, 12, 182, 21].

2.4 Chapter Summary and Conclusion

In this chapter we have presented generalizations of the RT prescription in various scenarios relevant to the derivations of the Page Curve for evaporating black holes and their Hawking radiation. The first was the case of an AdS spacetime coupled to an auxiliary system, which is the setting relevant to Refs. [151, 16]. We argued that the correct prescription is fully determined by physical considerations.

The remaining settings involved a "doubly-holographic" model relevant to the works [18, 167, 55, 12, 182, 21], in which matter in an AdS spacetime is assumed holographic. This introduces an additional layer of holography: the higher-dimensional bulk dual of the holographic matter. The fundamental object in this case is the auxiliary system containing the radiation: a "Boundary" conformal field theory or BCFT (in the sense of Refs. [53, 1]), with an apparently different RT prescription [188, 79]. To explicate the RT prescription that applies here, we deconstructed the prescription for BCFTs as a repeated application of the original RT prescription.

For the sake of clarity, we first developed an RT prescription for a doubly holographic setting *without* auxiliary system, in Section 2.2. In this case, the fundamental object is a regular CFT_{d-1} dual to an AdS_d bulk. The bulk matter sector is assumed to consist of a holographic CFT_d coupled to gravity. Then there exists a second holographic dual with $d+1$ dimensions. The original RT prescription computes the von Neumann entropy of a CFT_{d-1} region as the generalized entropy of its entanglement wedge in the AdS_d bulk. An adaptation of the RT prescription to braneworlds [73, 142] can be used to compute generalized entropy in the AdS_d bulk using the $d+1$ dimensional bulk. We showed that these steps can be combined into a one-step "squared RT" prescription for computing CFT_{d-1} entropy from a "squared entanglement wedge," EW^2, in the $d+1$ dimensional bulk.

In Section 2.3, we combined the settings of the previous two sections by considering a doubly holographic CFT_{d-1}, coupled to a (singly) holographic CFT_d that plays the role of the auxiliary system of Section 2.1. In the second holographic dual, the CFT_d is part of the conformal boundary of the $d+1$ dimensional bulk. Like in Section 2.2, we showed that the RT prescriptions for each holographic layer can be combined into a (one-step) squared RT prescription that uses the $d+1$ bulk to compute the von Neumann entropy of any union of subregions of the above top-level CFT_{d-1} and CFT_d. Our squared RT prescription agrees with the known RT prescription for BCFTs [188, 79]. It follows that [188, 79] can be deconstructed as two applications of the RT prescription.

Having clarified the RT prescription in these settings, we are prepared to discuss a puzzle that arises in these calculations of the Page curve. It is to this puzzle that we turn in the next chapter.

Chapter 3

The State Paradox and Gravity/Ensemble Duality

The derivations of the Page curve for evaporating black holes and their Hawking radiation using the RT prescription (Refs. [151, 16]) amount to a remarkable step forward in understanding the black hole information paradox and quantum gravity more broadly. They suggest that semiclassical gravity is more powerful than it originally seemed. The calculations are not, however, free of puzzles of their own.

Recall that the Page curve calculation reviewed in Chapter 1 makes use of the Ryu-Takayanagi (RT) prescription to compute the entropy of the Hawking radiation for an evaporating black hole coupled to an auxiliary system with absorbing boundary conditions. The prescription, as applied in this case, takes the general form

$$S(\text{radiation}) = S_{\text{gen}}[\text{EW}(\text{radiation})] \ . \tag{3.1}$$

Before the Page time, the entanglement wedge of the radiation is the radiation itself (refer back to Figure 1.1, left Penrose diagram), and the RT prescription implies that the entropy rises because it does so in Hawking's calculation of thermal Hawking radiation. After the Page time (refer back to Figure 1.1, right Penrose diagram), the entanglement wedge contains a disconnected "island," which is roughly the black hole interior:

$$\text{EW}(\text{radiation}) = \text{radiation} + \text{black hole interior} \qquad (t > t_{\text{Page}}) \ . \tag{3.2}$$

By Hawking's calculation, the modes in the interior and the radiation purify each other, so their von Neumann entropy $S(\text{EW})$ together is zero. Therefore, only the area term of the RT prescription contributes to the entropy. The boundary of the island is approximately the black hole horizon, so

$$S_{\text{gen}}[\text{EW}(\text{radiation})] = \frac{\mathcal{A}(\text{horizon})}{4G} \qquad (t > t_{\text{Page}}) \ . \tag{3.3}$$

As the black hole evaporates, the horizon shrinks, which yields the falling part of the Page curve.

Through Eq. (3.3), the radiation appears on both sides of Eq. (3.1). Hawking's equation for the quantum state of the black hole radiation, Eq. (1.4), is invoked in evaluating its entropy on the RHS of Eq. (3.1). Thus on the RHS, S(radiation) (without the island) follows Hawking's monotonically increasing curve. This is a crucial ingredient, because it triggers the inclusion of the black hole interior in EW(radiation) after the Page time. On the LHS, S(radiation) then follows the Page curve.

It seems, then, that the calculations of Refs. [151, 16] curiously make use of Hawking's result that S(radiation) increases monotonically for all times, in order to reach the final conclusion that it does not. This is a contradiction. The S-matrix is an observable, so the state of the Hawking radiation cannot be ambiguous. Therefore, its von Neumann entropy cannot have two different values.[1] We call this contradiction the *state paradox*.

One possible resolution of the paradox is that the RT prescription is an uncontrolled approximation. Our confidence in the RT prescription derives from its success in the context of AdS/CFT, where the CFT entropy can often be independently computed and shown to agree. However, under certain assumptions, the RT prescription follows directly from a bulk path integral computation [129], evaluated in the saddle point approximation. It is obtained as the analytic continuation to $n = 1$ of the n-th Renyi entropies of the radiation, which can be computed from a path integral using the replica trick. After the Page time, one finds that the dominant saddle point has wormholes connecting the replicas [152, 15]; see Ref. [17] for a pedagogical review.

Thus the RT prescription has nothing to do with AdS/CFT; the nonperturbative completeness of the CFT is not used. RT can be applied even in asymptotically flat space, for example to compute the entropy of radiation that has arrived at the conformal boundary [97, 80]. RT is an advanced analogue of the Euclidean computation of the thermodynamic entropy of a black hole by Gibbons and Hawking [83]. It cleverly extracts information about the full quantum gravity theory from a path integral approximation.

This is not a controlled approximation. It need not agree with the full quantum gravity theory, and when it does, it need not be self-consistent. This could explain the state paradox: perhaps Eq. (1.6) just happens to compute the correct statistical entropy from the incorrect state. (See Ref. [5] for a discussion of related ideas.) And one day, perhaps, an even more sophisticated application of the Euclidean gravity path integral will be shown to yield the correct state of the Hawking radiation.

[1] One might be tempted to declare that S computed from Eq. (1.4) is only a coarse-grained entropy (even though no coarse-graining is manifest in Hawking's calculation). But the second term on the right side of Eq. (1.5) is a fine-grained von Neumann entropy, and it is this fine-grained entropy that determines EW(radiation) in Eq. (1.6). The island that leads to the Page curve can only be included if the *fine-grained* entropy of the radiation continues to grow after the Page time. This is achieved by taking Hawking's calculation seriously at this step in the calculation, as a fine-grained entropy. Moreover, if the Page curve was assumed from the beginning, then the smooth horizon shown in the top diagrams in Figure 1.1 would be inconsistent [14] and so cannot enter the analysis at all. Finally, rejecting Eq. (1.4) as a fine-grained entropy would amount to putting in the Page curve by hand. With the Page curve for the radiation as input, Eq. (1.6) would reproduce the Page curve trivially as an identity, not by inclusion of an island.

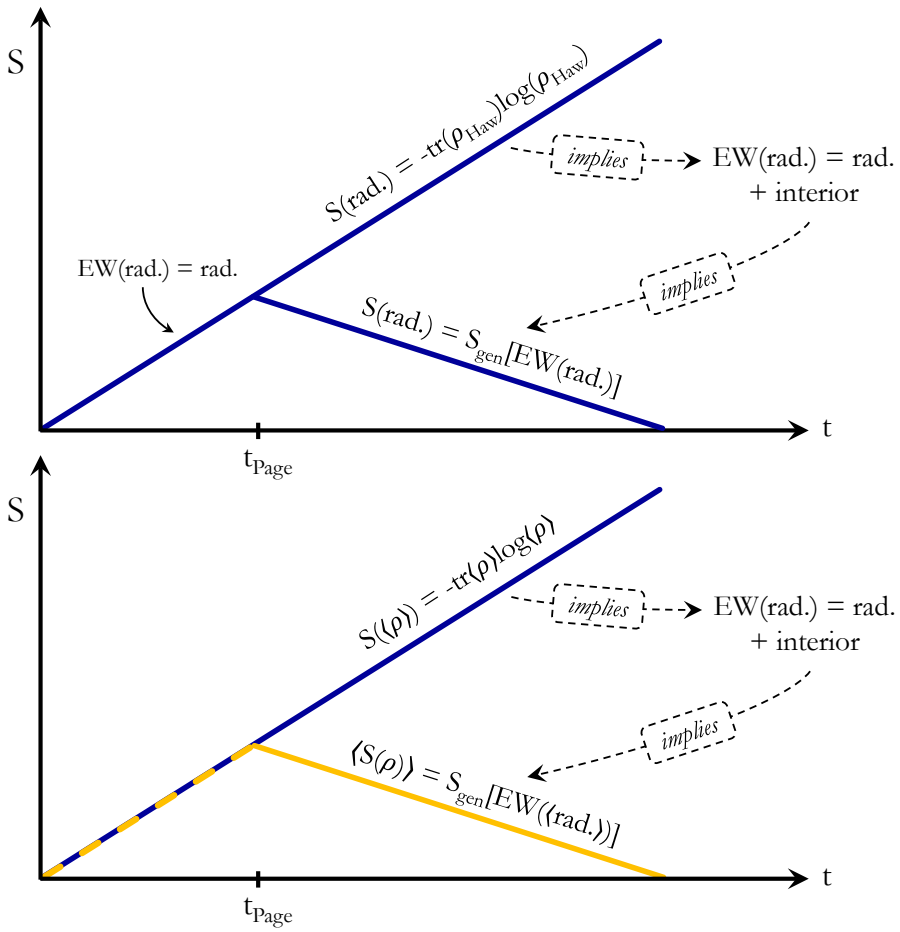

Figure 3.1: *Top:* State paradox. The rising blue curve corresponds to Hawking's calculation, while the falling blue curve is the Page curve. The RT prescription yields the Page curve for the entropy of the radiation, but only if the same entropy is assumed to follow Hawking's rising curve when determining the entanglement wedge. *Bottom:* Resolution of the state paradox by gravity/ensemble duality. The blue curve is that of Hawking's calculation, and the yellow curve is the Page curve. The ensemble-averaged state is mixed, and its entropy follows Hawking's curve. The ensemble-averaged entropy follows the Page curve.

A different, intriguing possibility is that there exists a novel kind of duality: between an appropriately defined version of the gravitational path integral, and an ensemble of quantum mechanical theories without gravity. This can resolve the state paradox [47]. According to this proposal, $S(\text{radiation})$ takes two different values on the two sides of Eq. (1.6) because it is not the same quantity on the two sides. On the left side, it is the ensemble average of the entropy, so we should replace $S(\text{radiation}) \to \langle S(\rho)\rangle$. See Figure 3.1 (bottom subfigure, lower graph). On the right side, the entanglement wedge is determined from the entropy of the

ensemble-averaged state of the radiation, $S(\langle\rho\rangle)$. See Figure 3.1 (bottom subfigure, upper graph). Because the von Neumann entropy is not a linear function of the state, generically $\langle S(\rho)\rangle \neq S(\langle\rho\rangle)$. We call this proposal *gravity/ensemble duality*.

We now describe this idea in more detail. Let ν label unitary theories, each capable of computing a pure Hawking radiation out-state from any pure in-state. Let

$$\langle x\rangle \equiv \int d\nu\, c(\nu)\, x^{(\nu)} \tag{3.4}$$

denote an appropriately weighted average of the quantity x computed in the different theories. Let $\rho_{\rm in}$ be the initial state before the black hole forms, and $\rho_{\rm out}^{(\nu)}$ be the final state of the radiation when the black hole has fully evaporated. Since each theory is unitary, we have

$$S(\rho_{\rm out}^{(\nu)}) = 0 \quad \text{for all } \nu\ , \tag{3.5}$$

and hence

$$\langle S(\rho_{\rm out})\rangle = 0\ . \tag{3.6}$$

But in general, the final states $\rho_{\rm out}^{(\nu)}$ will be different in different theories. We now assume that their ensemble average is the thermal state predicted by Hawking:

$$\langle\rho_{\rm out}\rangle = \rho_{\rm Haw}\ . \tag{3.7}$$

With these assumptions, Hawking's calculation computes the averaged out-state $\langle\rho_{\rm out}\rangle$; and in the same spacetime, the RT prescription correctly computes the averaged entropy:

$$\langle S[\rho_{\rm out}]\rangle = S_{\rm gen}[{\rm EW}(\langle\rho_{\rm out}\rangle)]\ . \tag{3.8}$$

Moreover, this holds at all times. Let $\rho(t) = {\rm tr}_{>t}\,\rho_{mathrmout}$ be the state of the radiation subsystem that has escaped to a distant region by the time t. The ensemble version of the RT prescription, Eq. (3.1) states that

$$\langle S[\rho(t)]\rangle = S_{\rm gen}[{\rm EW}(\langle\rho(t)\rangle)]\ . \tag{3.9}$$

No contradiction arises. The ensemble average of the entropy will follow the Page curve, while the entropy of the ensemble average follows Hawking's curve.

The state paradox and its resolution by gravity/ensemble duality was first described in a slightly different setting [47], which we will review in Section 3.1. Another compelling argument for gravity/ensemble duality comes from the fact that the partition function on multiple copies of a boundary need not factorize when it is computed from a bulk gravity dual, because connected geometries can contribute [152, 15]. It would be interesting to understand the detailed relation between these arguments.

The duality between JT gravity [189, 110] and a random matrix ensemble furnishes an important concrete example of gravity/ensemble duality [171, 172, 179, 170, 194]. Recently, an average over certain two-dimensional CFTs was shown to exhibit properties of an exotic

three-dimensional gravity theory [2, 135]. Conversely, starting with three-dimensional Einstein gravity, properties of a putative ensemble dual have been explored [62]; see also [153, 140].

An ensemble of theories satisfying Eqs. (3.5) and (3.7) may not exist in all cases where the RT prescription can be applied. If it does not, then the state paradox remains unresolved. For example, type IIB supergravity on $\mathrm{AdS}_5 \times \mathbf{S}^5$ is dual to a specific CFT [134], and no other boundary theories are presently known that have the same bulk as a coarse-grained description. If none exist, the gravitational path integral may still be expected to compute quantities that *would* be self-averaging if an ensemble *did* exist [172]. It would determine the entropy $S(\rho_{\mathrm{out}})$ but not the state ρ_{out}.

Notation and Conventions We use the same notations and conventions as the previous chapter.

3.1 Gravity/Ensemble Duality without a Bath

In this section, we exhibit a version of the state paradox in which only the standard RT prescription is needed [47]. There is no auxiliary system or bath, and there is only one layer of holography.

Simple Boundary Unitarity from a Semiclassical Bulk

It was recently shown that the RT prescription applied to semiclassical bulk evolution yields an entropy consistent with boundary unitarity [151, 16], for Hawking radiation extracted into an auxiliary system. This argument requires an extension of the RT prescription that includes auxiliary systems. We showed in Section 2.1 that this extension is uniquely determined by physical considerations.

However, the main result of Refs. [151, 16] can be obtained without involving an auxiliary system, using only the standard RT prescription, Eq. (2.5). Here we summarize this argument; further details are discussed in Ref. [47].

Consider a CFT_{d-1} on $M_{d-1} = \mathbf{S}^{d-2} \times \mathbf{R}$. In the vacuum, the gravity dual M_d would be global AdS_d. However, we shall take M_d to be a black hole formed from collapse of matter in a pure quantum state. The black hole is surrounded by a distant detector sphere ("Dyson sphere"), initially in some pure reference state. By the extrapolate dictionary, the initial boundary state must be pure. As the black hole evaporates, the Dyson sphere absorbs all of the Hawking radiation (see Figure 3.2).

Let $\Sigma_{d-1}(t)$ be a family of Cauchy surfaces (time slices) of the boundary M_{d-1}. Each such slice will be a sphere $\mathbf{S}^{d-2}$. Three slices are shown in Figure 3.2. We will apply the RT prescription to every slice, but first it will be useful to make some further definitions. Let $\Sigma_d(t)$ be a Cauchy surface of $M_d(t)$ bounded by $\Sigma_{d-1}(t)$. (In $\tilde{M}_d$, $\Sigma_{d-1} = \partial\Sigma_d$.) For boundary slices that lie in the future of the endpoint of the evaporation process, we define

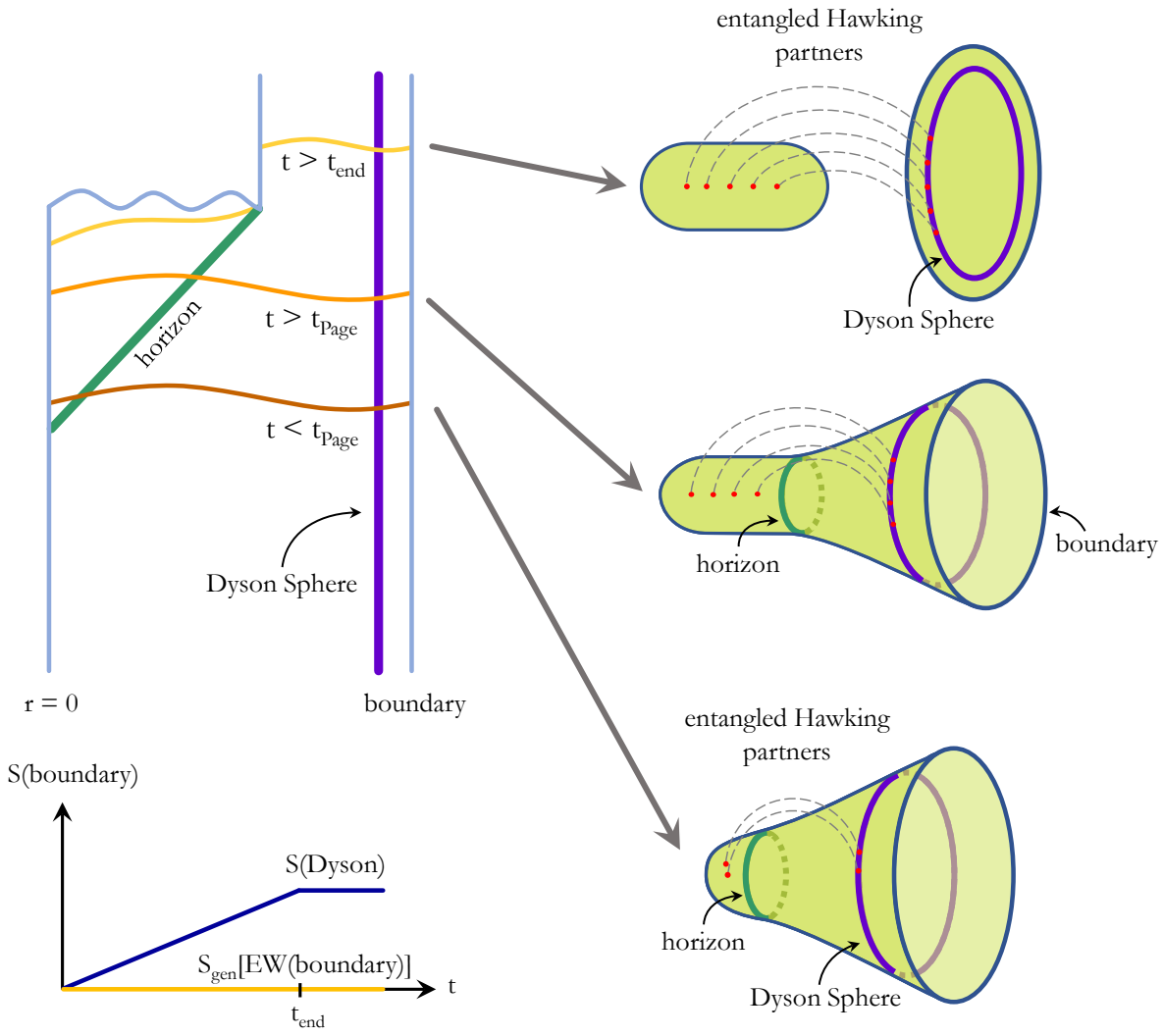

Figure 3.2: Hawking radiation is absorbed by a distant Dyson sphere near the boundary. In Hawking's semiclassical analysis, the Dyson sphere entropy will grow monotonically. The quantum state on the global bulk slices shown is pure. Each global slice is the entanglement wedge of its respective boundary slices. Thus the RT prescription implies that the entropy of the global boundary vanishes, as required by CFT unitarity. However, at late times the extrapolate dictionary demands that $S(\text{boundary}) = S(\text{Dyson})$. This contradiction is the state paradox.

$\Sigma_d(t)$ to include a disconnected component, a Cauchy slice of the black hole interior (see Figure 3.2, yellow slice at top). This can be chosen far enough from the singularity so that semiclassical gravity is applicable everywhere but in the neighborhood of the endpoint [132].

The key observation is that the entanglement wedge is the entire bulk:

$$\Sigma_d(t) = \mathrm{EW}[\Sigma_{d-1}(t)] \ , \tag{3.10}$$

for all t. To see this, note that the homology condition is satisfied, with $\gamma_d = \varnothing$. The stationarity condition is satisfied because no variations of γ_d exist. The minimality condition is satisfied because

$$S_{\mathrm{gen}}[\Sigma_d(t)] = 0 \tag{3.11}$$

for all t, and the generalized entropy cannot be negative.

Strictly, one could question all three of these statements due to the breakdown of the semiclassical description at the evaporation endpoint. We assume that this small region does not contribute significant effects that invalidate our treatment of the post-evaporation entanglement wedge. In any case, the essence of our discussion requires us only to go past the Page time, but not close to or beyond the endpoint of evaporation.

It is important to understand why Eq. (3.11) holds. The area term in the standard RT prescription, Eq. (2.6), vanishes since $\gamma_d = \varnothing$. The von Neumann entropy of the matter fields vanishes because the initial bulk state is pure, and the semiclassical bulk evolution of the *global* bulk state is unitary. (Information is lost to an observer outside the black hole in this description [100], but globally the state remains pure. The interior Hawking partners and the exterior Hawking radiation together form a pure state, the vacuum at the horizon.)

By Eq. (2.5), it follows that

$$S[\Sigma_{d-1}(t)] = 0 \tag{3.12}$$

for all t. The RT prescription "predicts" that the entropy of the boundary theory vanishes at all times. Of course, this is exactly what is expected from the unitarity of the boundary CFT_{d-1}. But it is remarkable that this result is reproduced by performing a semiclassical analysis in the bulk—the same calculation that led Hawking to conclude that information is lost to bulk observers outside the black hole. This fact was perhaps not widely appreciated prior to the recent work [151, 16] that derives the entire Page curve, even though it has the same import and is simpler to obtain.

Island and Page Curve

The previous subsection explained how the RT prescription yields the vanishing global boundary entropy consistent with unitarity, despite using Hawking's semiclassical evolution in the bulk. In this subsection, we introduce a refined scenario, such that the RT prescription yields the Page curve for two complementary subsystems, the Hawking radiation and the remaining black hole. In order to implement this without introducing an external bath or auxiliary system, any absorbed Hawking radiation is immediately transferred to a localized

reservoir RES taking up a small solid angle on the Dyson sphere, without loss of quantum coherence (see Figure 3.3) [47].

Gravitational backreaction in the asymptotic region can be kept arbitrarily small, so the shape of any stationary surface anchored to a small boundary region R_{d-1} will be similar to that in the vacuum. We take $R_{d-1}(t) \subset \Sigma_{d-1}(t)$ to be at the same angular position as the reservoir, and just large enough so that $\mathrm{EW}[R_{d-1}(t)]$ will barely contain the reservoir (see Figure 3.3). Before the Page time, the entanglement wedge has only one connected component, and we find

$$S[R_{d-1}(t)] = S_{\mathrm{gen}}[\mathrm{EW}(R_{d-1}(t))] = \frac{\mathcal{A}[\gamma_d^{\mathrm{conn}}]}{4G} + S_{\mathrm{RES}}(t) \ . \tag{3.13}$$

The superscript refers to the fact that $\gamma_d = \gamma_d^{\mathrm{conn}}$ is connected to R_{d-1} before the Page time. By moving around ballast on the Dyson sphere, one can arrange for the asymptotic geometry in an open neighborhood of γ_d^{conn}, and hence for $\mathcal{A}[\gamma_d^{\mathrm{conn}}]$ to remain fixed [47]. The entropy of the reservoir $S_{\mathrm{RES}}(t)$, however, increases as more radiation arrives. This yields the rising part of the Page curve shown in Figure 3.3.

The entropy of the Dyson sphere, and of S_{RES} in particular, increases monotonically even after the Page time. Its state is always purified by the "Hawking partners" in the black hole interior. Inclusion of the black hole interior in the entanglement wedge will entirely wipe out the contribution $S_{\mathrm{RES}S}$ to $S_{\mathrm{gen}}(R_{d-1})$ at a cost of increasing the area term by the area of the black hole. This preserves the homology condition, since it merely adds an extra component to γ_d. By its very definition, this choice becomes favorable at the Page time, when the black hole and radiation entropy are equal.

After the Page time, the minimality condition thus requires that $\mathrm{EW}(R_{d-1})$ contains a second, disconnected component I (see Figure 3.3). This is called an island, in the terminology of Ref. [18]. The island is the black hole interior, bounded by a disconnected component $\gamma_d^{\mathrm{island}}(t)$ that nearly coincides with the horizon.[2] The interior of $\gamma_d^{\mathrm{island}}$ purifies the Hawking radiation, so the entropy of the reservoir no longer contributes, and $S_{\mathrm{gen}}[\mathrm{EW}(R_{d-1})]$ is given just by the area of the RT surface $\gamma_d = \gamma_d^{\mathrm{conn}} \cup \gamma_d^{\mathrm{island}}$:

$$S_{\mathrm{gen}}[\mathrm{EW}(R_{d-1})] = \frac{\mathcal{A}[\gamma_d^{\mathrm{conn}}]}{4G} + \frac{\mathcal{A}[\gamma_d^{\mathrm{island}}(t)]}{4G} \ . \tag{3.14}$$

The first term remains constant. But $\gamma_d^{\mathrm{island}}(t)$ shrinks with the black hole horizon as the black hole evaporates, yielding the decreasing part of the Page curve.

Thus, in the refined scenario, the RT prescription (i.e., a bulk path integral that computes the entropy) yields the Page curve for the boundary region R_{d-1}. It rises during the first half of the evaporation process, then decreases. Again, this is consistent with our expectations from boundary unitarity. Entanglement wedge complementarity is manifest in the present setting, so a Page curve is also obtained for the complementary boundary region $\bar{R}_{d-1}$.

[2]The precise location of $\gamma_d^{\mathrm{island}}$ is determined by the stationarity condition. It sits about a Planck length inside the horizon. Temporally, $\gamma_d^{\mathrm{island}}(t)$ is located at $t - t_{\mathrm{scr}}$, where $t_{\mathrm{scr}} \sim \beta \ln\left(\mathcal{A}[\gamma_d^{\mathrm{island}}]/4G\right)$ and β is the inverse temperature of the black hole [151, 16].

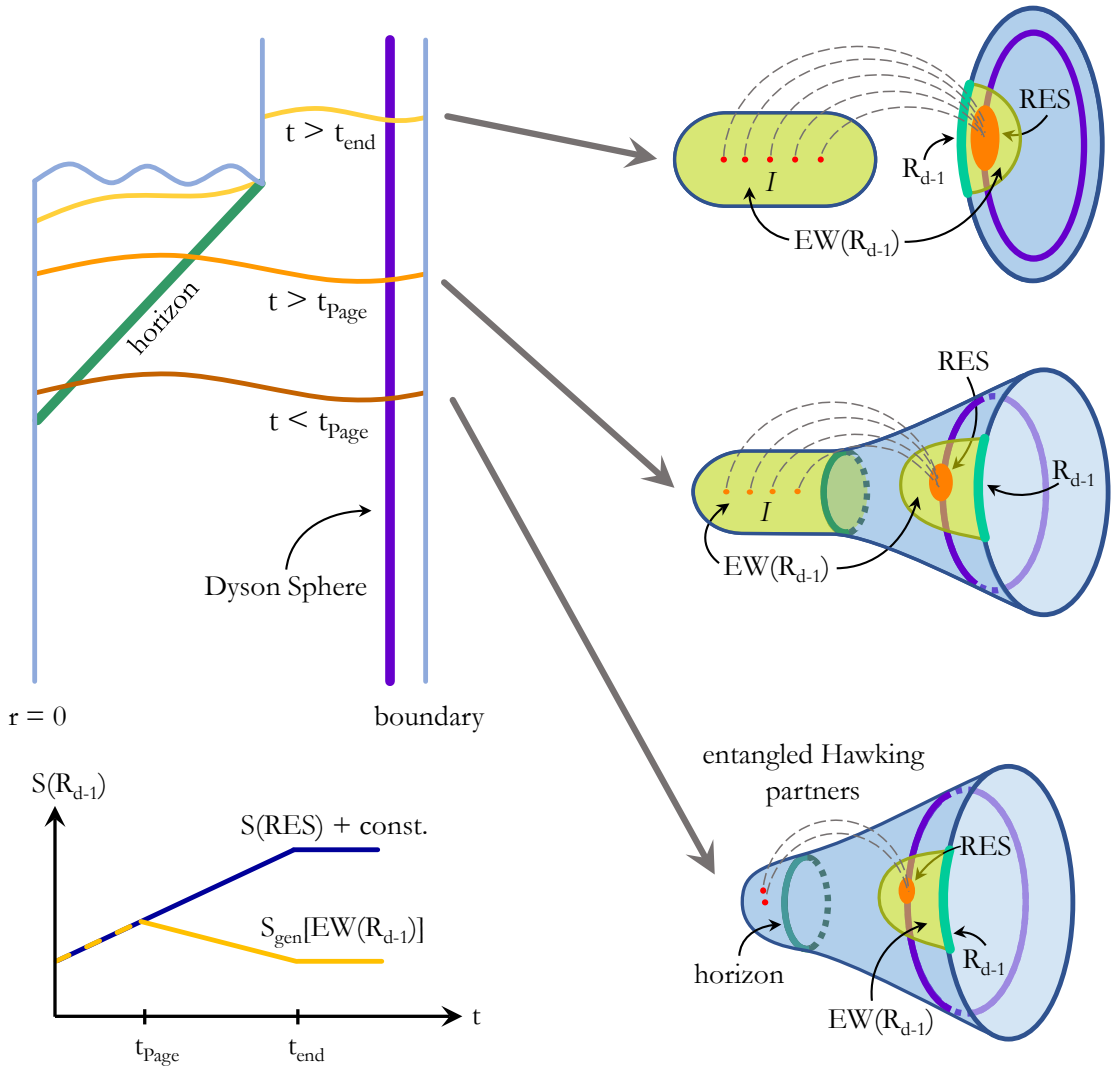

Figure 3.3: Compared to Figure 3.2, the Hawking radiation is collected in a localized reservoir on the Dyson sphere. The RT prescription is applied to a nearby boundary region R_{d-1}. The entanglement wedge $\mathrm{EW}(R_{d-1})$ is shown in light green. After the Page time, it contains a disconnected island I, the black hole interior, because this choice minimizes the generalized entropy. This yields the Page curve for $S(R_{d-1})$. However, the extrapolate dictionary would yield Hawking's curve; this is the state paradox.

State Paradox and Ensemble Interpretation

The large entropy of the Dyson sphere at late times leads to the state paradox. After the evaporation is complete, all of the (conserved) mass is in the Dyson sphere. The standard AdS/CFT dictionary can be used to construct the boundary state from the mixed state of the Dyson sphere [90]. It dictates that the boundary state must have the same entropy as the Dyson sphere. Energetic arguments preclude purification of this state by some nonlocal CFT excitations [47]. The entropy of the CFT_{d-1} should therefore grow monotonically throughout the evaporation process. But this contradicts both the RT result and the expected unitarity of the boundary theory.

We stress again that one cannot dismiss the large Dyson sphere entropy as an artifact of the semiclassical approximation, without discarding the entire RT calculation. If the reservoir RES did not have large entropy after the Page time, the black hole interior could not purify it. Then there would be no reason to include the island.

In the setting of this section, the paradox does not arise for the state of the bulk radiation, but for the boundary state, since we are using the RT prescription to compute the entropy of the latter. A resolution of the state paradox can then be obtained by assuming that the boundary CFT is an *ensemble* of unitary theories, and that the boundary quantities computed using the bulk are ensemble averages (see Figure 3.4). This proposal is consistent both with the smallness of $S[R_{d-1}(t)]$ and the fact that the reservoir contains a mixed state, for $t > t_{\mathrm{Page}}$. Since each member of the ensemble is unitary, $S(R_{d-1})$ must follow the Page curve in each theory. Hence the ensemble average of $S(R_{d-1})$ also follows the Page curve.

But the state of R_{d-1} need not be self-averaging. Each member of the ensemble predicts a pure out-state, but this need not be the *same* pure out-state in each theory. Hence the ensemble average of the out-state is a mixed state whose entropy can continue to grow after the Page time. Under the ensemble interpretation, the ensemble-averaged boundary state can be obtained by applying the standard AdS/CFT dictionary to the semiclassical bulk state.

The most explicit calculations of entanglement islands so far [16] were done for the case where the bulk is JT gravity, which is indeed dual to a matrix ensemble. However, we stress that the above argument is unrelated to this observation. The state paradox should be viewed as independent evidence that the gravity path integral, if it is well defined, must be dual to an ensemble, even in settings where no suitable ensemble dual is currently known.

3.2 Gravity/Ensemble Duality with a Bath

In this section, we turn to the settings studied by Penington [151] and by Almheiri *et al.* [16]. We will exhibit the state paradox and discuss its resolution by gravity/ensemble duality.

In contrast to Section 3.1, the Dyson sphere in AdS_d is eliminated and replaced by an auxiliary (external) system AUX: a "bath" that couples to the boundary CFT_{d-1} and absorbs

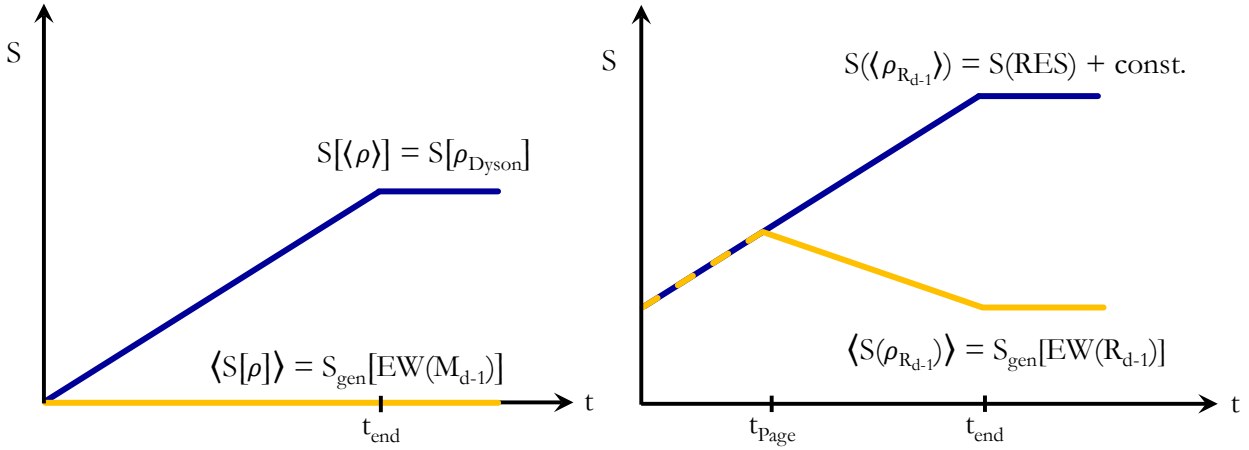

Figure 3.4: Here we assume the gravity/ensemble interpretation, in the examples studied in Section 3.1 (left) and Section 3.1 (right). This resolves the state paradox. The RT prescription (yellow) computes the ensemble averaged entropy $\langle S \rangle$ of the full boundary (left) or of R_{d-1} (right). The extrapolate dictionary (blue) yields the average state of the ensemble, $\langle \rho \rangle$, in these regions.

the Hawking radiation (see Figure 3.5). Thus we study the holographic duality

$$M_{d-1} \cup \text{AUX} \longrightarrow M_d \cup \text{AUX} \ . \tag{3.15}$$

In Ref. [16], AUX is a 1+1 dimensional CFT, and the black hole has two asymptotic regions. For definiteness, we will follow Penington [151], who considered the more physical setting of a black hole formed from collapse. The auxiliary system AUX will remain unspecified in this section.

We use the extension of the RT prescription to include AUX, derived in Section 2.1. In Section 3.2 we apply the RT prescription to black hole evaporation into AUX. This is just for completeness: we summarize Refs. [151, 16] and restate the analysis in Section 3.1 in this modified setting. The paradox identified in Ref. [47] and reviewed in Section 3.1 also has an analogue in this setting. In Section 3.2 we discuss this and its resolution if the bulk is dual to an ensemble of boundary theories.

Island and Page Curve

We now consider the specific setting of a black hole evaporating into AUX [151] and examine the implications of the RT prescription, Eq. (2.7). These follow immediately from the results of Section 3.1, upon substituting $R_{d-1} \to \text{AUX}$ and $\bar{R}_{d-1} \to M_{d-1}$. The entropy of each system follows a Page curve, as we will now verify.

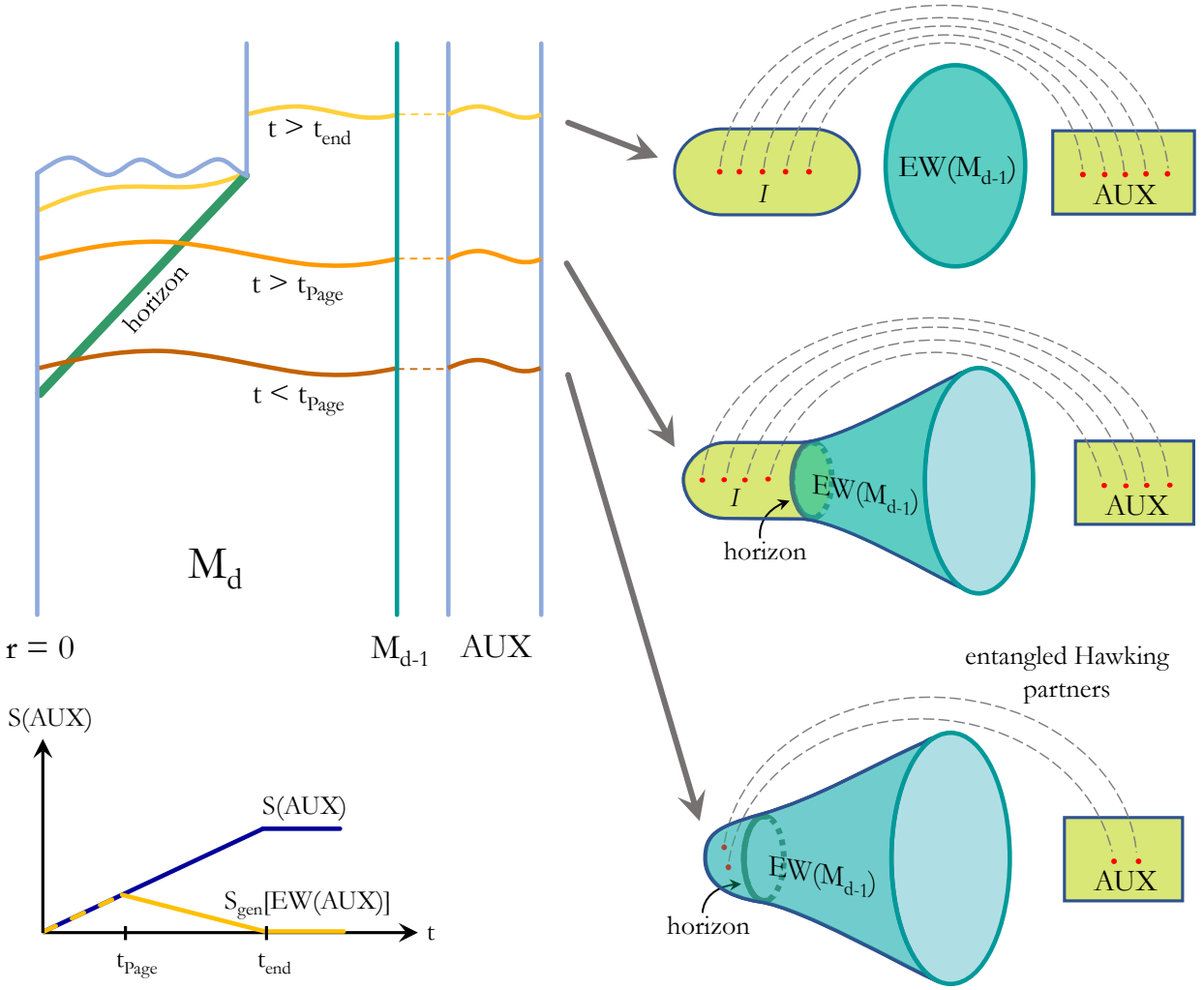

Figure 3.5: Hawking radiation escapes into an auxiliary system without gravity. The RT prescription can be applied to the boundary M_{d-1}, yielding the dark green entanglement wedge. A version of the RT prescription for AUX can be developed by requiring consistency with the analysis in Section 3.1. One finds that EW(AUX) (light green) includes AUX itself, and after the Page time, it also the bulk region I complementary to $EW(M_{d-1})$. The state paradox arises in AUX: the entropy must follow Hawking's rising curve for the island I to be part of EW(AUX), but with I included, RT yields the Page curve for AUX.

Recall that $\Sigma_{d-1}(t)$ defines a foliation of the boundary M_{d-1}, and $\Sigma_d(t)$ are bulk Cauchy slices whose boundary is $\Sigma_{d-1}(t)$. Before the Page time, one finds that the entanglement wedge of the CFT_{d-1} includes the entire bulk:

$$\mathrm{EW}[\Sigma_{d-1}(t)] = \Sigma_d(t) \ . \tag{3.16}$$

Since $\gamma_d = \varnothing$ and hence $\mathcal{A}(\gamma_d) = 0$,

$$S[\Sigma_{d-1}(t)] = S_{\mathrm{gen}}[\Sigma_d(t))] = S[\Sigma_d(t)] \ . \tag{3.17}$$

This grows with time, because $\Sigma_d(t)$ contains the black hole interior, which in turn contains more and more unpartnered interior Hawking modes as the Hawking radiation escapes into AUX.

After the Page time, the entanglement wedge of the full boundary slices $\Sigma_{d-1}(t)$ ends at a quantum extremal surface $\gamma_d(t)$ near the horizon [151]:

$$\mathrm{EW}[\Sigma_{d-1}(t)] = \Sigma_d(t) \cap \mathrm{Ext}[\gamma_d(t)] \ . \tag{3.18}$$

Here we have chosen $\Sigma_d(t)$ to contain $\gamma_d(t)$, and Ext denotes the spacelike exterior of γ_d. Since the interior Hawking modes are no longer part of $\mathrm{EW}[\Sigma_{d-1}(t)]$, the von Neumann entropy of the entanglement wedge vanishes and so

$$S[\Sigma_{d-1}(t)] = S_{\mathrm{gen}}[\mathrm{EW}(\Sigma_{d-1}(t))] = \frac{\mathcal{A}[\gamma_d(t)]}{4G_d} \ , \tag{3.19}$$

which decreases to zero as the black hole evaporates.

By entanglement wedge complementarity, Eq. (2.12), $\mathrm{EW}[\mathrm{AUX}(t)]$ is the complement of $\mathrm{EW}[\Sigma_{d-1}(t)]$. Thus, the entropy of AUX will follow the same Page curve. Before the Page time, EW(AUX) only contains AUX, i.e., the early Hawking radiation that has been extracted from the AdS_d spacetime. Its entropy grows as more radiation is produced:

$$S_{\mathrm{gen}}[\mathrm{EW}(\mathrm{AUX(t)})] = S(\mathrm{AUX}) \quad (t < t_{\mathrm{Page}}) \ . \tag{3.20}$$

After the Page time, EW(AUX) in addition contains an island I:

$$\mathrm{EW}(\mathrm{AUX(t)}) = \mathrm{AUX(t)} \cup I(t) \quad , \ I = \mathrm{Int}(\gamma_d) \ , \tag{3.21}$$

where Int denotes the spatial interior of γ_d on Σ_d. I is the black hole interior, which contains Hawking partners that purify the radiation in AUX. Hence, the generalized entropy is then given by the (decreasing) boundary area of this island:

$$S_{\mathrm{gen}}[\mathrm{EW}(\mathrm{AUX(t)})] = \frac{\mathcal{A}[\gamma_d(t)]}{4G_d} \quad (t > t_{\mathrm{Page}}) \ . \tag{3.22}$$

After the black hole has completely evaporated and all of the Hawking radiation is in AUX, EW(AUX) continues to contain the black hole interior I, now a separate "island universe" without boundary (see Figure 3.5).

State Paradox and Ensemble Interpretation

In the present setting, the state paradox arises in AUX. On the one hand, the Hawking radiation in AUX is manifestly in a mixed state, whose entropy continues to increase even after the Page time. (In the notation of Ref. [11], this is the "non-bold state.") If its entropy did not increase, then there would be no justification for including the black hole interior island in EW(AUX) after the Page time. On the other hand, the generalized entropy of EW(AUX) after the Page time is given by the area of the black hole, which decreases and eventually vanishes. According to the RT prescription, $S_{\text{gen}}[\text{EW(AUX)}]$ computes the von Neumann entropy of AUX. Hence AUX must be in a different state from what we originally assumed: one whose entropy follows the Page curve. (In the notation of Ref. [11], this is the "bold state.") This is a contradiction [47].

It is interesting to compare this instantiation of the state paradox to the version that arose in Section 3.1. In Section 3.1, the extrapolate dictionary is used at the last step, to translate the mixed Dyson sphere state to a mixed boundary state, in conflict with the pure state obtained from RT. In the present setting, the extrapolate dictionary is used earlier, when the *bulk* Hawking radiation is allowed to escape into AUX by coupling the *boundary* to AUX. Strictly it is not possible to couple radiation inside a spacetime to an auxiliary system, since the resulting nonconservation of the stress tensor would violate the Bianchi identity. Thus the coupling is defined through the boundary, and the extrapolate dictionary is used in interpreting this as a transparent boundary condition for the Hawking radiation. As a result of this coupling, the two conflicting quantum states are both in AUX in the end.

As in the previous section, the paradox is resolved if we assume that the bulk calculation computes both the average state (via Hawking's calculation), and the average entropy (via the RT prescription), in an ensemble of unitary boundary theories. The average entropy of M_{d-1} (and also of AUX) follows the Page curve, because it does so in each (unitary) theory. Different members of the ensemble evolve the same initial state to different final states, so the ensemble average of the state is mixed, and *its* entropy grows monotonically even after the Page time. Both sides of the gravity/ensemble duality exhibit a mixed state: in the bulk because we performed Hawking's calculation, and on the boundary because we averaged over the final state produced by different theories. (In the notation of Ref. [11], the ensemble-averaged bold state equals the non-bold state.)

3.3 Double Holography with a Holographic Bath

Next we turn to the "doubly holographic" setting introduced in Ref. [18] and expanded upon in [167, 55, 12, 182, 21, 56]. This setting contains a black hole whose radiation escapes to a reference system, and all matter is assumed to be holographic. This implies that there is a higher-dimensional bulk dual description, as discussed in the previous chapter. We will apply the generalizations of the RT prescription derived in Section 2.3 to exhibit how the state paradox arises in this setting.

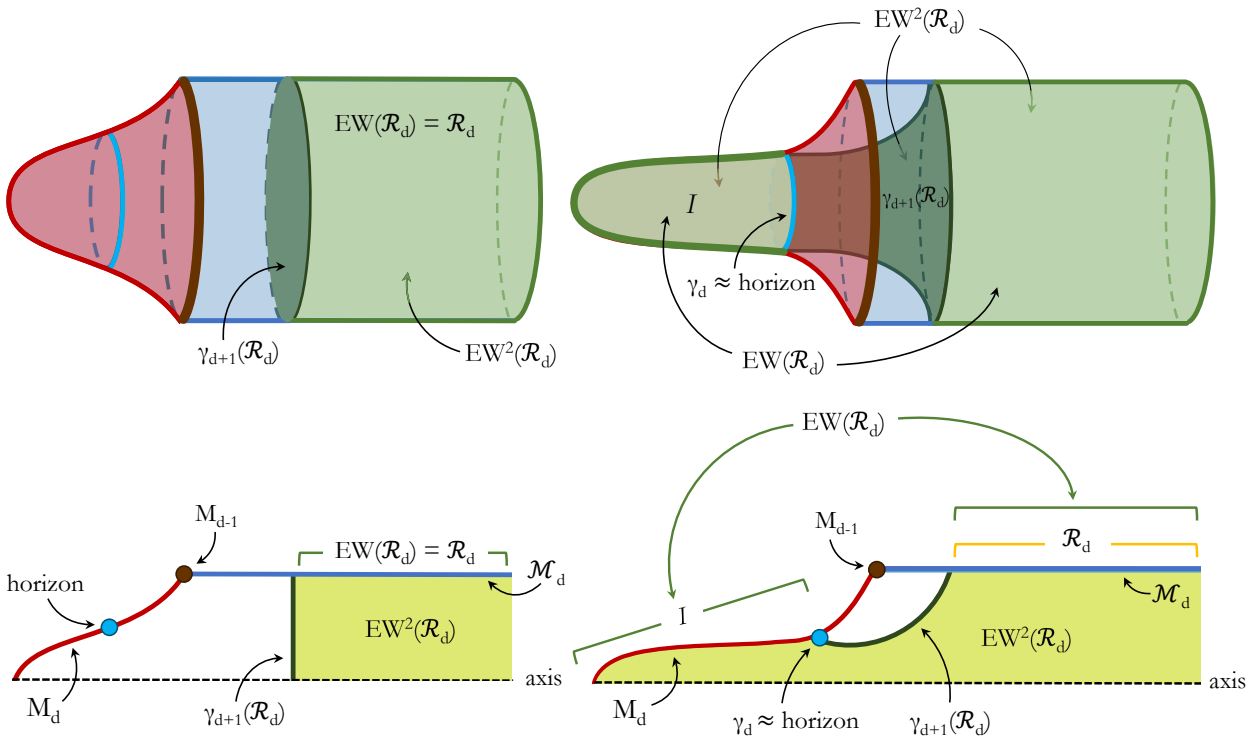

Figure 3.6: Entanglement wedges of the bath region $\mathcal{R}_d$ before (left) and after (right) the Page time, when $\mathrm{EW}(\mathcal{R}_d)$ has a disconnected island I. Each top figure is simply the bottom figure rotated around the axis. The "squared" entanglement wedge EW^2 is always connected. It can be found iteratively as $\mathrm{EW}(\mathrm{EW}(\mathcal{R}_d))$, or in one step from Eq. (2.34) [188, 79]. As in Section 3.3, γ_d is a quantum extremal surface, but γ_{d+1} is an ordinary extremal surface.

Island and Page Curve

In the language of Section 3.2, the first holographic dual, $M_d \cup \mathcal{M}_d$, M_d contains a black hole whose radiation propagates to $\mathcal{M}_d$. First, let us consider the top level, the BCFT_d on $M_{d-1} \cup \mathcal{M}_d$. There are now two ways to compute the von Neumann entropy of a subregion $\mathcal{R}_d \subset \mathcal{M}_d$ that contains the radiation.

One option is to ignore the second holographic dual and use RT only for the first holographic duality, Eq. (2.27). Setting $R_{d-1} \to \varnothing$ in Eq. (2.31), we find

$$S(\mathcal{R}_d) = S_{\mathrm{gen}}[\mathrm{EW}(\mathcal{R}_d)] \ . \tag{3.23}$$

Before the Page time, $\mathrm{EW}(\mathcal{R}_d) = \mathcal{R}_d$ (see Figure 3.6). Since $\mathcal{R}_d$ is a true boundary region, $S_{\mathrm{gen}}(\mathcal{R}_d) = S(\mathcal{R}_d)$. Thus, the above equation is a trivial identity before the Page time. After the Page time,

$$\mathrm{EW}(\mathcal{R}_d) = \mathcal{R}_d \cup I \quad (t > t_{\mathrm{Page}}) \ , \tag{3.24}$$

where the island $I \subset M_d$ is the black hole interior (see Figure 3.6). The Hawking radiation in $\mathcal{R}_d$ is purified by the Hawking partners in I, so

$$S_{\text{gen}}[\text{EW}(\mathcal{R}_d)] = \frac{\mathcal{A}(\gamma_d)}{4G_d} \quad (t > t_{\text{Page}}) \ , \tag{3.25}$$

where $\gamma_d = \partial I$ nearly coincides with the horizon. Note that the radiation appears on both sides of the duality, and that we have made no reference to the second holographic bulk dual M_{d+1}.

Another option is to use the doubly holographic duality derived in Chapter 2, Eq. (2.29). By the one-step RT prescription for double holography, Eq. (2.34),

$$S(\mathcal{R}_d) = S_{\text{gen}}[\text{EW}^2(\mathcal{R}_d)] \ . \tag{3.26}$$

With the one-step prescription following Eq. (2.34) one finds $\text{EW}^2(\mathcal{R}_d)$ as shown in Figure 3.6. Unlike $\text{EW}(\mathcal{R}_d)$ in Eq. (3.24), $\text{EW}^2(\mathcal{R}_d)$ is always a connected region. After the Page time, γ_{d+1} ends on the quantum extremal surface γ_d, and the island I forms part of the boundary of $\text{EW}^2(\mathcal{R}_d)$. But neither the radiation in $\mathcal{R}_d$ nor the Hawking partners in the black hole interior on M_d contribute to $S_{\text{gen}}[\text{EW}^2(\mathcal{R}_d)]$, since they are not part of M_{d+1}. Both before and after the Page time, the generalized entropy of the squared entanglement wedge is given just by the classical area of γ_{d+1}, in line with the discussion at the end of Section 2.2:

$$S_{\text{gen}}[\text{EW}^2(\mathcal{R}_d(t))] = \frac{\mathcal{A}[\gamma_{d+1}(t)]}{4G_{d+1}} \ . \tag{3.27}$$

State Paradox and Ensemble Interpretation

Agreement between Eqs. (3.23) and (3.26) is a nontrivial consequence of the "second step" of the RT prescription for double holography, Eq. (2.32). That equation, in turn, was obtained by applying the RT prescription for braneworlds, (2.22), which is relevant for the duality (2.28), to the region $\text{EW}(\mathcal{R}_d)$. But Eq. (2.22) allows us to choose any other subregion of the first bulk dual $M_d \cup \mathcal{M}_d$ and compute its generalized entropy. Thus we may ask questions that have no obvious analogue in the dualities of Eqs. (2.27) and (2.29).

For example, after the Page time, $\text{EW}(\mathcal{R}_d) = \mathcal{R}_d \cup I$. But we could instead use Eq. (2.22) to compute the generalized entropy of just $\mathcal{R}_d$. Because the RT prescription for braneworlds, Eq. (2.22), prohibits the RT surface γ'_{d+1} from ending on M_d (see Figure 3.7), its area continues to grow after the Page time, and we find the entropy computed by Hawking. Thus, Eq. (2.22) will not give the same answer for $S(\mathcal{R}_d)$ as Eqs. (3.23) and (3.26)! This contradiction is the bulk dual of the state paradox.

In Section 3.2 (with $\text{AUX} \to \mathcal{R}_d$), the state paradox appeared as a contradiction between $S(\mathcal{R}_d)$ computed from the semiclassical Hawking analysis on $M_d \cup \mathcal{M}_d$, and $S(\mathcal{R}_d)$ computed from Eq. (3.23). Either quantity can now also be computed using the second holographic dual M_{d+1}. As noted in the previous paragraph, the results (given by Eq. (2.22) and (3.26) respectively) disagree.

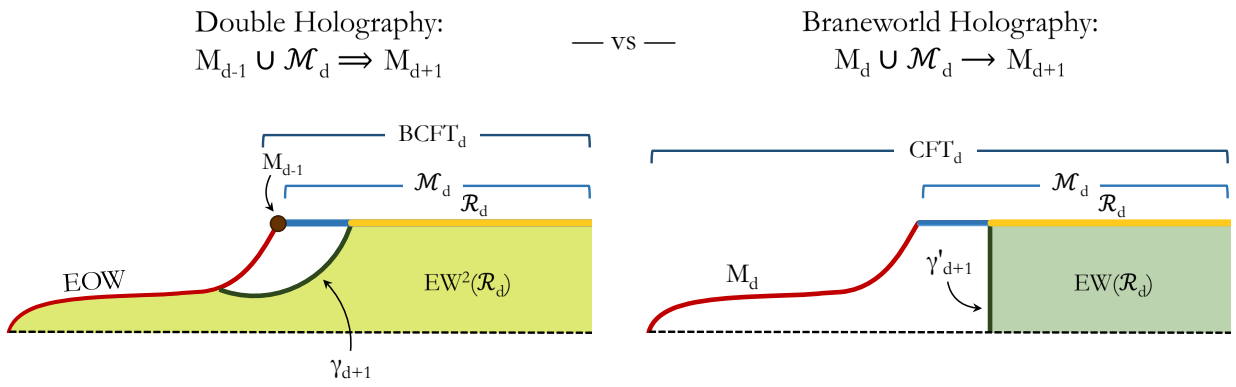

Figure 3.7: Bulk dual of the state paradox. *Left:* We regard $\mathcal{R}_d$ as a BCFT$_d$ subregion (top level). The homology rule following Eq. (2.34) applies: γ_{d+1} is allowed to end on the braneworld which here appears as an EOW brane. At late times, $\mathcal{A}(\gamma_{d+1}) \to 0$, resulting in the Page curve for $S(\mathcal{R}_d)$. *Right:* We consider $\mathcal{R}_d$ as a subregion of the CFT$_d$ on $M_d \cup \mathcal{M}_d$. The homology rule following Eq. (2.22) applies. The braneworld M_d is now part of the boundary; since we are computing the entropy only for the region $\mathcal{R}_d$, γ'_{d+1} is not allowed to end on M_d. $\mathcal{A}(\gamma'_{d+1})$ grows monotonically, resulting in Hawking's curve.

Gravity/ensemble duality can again resolve this paradox. Suppose that the CFT$_{d-1}$ on M_{d-1} is really an ensemble of unitary theories as discussed in the introduction. From the top-level viewpoint, the CFT$_{d-1}$ emits radiation into the CFT$_d$ on $\mathcal{M}_d$. In each theory, this process is unitary and the radiation entropy in $\mathcal{R}_d \subset \mathcal{M}_d$ follows the Page curve. Hence the average entropy $\langle S(\rho_{\mathcal{R}_d})\rangle$ follows the Page curve. But the ensemble-averaged state of the radiation, $S(\langle\rho_{\mathcal{R}_d}\rangle)$, follows Hawking's monotonically rising curve.

The first holographic dual of this process is the escape of Hawking radiation from M_d into $\mathcal{M}_d$. Assuming gravity/ensemble duality, the semiclassical analysis of black hole evaporation computes $\langle\rho_{\mathcal{R}_d}\rangle$ directly, and it determines $\langle S(\rho_{\mathcal{R}_d})\rangle$ via the first RT prescription, Eq. (3.23). The second layer of holography, Eq. (2.28), gives us an alternative way of computing $\langle S(\rho_{\mathcal{R}_d})\rangle$ and $S(\langle\rho_{\mathcal{R}_d}\rangle)$ using the braneworld version of the RT prescription, Eq. (2.22). To compute $\langle S(\rho_{\mathcal{R}_d})\rangle$, choose $R_d \to \mathrm{EW}(\mathcal{R}_d) = \mathcal{R}_d \cup I$ in Eq. (2.22). To compute $S(\langle\rho_{\mathcal{R}_d}\rangle)$, set $R_d \to \mathcal{R}_d$ in Eq. (2.22).

It is interesting to note that it does not matter whether Eq. (2.28) is a gravity/ensemble duality. Suppose that it is. Then there exists an ensemble of CFT$_d$ theories on $M_d \cup \mathcal{M}_d$. On what is now the boundary side, we would have to perform a gravity path integral involving each of these different theories, then average. But regardless of the details of each CFT$_d$, the state in $\mathcal{R}_d$ will be thermal and purified by the excitation in I. Therefore, unlike the state of the Hawking radiation in $\mathcal{R}_d$ in the BCFT$_d$ (the top level), the state of the semiclassically evolved CFT$_d$ theories is self-averaging in the region $\mathcal{R}_d \cup I$, and also in the region $\mathcal{R}_d$.

Of course, in a different state (for example, a setup analogous to Section 3.1 in the $d+1$ dimensional bulk), a state paradox can arise in $M_d \cup \mathcal{M}_d$, and we would need to appeal to state gravity/ensemble duality for a resolution.

So far, we have discussed the first and second holographic duality separately. We can also consider the one-step doubly holographic RT prescription of Eq. (2.34). This evaluates the entropy of the BCFT$_d$ region $\mathcal{R}_d$ directly in the M_{d+1} bulk as the area of γ_{d+1}; see Eq. (3.27). By "jumping" over the middle level, we have missed the paradox. Namely, the paradox involved the apparent discrepancy of the states in the region $\mathcal{R}_d$, depending on whether it is viewed as a state of the BCFT$_d$ or a state of the CFT$_d$ on $M_d \cup \mathcal{M}_d$. The CFT$_d$ is not present in the second holographic dual. It has now been replaced by the classical bulk state in M_{d+1}; thus we are no longer comparing two states of the same region.

Therefore, an ensemble interpretation is not required to make sense of the doubly holographic duality (2.29), so long as we never consider the intermediate level. Unfortunately, without the intermediate level $M_d \cup \mathcal{M}_d$, we also lose contact with the process of black hole evaporation, which is manifest only at this level.

3.4 Chapter Summary and Conclusion

In this chapter, we have discussed the seemingly contradictory use of Hawking's result for the radiation entropy in the calculations of Refs. [151, 16]. We called this puzzle the state paradox, and we considered several distinct settings in which it appears. In each case, we discussed its possible resolution by gravity/ensemble duality, the proposal that the gravitational path integral is dual to an appropriately defined ensemble of theories on the boundary.

In Section 3.1, we used the RT prescription in an AdS$_d$ bulk spacetime to derive the Page curve in the dual CFT$_{d-1}$ [47]. The setting is distinct from that of of Refs. [151, 16] in that there is no external bath or auxiliary system. The radiation remains in an AdS bulk and appears only on the right side of Eq. (1.6). The left hand side corresponds to the entropy of the CFT dual, for which a Page curve is obtained. The state paradox then arises in the CFT. The CFT entropy can also be computed as the von Neumann entropy of a CFT state constructed by applying the standard AdS/CFT extrapolate dictionary to the bulk. With this method, we found that the CFT entropy should grow monotonically. These results are consistent only if the CFT is actually an ensemble of CFTs.

In Section 3.2, we turned to the setting of Refs. [151, 16]. The gravitating spacetime is coupled to an auxiliary system without gravity, into which the Hawking radiation escapes. The entropy of the auxiliary system is computed using the extension of the RT prescription derived in Chapter 2. The radiation appears on both sides of Eq. (1.6), leading to the state paradox unless gravity/ensemble duality is invoked.

Several works [18, 167, 55, 12, 182, 21] have computed the Page curve using the entanglement wedge in a "doubly holographic" dual. The state paradox is somewhat obscured in this approach. To exhibit it, we used the deconstructed RT prescription for BCFTs as a repeated application of the original RT prescription, as discussed in Chapter 2. This allowed

us to shed light on a number of puzzling features in Refs. [18, 167, 55, 12, 182, 21]. We found that the state paradox arises at the first step, for the Hawking radiation that has escaped to the "auxiliary" CFT$_d$. At this level the paradox can be resolved by replacing (at least) the CFT$_{d-1}$ with an ensemble of such theories.

We found that the second level of holography furnished a bulk dual of the original state paradox. The RT prescription for braneworlds computes the entropy of subregions of the first holographic dual, in terms of bulk quantities in the second dual. Choosing the subregion to be just the radiation region, this reproduces Hawking's rising curve; choosing it to include the island as well, one again obtains the Page curve.

Finally, we observed that when the entropy of a top level CFT$_d$ region is computed directly using the squared RT prescription [188, 79], no paradox is manifest, because the $d+1$ bulk dual does not contain the radiation.

Having examined and proposed a resolution to the state paradox, we are now prepared to take another step in investigating what we can learn from the Page curve calculations: namely, how they apply to cosmology.

Chapter 4

Islands in Closed and Open Universes

The derivation of the Page curve via the Ryu-Takayanagi (Quantum Extremal Surface) prescription that we have discussed in the previous chapters comes on the heels of significant indirect evidence for the unitarity of black hole evaporation, most prominently via the AdS/CFT duality [134]. In these calculations, the QES formula manages to capture a highly nontrivial aspect of quantum gravity from a semiclassical analysis.

It is vital, therefore, to study the implications of these calculations in cosmological spacetimes, where we have no other handle on quantum gravity. A first objective in this direction is to understand whether islands can appear in cosmology. For an evaporating black hole, islands appear naturally when the QES formula is applied to the Hawking radiation. In cosmology, however, it is not clear a priori what process or setup should be considered: what would give rise to the large amounts of entanglement necessary for the formation of an island? What is the relevant reference system (the analogue of the Hawking radiation)?

One approach to this problem is not to require a natural dynamical origin for the entanglement. Instead, one can consider a simple cosmological solution and make assumptions about the entanglement structure that favor the existence of islands. If islands are absent even under favorable assumptions, this already constitutes an interesting finding.

In this spirit, Hartman *et al.* [95] searched for islands in a radiation-dominated, spatially flat Friedman-Robertson-Walker (FRW) spacetime M, entangled with a second nongravitating reference spacetime M_R, in a thermofield-double-like state. Instead of first specifying a reference system analogous to the Hawking radiation, Ref. [95] specified spherically symmetric candidate regions I on a Cauchy slice Σ_M of M and asked whether there *exists* a reference region R on a Cauchy slice Σ_R of M_R such that I is an island of R. (See [136, 59, 23] for other work on cosmological islands and thermofield-doubled universes.)

Hartman *et al.* found that no islands exist unless the cosmological constant is negative, $\Lambda < 0$. A flat FRW universe with $\Lambda < 0$ expands and then collapses, on a characteristic time scale of order $t_\Lambda \sim |\Lambda|^{-1/2}$. Islands are located in a narrow time band, of order the thermal timescale $\beta \ll t_\Lambda$, before and after the turnaround time; and they must be very large, with proper radius $\gg t_\Lambda$.

Ref. [95] considered only spatially flat FRW universes. In this chapter, we will relax this

Table 4.1: Summary of Results

Case	**Island Location(s)**
closed, $\Lambda > 0$	$I = M$
closed, $\Lambda = 0$	$I = M$
closed, $\Lambda < 0$	$I = M$; and if $t_\Lambda/t_C \lesssim (l_P/t_C)^{1/2} \ll 1$, then also $I \subsetneq \Sigma_M$, with comoving radius $\chi \in (\chi_*, \pi - \chi_*)$, near turnaround
open, $\Lambda \geq 0$	None
open, $\Lambda < 0$	$I \subsetneq \Sigma_M$, with $\chi > \chi^*$, near turnaround, if $t_\Lambda/t_C \lesssim (l_P/t_C)^{1/2} \ll 1$

assumption and search for islands in spatially closed and open FRW cosmologies. We will show that a small amount of spatial curvature can have a significant effect. Arbitrarily small positive curvature guarantees that the entire spacetime is an island. It also allows for a new class of islands consisting of more than half (but not all) of the universe. A small—but not arbitrarily small—amount of negative curvature eliminates cosmological islands entirely at fixed $\Lambda < 0$. Our results are summarized in Table 4.1.

4.1 Preliminaries

Quantum Extremal Surface Prescription

For ease of reference, we remind the reader of the Quantum Extremal Surface (or Ryu-Takayanagi) prescription for computing von Neumann entropies. The all-orders [75] quantum-corrected [78], covariant [108] Ryu-Takayanagi [169, 168] prescription computes the entropy of a nongravitating system R in terms of a dual spacetime with gravity, M, whose state and geometry are computed semiclassically:

$$S(\mathbf{R}) = S_{\text{gen}}[\text{EW}(R)] \ . \tag{4.1}$$

The bold-face notation [11] distinguishes the (presumably correct) entropy computed by the QES formula from the von Neumann entropy $S(R)$ computed directly from the semiclassical state. Here $\text{EW}(R)$ is the entanglement wedge and S_{gen} is its generalized entropy. We will now briefly summarize their definitions.

For a partial Cauchy surface $X \subset \Sigma_M$,

$$S_{\text{gen}}(X) = \frac{\text{Area}[\partial X]}{4G_N\hbar} + S(X) \ , \tag{4.2}$$

where $S(X)$ is the von Neumann entropy of the density operator of the quantum field theory state reduced to X. Both terms are cutoff-dependent, but their sum is well-defined (see the appendix in Ref. [48] for a detailed discussion).

$\mathrm{EW}(R)$ is a spacetime region whose generalized entropy is "extremal" (really, stationary) with respect to small shape deformations of its boundary surface in M, subject to certain homology and global minimality conditions. (Settings with highly incompressible quantum states require a more precise definition [6]. In doubly holographic settings, the appropriate homology rule must be chosen with care, as discussed in Chapter 2. Neither subtlety will arise here. The entanglement wedge is in general state-dependent; it is related through a choice of code subspace to the reconstructible wedge [102, 7], which is not. We implicitly assume a small code subspace in this work, so that we can neglect this distinction.)

Now let us specialize to the case where $R \subset \Sigma_R$ is a partial Cauchy surface in a nongravitating spacetime M_R distinct from M. Then the definition of $\mathrm{EW}(R)$ reduces to the "island rule" [18]:

1. $\mathrm{EW}(R) = I \cup R$, where $I \subset \Sigma_M$ and I is compact;[1]
2. $S_{\mathrm{gen}}(I \cup R)$ is stationary under any local variations of the boundary surface ∂I;
3. Among all such regions globally, I yields the smallest $S_{\mathrm{gen}}(I \cup R)$.

Note that $I = \varnothing$ is allowed.

For example, suppose that M_R is coupled to M, and that R contains the Hawking radiation emitted by an evaporating black hole prior to the time t [151, 16]. (R could also be a weakly gravitating distant region containing the radiation [47].) In the semiclassical approximation, the radiation is thermal [100]. Its entropy $S(R(t))$ increases monotonically, implying information loss [99]. However, after the Page time, the entanglement wedge $\mathrm{EW}(R)$ includes an island $I \neq \varnothing$ that purifies the radiation [151, 16]. The island is the black hole interior slightly before the most recent radiation in R was emitted. Thus, $S_{\mathrm{gen}}[\mathrm{EW}(R)]$ is dominated by the area term $A[\partial I]/4G_N$, which decreases as the black hole shrinks.

Four Necessary Conditions for Islands

A nonempty island I must satisfy four conditions that do not depend on R. We will begin by deriving the first three, following Ref. [95]. Since $I \neq \varnothing$, we have

$$S(R) > S_{\mathrm{gen}}(I \cup R) = \frac{A(\partial I)}{4G_N} + S(I \cup R) \geq \frac{A(\partial I)}{4G_N} + S(R) - S(I) \tag{4.3}$$

by subadditivity of the von Neumann entropy; hence

$$S(I) > \frac{A(\partial I)}{4G_N} \ . \quad \text{(Condition 1)} \tag{4.4}$$

[1] More precisely, the homology rule requires that in the conformally compactified spacetime, the boundary of the image of I does not intersect with the conformal boundary of M.

By assumption, $I \cup R$ is quantum extremal, *i.e.*, $S_{\text{gen}}(I \cup R)$ is stationary under shape deformations of ∂I. The area contribution to this variation does not change when we consider $S_{\text{gen}}(I)$ instead; and by strong subadditivity, the shape derivative of the von Neumann entropy in the past or future directions outward from I can only increase when R is dropped [48]. Hence it must be non-negative:

$$I \text{ is quantum normal.} \quad \text{(Condition 2)} \tag{4.5}$$

We will take the global quantum state on $\Sigma_M \cup \Sigma_R$ to be pure. (This can always be arranged by adding a purifying auxiliary system to M_R.) Hence $G \cup Q$ is also quantum extremal, where $G \equiv \Sigma_M \backslash I$ and $Q \equiv \Sigma_R \backslash R$. The above argument implies that

$$G \text{ is quantum normal.} \quad \text{(Condition 3)} \tag{4.6}$$

M always satisfies extremality. However, it satisfies the homology condition only if its Cauchy surfaces are closed. For a proper subset $I \subsetneq \Sigma_M$ to be an island, in this case, it must be a better candidate than the whole of M:

$$S_{\text{gen}}(M \cup R) > S_{\text{gen}}(I \cup R) \ . \tag{4.7}$$

Since M is spatially closed, $S_{\text{gen}}(M \cup R) = S(M \cup R)$, and Eq. (4.7) implies

$$S(I \cup R) + \frac{A(\partial I)}{4G_N} < S(M \cup R) \leq S(G) + S(I \cup R) \tag{4.8}$$

by subadditivity of the von Neumann entropy. Hence we find a fourth condition:

$$\text{For spatially closed } M \text{ and } I \subsetneq \Sigma_M \ : \quad S(G) > \frac{A(\partial I)}{4G_N} \ . \quad \text{(Condition 4)} \tag{4.9}$$

Thermofield-doubled FRW Universes

In the next two sections, we shall search for islands in cosmological spacetimes. We will consider a spatially homogeneous and isotropic universe M in 4 dimensions with positive or negative spatial curvature, thermal radiation, and arbitrary cosmological constant Λ. The metric is

$$ds^2 = -dt^2 + a(t)^2 \left(d\chi^2 + f^2(\chi) d\Omega^2 \right) \ , \tag{4.10}$$

where $a(t)$ is the scale factor. The function $f(\chi)$ depends on the curvature: $f(\chi) = \sinh(\chi), \chi,$ or $\sin(\chi)$ for open, flat, and closed universes respectively. Another convenient coordinate system uses conformal time η, defined via

$$d\eta = \frac{dt}{a(t)} \ . \tag{4.11}$$

In these coordinates, the FRW metric takes the form

$$ds^2 = a^2(\eta)\left(-d\eta^2 + d\chi^2 + f^2(\chi)d\Omega^2\right). \tag{4.12}$$

The scale factor $a(t)$ obeys the Friedmann equation:

$$\left(\frac{\dot{a}}{a}\right)^2 = \frac{8\pi G_N \rho_r}{3} + \frac{\Lambda}{3} - \frac{k}{a^2}\ , \tag{4.13}$$

where ρ_r is the energy density of radiation and Λ is the cosmological constant.

We will mainly be interested in universes with an initial curvature singularity (a big bang). Solutions with a big crunch but no big bang are trivially related by time-reversal. Radiation redshifts as $\rho_r \propto a^{-4}$, so its energy density will dominate near the big bang, *i.e.*, at sufficiently early times.

The cosmological constant will come to dominate the evolution within a time of order

$$t_\Lambda \equiv \sqrt{3/|\Lambda|} \tag{4.14}$$

after the big bang, if the universe reaches this age.

At the time

$$t_C \equiv \left(\frac{8\pi G_N \rho_r a^4}{3}\right)^{1/2}\ , \tag{4.15}$$

after the big bang, the curvature term in the Friedmann equation begins to dominate over the radiation term. If the universe reaches this age, and if $t_C < t_\Lambda$, a curvature-dominated era begins at t_C and ends at t_Λ. For recollapsing solutions, the same sequence happens in reverse after the turnaround time.

Solutions without a singularity arise only if the cosmological constant and curvature are both positive and the radiation density at the turnaround time is sufficiently small. Then the above definitions can be still be made, but they do not have the stated physical interpretation. Moreover, t_C and t_Λ do not fix a solution uniquely. Hence we will use a different parametrization of solutions in Section 4.2.

It will be convenient to express the Friedmann equation in terms of t_C and t_Λ:

$$\left(\frac{\dot{a}}{a}\right)^2 = \frac{t_C^2}{a^4} \pm \frac{1}{t_\Lambda^2} - \frac{k}{a^2}\ . \tag{4.16}$$

The $\pm$ corresponds to the sign of Λ.

Throughout this chapter we shall assume that the effective number of light fields is of order unity. (It is easy to generalize to a larger number of fields, and strictly it is necessary to do so in order to justify neglecting the contribution of gravitons to the entropy. But increasing the number of radiation species does not lead to new regimes in our analysis, while it does complicate the formulas.) Then the physical entropy density of the thermal radiation is

$$s \sim \rho_r^{3/4}\ , \tag{4.17}$$

and the comoving entropy density is

$$s_c \equiv sa^3 \sim \left(\frac{t_C}{l_P}\right)^{3/2} , \tag{4.18}$$

where $l_P \equiv G_N^{1/2}$ is the Planck length.

Following Ref. [95], we purify the thermal radiation by invoking a second, nongravitating spacetime M_R and constructing a thermofield double. M_R is defined up to conformal transformations; here we choose

$$ds_R^2/\ell^2 = -d\eta_R^2 + d\chi_R^2 + f^2(\chi_R)d\Omega_R^2 , \tag{4.19}$$

where ℓ is an arbitrary fixed length scale. The thermofield double is first constructed using two copies of M_R:

$$|\mathrm{TFD}\rangle \propto \sum_n e^{-\beta E_n} |n\rangle_1^* |n\rangle_2 \ ; \tag{4.20}$$

then a conformal transformation by a^2 is applied to transform one copy to M. Here $\beta = \ell/(aT)$, where T is the radiation temperature in the physical spacetime M at scale factor a. Our convention for the respective time orientations is opposite to that of Ref. [96]; see Refs. [95] for further details.

We note an important property of the thermofield double which will be useful below. For regions $I \subset \Sigma_M$ and $R \subset \Sigma_R$ with equal coordinate position, the renormalized[2] entropy of $I \cup R$ is small and increases when I and R are separated in time at fixed comoving size. It also increases if the size of either I or R is increased or decreased at fixed time:

$$S(I \cup R) \approx s_c |\Delta V_c| , \tag{4.21}$$

where $\Delta V_c = V_c^R - V_c^I$, and V_c denotes comoving volume (*i.e.*, $V_c^R = V(R)/\ell^3$ and $V_c^I = V(I)/a^3$). The sharp transition in Eq. (4.21) when I and R coincide is smoothed on the thermal scale β [95].

General Analysis and Restriction to Time-Symmetric Slices

For each class of universes, we will search for spherical[3] islands by checking the four necessary conditions laid out in Section 4.1. This check is performed using solutions for the full spacetime, and the results are displayed in plots showing where each condition is satisfied.

[2]The entropy of bounded regions in QFT has universal short-distance divergences that can be stripped off so long as the characteristic wavelength of excitations is greater than the Planck scale. In this chapter, we only consider regions that are under semiclassical control, $(a/\ell)\beta \gg l_P$.

[3]If I is a spherical island of the region R, then one expects that deformations of R will still have an island that is a small deformation of I. Area is "expensive" so generally I will deviate less from spherical symmetry than R. Our analysis does not rule out the existence of different classes of islands that are not approximately spherical.

The solutions for the full spacetime are relatively complicated. In order to develop some intuition, we precede each full analysis by searching for islands only on time-symmetric slices. Ultimately, this where we expect to find islands, because quantum extremality is difficult to satisfy when the universe is expanding or contracting.

Quantum extremality requires that the classical expansion is compensated by the time-derivative of the renormalized entropy at fixed χ. This is possible if the classical expansion is itself very small, of order G, *i.e.*, in a small time interval around the turn-around time. In the spatially flat case, the size of this interval is of order β [95]. The same conclusion applies to open and closed universes: as we shall see below, curvature is dynamically negligible at the turnaround time in all cases where we find islands at that time.

On time-symmetric slices, the necessary conditions of Section 4.1 take a special form. The scale factor at the turnaround time, a_0, is found by setting $\dot{a} = 0$ in Eq. (4.16). Then the conditions become

$$s_c V_c(\chi) \geq \frac{a_0^2 A_c(\chi)}{4l_P^2} \qquad \text{(Condition 1)} \tag{4.22}$$

$$\frac{\partial}{\partial \chi} S_{\text{gen}}[I(\chi)] \geq 0 \qquad \text{(Condition 2)} \tag{4.23}$$

$$-\frac{\partial}{\partial \chi} S_{\text{gen}}[G(\chi)] \geq 0 \qquad \text{(Condition 3)} \tag{4.24}$$

$$s_c \left(V_c^{\text{tot}} - V_c(\chi)\right) \geq \frac{a_0^2 A_c(\chi)}{4l_P^2} \qquad \text{(Condition 4)} \tag{4.25}$$

for a spherical island candidate of radius χ. Here V_c^{tot} is the comoving volume of the entire closed universe at the turnaround time, and

$$S_{\text{gen}} = s_c V_c(\chi) + \frac{A(\chi)}{4G_N} \ . \tag{4.26}$$

In the next two sections, we will analyze the closed and open cases, respectively. We will examine whether the necessary conditions can be satisfied, and if so, we will check whether they are sufficient.

4.2 Closed Universes

In this section, we consider solutions with positive spatial curvature (closed FRW). In such a geometry, the coming volume and area functions on the unit three-sphere are

$$V_c = \pi(2\chi - \sin 2\chi) \ , \tag{4.27}$$

$$A_c = 4\pi \sin^2 \chi \ . \tag{4.28}$$

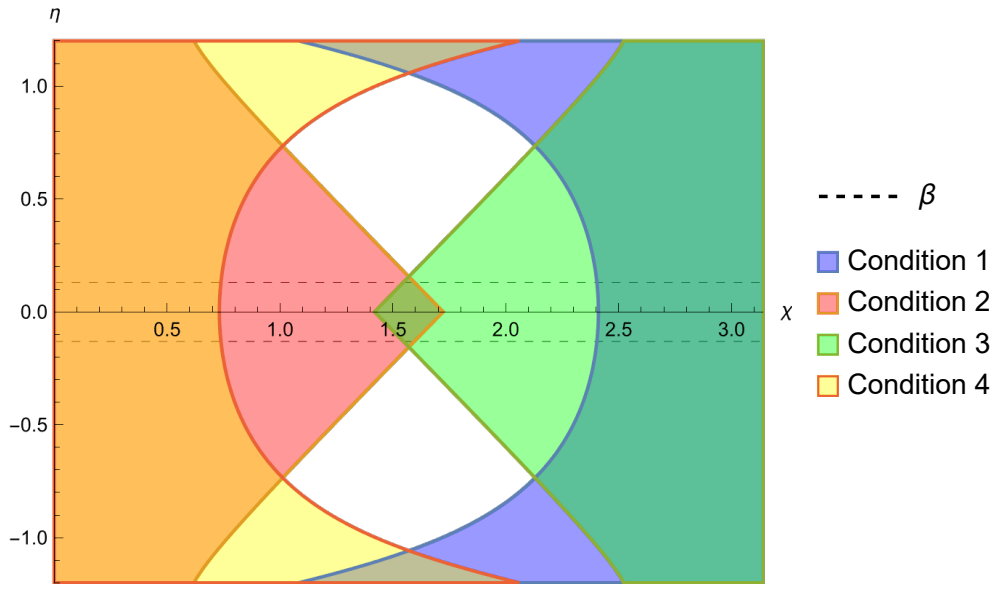

Figure 4.1: Regions satisfying the four island conditions are shown for a closed universe with $\Lambda = 0$. The radiation temperature is β^{-1} at the turnaround time $t = \eta = 0$. Chosen for display is $t_C = 170 t_P$. Top and bottom cutoffs are chosen so as to eliminate artifacts of the Planck regime near the big bang and big crunch. The lack of four-way overlap shows that no region satisfies all four conditions, so there cannot be any islands.

Positive Curvature, Zero Cosmological Constant

The first closed universe we consider is the simplest: one with $\Lambda = 0$. We begin our search for islands by restricting our attention to the time-symmetric slice. We consider spherically symmetric regions, $I(\chi)$, which extend from the origin to the sphere at χ at the turnaround time. For $\Lambda = 0$ and $k = 1$, the scale factor at the turnaround time satisfies

$$0 = \frac{t_C^2}{a_0^4} - \frac{1}{a_0^2} \tag{4.29}$$

by Eq. (4.16). Hence

$$a_0 = t_C \ . \tag{4.30}$$

Since the universe is closed, we can consider either the entire universe M, or a proper subset $I(\chi)$, $\chi < \pi$, of its time-symmetric slice, as an island candidate. We begin by ruling out the latter, by showing that conditions 1 and 4 are mutually incompatible.

Condition 1 is that the radiation entropy in I exceed the Bekenstein-Hawking entropy of the boundary. Using the time-symmetric version of condition 1, Eq. (4.22), and Eq. (4.18),

this becomes

$$\left(\frac{t_C}{l_P}\right)^{3/2} V_c \gtrsim \frac{t_C^2 A_c(\chi)}{l_P^2} \ , \tag{4.31}$$

which is equivalent to

$$\frac{V_c(\chi)}{A_c(\chi)} \gtrsim \left(\frac{t_C}{l_P}\right)^{1/2} \ . \tag{4.32}$$

The ratio of comoving volume to area is of order χ for small χ and grows monotonically, diverging as $\chi \to \pi$. We are only interested in the semiclassical regime,

$$\frac{t_C}{l_P} \gg 1 \ . \tag{4.33}$$

Thus condition 1 requires $\pi - \chi \ll 1$; that is, the island must be nearly the whole universe. In this regime,

$$\frac{V_c}{A_c} \approx \frac{2\pi^2}{4\pi(\pi-\chi)^2} = \frac{\pi}{2(\pi-\chi)^2} \ . \tag{4.34}$$

and condition 1 becomes

$$\pi - \chi \lesssim \left(\frac{l_P}{t_C}\right)^{1/4} \ , \tag{4.35}$$

Condition 4 requires that the radiation entropy in G, the complement of I in M, should also exceed the Bekenstein-Hawking entropy of its boundary. Hence G must also consist of nearly the entire time-symmetric slice. But this contradicts the definition of G: G and I cannot be mutual complements and both consist of nearly all of Σ_M. Since the necessary conditions 1 and 4 cannot be simultaneously satisfied, no proper subset of the time-symmetric slice can be an island.

To check that the restriction to the time-symmetric slice did not miss viable island candidates, we examine the full solution. The scale factor is:

$$a(\eta) = t_C \cos(\eta) \ , \tag{4.36}$$

with the turnaround time set at $\eta = 0$. Figure 4.1 shows the regions in which the four conditions are satisfied. As expected, there is no region of four-way overlap. Therefore, no proper subset of a closed universe with $\Lambda = 0$ can be an island.

Next, we turn to M itself as an island candidate. M trivially satisfies all necessary conditions, since it has no boundary. But for M to be an island, it must beat the empty set; we require $S(R \cup M) < S(R)$. Since $S(R \cup M) \approx s_c[V_c(\Sigma_R) - V_c(R)]$, M is an island of R if and only if R is more than half of Σ_R.

Positive Curvature, Negative Cosmological Constant

Now we consider closed universes with $\Lambda < 0$. As before, we begin with a restriction to time-symmetric slices. If $t_\Lambda \gg t_C$, then Λ is insignificant at the turnaround time. Then Λ

never plays a dynamical role, and we expect the results to be the same as the $\Lambda = 0$ case. Thus, we will consider the regime

$$t_\Lambda \lesssim t_C \ . \tag{4.37}$$

By Eq. (4.16), the scale factor satisfies

$$0 = \frac{t_C^2}{a_0^4} - \frac{1}{t_\Lambda^2} - \frac{1}{a_0^2} \tag{4.38}$$

at the turnaround time, so with Eq. (4.37) we find

$$a_0 \sim \sqrt{t_\Lambda t_C} \ . \tag{4.39}$$

Consider first a proper subset of the universe as the island candidate: $I(\chi)$ with $\chi < \pi$. Condition 1 was given in Eq. (4.22). Substituting the above expression for a_0 we find

$$\frac{V_c(\chi)}{A_c(\chi)} > \alpha \sim \left(\frac{t_\Lambda}{t_C}\right)\left(\frac{t_C}{l_P}\right)^{1/2} \ , \tag{4.40}$$

where we have defined the combination of parameters α for later convenience.

Condition 4 yields the same inequality with $\chi \to \pi - \chi$. Since V_c/A_c is monotonic in χ, conditions 1 and 4 can be satisfied simultaneously only if

$$\alpha < \frac{V_c(\pi/2)}{A_c(\pi/2)} = \frac{\pi}{4} \ . \tag{4.41}$$

Hence we require

$$\frac{t_\Lambda}{t_C} \lesssim \left(\frac{l_P}{t_C}\right)^{1/2} \ll 1 \ , \tag{4.42}$$

where the second inequality is the condition for a classical solution. Note that this conclusion disallows $t_\Lambda \sim t_C$ and hence is stronger than Eq. (4.37).

In the regime characterized by Eq. (4.42), solving Eq. (4.40) as an equality yields a critical value $\chi_1 < \pi$ such that the inequality (4.40) will be satisfied for all $\chi > \chi_1$. Hence, conditions 1 and 4 will be simultaneously satisfied for

$$\chi_1 < \chi < \pi - \chi_1 \ . \tag{4.43}$$

In the limit as $\alpha \ll 1$, one finds $\chi_1 \sim \alpha$.

We turn to conditions 2 and 3. Condition 2 is the requirement that the island be quantum normal. Using the time-symmetric version of condition 2, Eq. (4.23), and Eqs. (4.18), (4.27), (4.28), and (4.39) we find

$$\cot(\chi) \gtrsim -\alpha^{-1} \ . \tag{4.44}$$

Note that the cotangent monotonically decreases in the range $\chi \in (0, \pi)$ and becomes negative for $\chi > \pi/2$. In the regime where conditions 1 and 4 can be satisfied, the magnitude

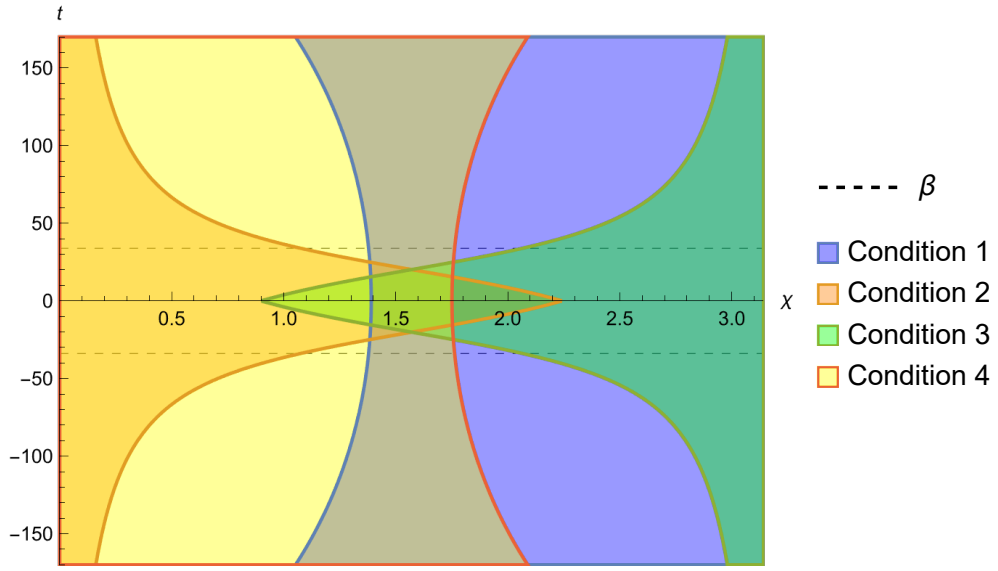

Figure 4.2: Island conditions in a closed universe with $\Lambda < 0$, $t_C \gg t_\Lambda$. Chosen for display is $t_C = 25000 t_P$, $t_\Lambda = 400 t_P$. All conditions overlap in a region centered on the equator with temporal width of order β around the turnaround time. We verify explicitly that any region at $t = 0$ whose only boundary lies in this overlap is an island.

of the right hand side is at least of order unity by Eq. (4.41). Hence, the above condition corresponds to

$$0 < \chi < \pi - \chi_2 \ , \tag{4.45}$$

where

$$\chi_2 < \frac{\pi}{2} \text{ and } \frac{\pi}{2} - \chi_2 \sim O(1) \ . \tag{4.46}$$

Condition 3 mandates that G (the complement of I) be quantum normal; by symmetry, this results in the condition

$$\chi_2 < \chi < \pi \ . \tag{4.47}$$

Hence, assuming that conditions 1 and 4 are satisfied, then conditions 2 and 3 will be simultaneously satisfied for

$$\chi_2 < \chi < \pi - \chi_2 \ . \tag{4.48}$$

In the regime where $\alpha \ll 1$, Eq. (4.44) implies $\chi_2 \sim \alpha$.

To summarize, for a subset of the time-symmetric slice to be an island, we require that

$$\chi_* < \chi < \pi - \chi_* \ , \tag{4.49}$$

where

$$\chi_* \equiv \max\{\chi_1, \chi_2\} \ . \tag{4.50}$$

Importantly, for the conditions 1 and 4 to be simultaneously satisfied, *i.e.*, for the range (4.43) to be nonempty, we found that Eq. (4.42) must be satisfied: $\alpha < \pi/4$. This means that curvature must be dynamically negligible at the turnaround time.

Near the critical value $\alpha = \pi/4$, χ_1 will be close to $\pi/2$ whereas $\pi/2 - \chi_2 \sim O(1)$, so $\chi_* = \chi_1$; that is, conditions 1 and 4 are the more stringent. For $\alpha \ll 1$, χ_1 and χ_2 are both of order α. A careful analysis keeping O(1) factors shows that $\chi_* = \chi_1$ for all α, meaning that conditions 1 and 4 are always more stringent than 2 and 3 at the turnaround time. Thus, to be an island, a subset of the time-symmetric slice must obey

$$\chi_1 < \chi < \pi - \chi_1 \ . \tag{4.51}$$

Next we examine the full spacetime. The scale factor is

$$a(t) = t_\Lambda \sqrt{\frac{1}{2}\left(\sqrt{1 + \frac{4t_C^2}{t_\Lambda^2}}\cos\left(\frac{2t}{t_\Lambda}\right) - 1\right)} \ , \tag{4.52}$$

with the turnaround time set to $t = 0$. Figure 4.2 shows a check of the four conditions with $t_C \gg t_\Lambda$. As expected from the time-symmetric analysis, the four conditions overlap only in a region centered on the equator with temporal width of order β around the turnaround time. (It is worth noting that far from the turnaround time, Conditions 1 and 4 are not always more stringent that conditions 2 and 3.) A check of the full solution with $t_C \sim t_\Lambda$ confirms that there are no islands in that regime.

While we have only verified four necessary conditions, it is easy to check that at the turnaround time, $I(\chi)$ in the range $\chi_1 < \chi < \pi - \chi_1$ is indeed an island of a region R of equal size and location on Σ_R.

Since we found that curvature must be dynamically negligible at the turnaround time for an island $I(\chi)$ to exist, we should be able to make contact with Ref. [95], which found that on the time-symmetric slice of a flat FRW universe with $\Lambda < 0$, any $I(r)$ with proper area radius $r \gtrsim t_\Lambda^{3/2}/l_P^{1/2}$ is an island. Indeed, in a closed universe, the proper area radius of the minimum island at the turnaround time is

$$r = a_0 \sin\chi_* \sim a_0\chi_* \sim (t_C t_\Lambda)^{1/2}\,\frac{t_\Lambda}{t_C}\left(\frac{t_C}{l_P}\right)^{1/2} = \frac{t_\Lambda^{3/2}}{l_P^{1/2}} \ . \tag{4.53}$$

As expected the curvature timescale drops out, and we recover the flat FRW result.

However, there is an important difference: in a flat universe there is no maximum island size. In a closed universe, there is; and it is not the trivial upper bound $\chi = \pi$, because condition 4 becomes violated already for smaller values of χ. For $\chi_R > \chi_1$, at $t = 0$, the favored island becomes the entire universe M. This is sensible: although curvature has no dynamical effect on the evolution of the universe at the turnaround time, it does affect the kinematics (the topology of space), and the island rule is sensitive to both.

As before, M itself trivially satisfies conditions 1–3, meaning it is a viable island candidate. Let us check when M is in fact an island for some region $R \subset \Sigma_R$. As in the $\Lambda = 0$

case, R must be more than half of Σ_R for $R \cup M$ to have less entropy than R, *i.e.*, for M to be preferred over the empty set. Now, however, M must also compete with its own subsets. M wins if and only if condition 4 is violated, *i.e.* if

$$\chi_R > \pi - \chi_1 \ . \tag{4.54}$$

Since $\chi_1 < \pi/2$, this is the only relevant condition.

Positive Curvature, Positive Cosmological Constant

Let us examine the case where both the cosmological constant and the curvature are positive. As before, we start by finding the scale factor at the turnaround time. In this case, it will be more convenient to work with the Friedmann equation in terms of ρ_r, Eq. (4.13). Setting $k = +1$ and $\dot{a} = 0$ implies that the scale factor at the turnaround time is

$$a_0 = \left(\frac{8\pi G_N \rho_r}{3} + \frac{\Lambda}{3} \right)^{-1/2} \ . \tag{4.55}$$

First let us consider islands that are a proper subset of the closed universe, *i.e.* $I(\chi)$ with $\chi < \pi$. Using the fact that $s \sim \rho_r^{3/4}$ and so $s_c \sim \rho_r^{3/4} a^3$, condition 1 becomes

$$\frac{V_c(\chi)}{A_c(\chi)} \geq \frac{1}{4\rho_r^{3/4} a_0 l_P^2} \ , \tag{4.56}$$

and condition 4 yields the same inequality with $(\chi \to \pi - \chi)$. As before, the fact that V_c/A_c is monotonic in χ implies that an island candidate can satisfy conditions 1 and 4 simultaneously only if

$$\frac{1}{4\rho_r^{3/4} a_0 l_P^2} < \frac{V_c(\pi/2)}{A_c(\pi/2)} = \frac{\pi}{4} \ . \tag{4.57}$$

First consider the case where the radiation density dominates at turnaround, $G_N \rho_r \gg \Lambda$. In this regime,

$$a_0 \sim \frac{1}{\sqrt{G_N \rho_r}} = \frac{1}{\rho_r^{1/2} l_P} \ , \tag{4.58}$$

and Eq. (4.57) becomes

$$\frac{1}{\rho_r^{1/4}} \lesssim l_P \ . \tag{4.59}$$

But the semiclassical regime requires $a_0 \gg l_P$ and hence

$$\frac{1}{\rho_r^{1/4}} \gg l_P \ . \tag{4.60}$$

Since these equations are mutually incompatible, conditions 1 and 4 cannot be simultaneously satisfied.

Next, consider the opposite regime where vacuum energy dominates at turnaround, $\Lambda \gg G_N \rho_r$. Then

$$a_0 \sim \frac{1}{\sqrt{\Lambda}} \sim t_\Lambda \ , \tag{4.61}$$

and Eq. (4.57) becomes

$$\sqrt{\frac{\Lambda}{\rho_r G_N}} \left(\frac{1}{\sqrt{G_N} \rho_r^{1/4}} \right) \lesssim 1 \ . \tag{4.62}$$

The first factor is large by assumption, and the second is large since ρ_r cannot approach the Planck density. Hence, this inequality cannot be satisfied for $\Lambda \gg G_N \rho_r$ in the semiclassical regime. It is easy to verify that the problem persists in the intermediate regime $\Lambda \sim G_N \rho_r$. Thus we have shown (within the parameters of our model) that no proper subset of a time-symmetric slice of a closed universe with positive cosmological constant can be an island.

Next we examine the full spacetime. The scale factor can take one of three forms:

$$a(t) = t_\Lambda \sqrt{\frac{1}{2} \left(1 - \cosh\left(\frac{2t}{t_\Lambda}\right) + \frac{2t_C}{t_\Lambda} \sinh\left(\frac{2t}{t_\Lambda}\right) \right)} \qquad \text{(expansion)} \tag{4.63}$$

$$a(t) = t_\Lambda \sqrt{\frac{1}{2} \left(1 - \cosh\left(\frac{2t}{t_\Lambda}\right) \sqrt{1 - \frac{4t_C^2}{t_\Lambda^2}} \right)} \qquad \text{(recollapse)} \tag{4.64}$$

$$a(t) = t_\Lambda \sqrt{\frac{1}{2} \left(1 + \frac{1 - \xi t_\Lambda^2}{1 + \xi t_\Lambda^2} \cosh\left(\frac{2t}{t_\Lambda}\right) \right)} \qquad \text{(bounce)} \tag{4.65}$$

where $\xi \equiv 8\pi G_N \rho_r(0)/3$. Eq. (4.63) describes a universe with a big bang at $t = 0$ which expands eternally if $t_C/t_\Lambda > 1/2$ or recollapses if $t_C/t_\Lambda < 1/2$. Eq. (4.64) is the same solution as Eq. (4.63) but defined only for $t_C/t_\Lambda < 1/2$ with the turnaround time set to $t = 0$. Eq. (4.65) describes a universe that bounces (the scale factor reaches a minimum) at $t = 0$.

The expanding solution has no turnaround time, and a check of the four conditions (Figure 4.3) confirms that there is no region of four-way overlap in its regime ($t_C \gtrsim t_\Lambda$). The recollapsing solution appears qualitatively like the $\Lambda = 0$ case and similarly disallows islands. The bounce solution also has no region of four-way overlap (Figure 4.4).

As in the $\Lambda \leq 0$ cases, the entire closed universe M satisfies all necessary conditions. M will be an island when R is more than half of Σ_R.

4.3 Open Universes

Next we search for islands in universes with negative spatial curvature (open FRW). As before, we start with time-symmetric slices. By Eq. (4.16), none exist for $\Lambda \geq 0$, so we shall take $\Lambda < 0$.

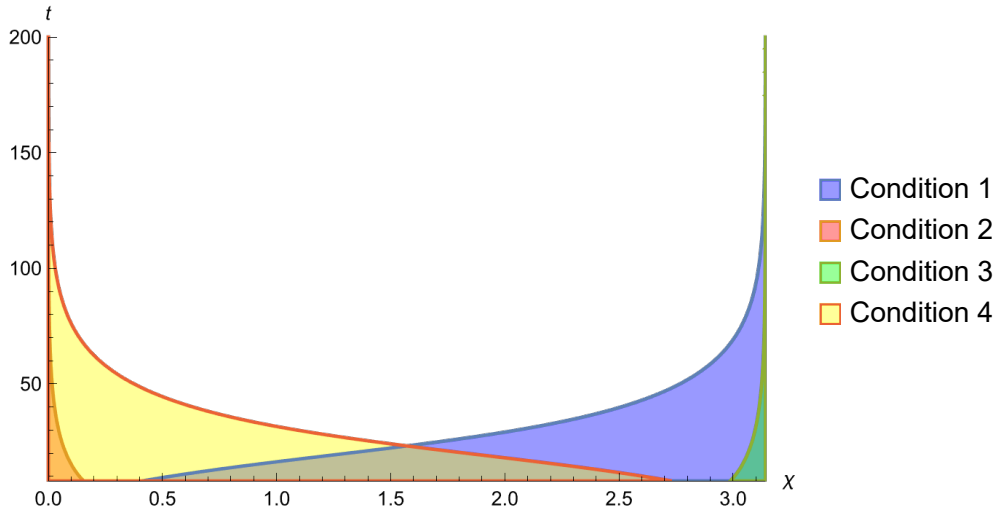

Figure 4.3: Island conditions in a closed universe with $\Lambda > 0$, $t_C \gg t_\Lambda$. Chosen for display is $t_C = 1000t_P$, $t_\Lambda = 20t_P$. Such a universe expands eternally and thus has no time-symmetric slice. There is no region in which all four conditions are satisfied, meaning there cannot be islands.

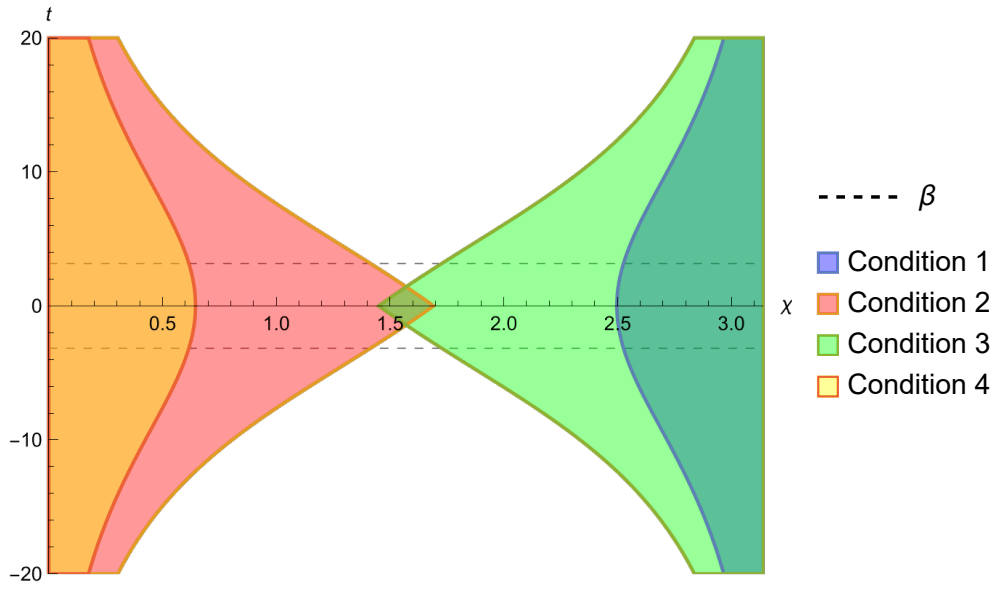

Figure 4.4: Regions satisfying the four island conditions for a closed universe with $\Lambda > 0$ that bounces at $t = 0$. The radiation temperature is β^{-1} at the turnaround time $t = 0$. Chosen for display is $\xi = 0.084t_P^{-2}$, $t_\Lambda = 10t_P$. There is no region of four-way overlap, so there cannot be islands.

The comoving volume and area of a spherical region of coordinate radius χ are

$$V_c(\chi) = \pi(\sinh(2\chi) - 2\chi) \ , \tag{4.66}$$

$$A_c(\chi) = 4\pi \sinh^2(\chi) \ . \tag{4.67}$$

Hence

$$\frac{V_c}{A_c} \leq \frac{1}{2} \ . \tag{4.68}$$

We begin by ruling out islands in the regime $t_\Lambda/t_C \gtrsim 1$. The scale factor at the turnaround time will be

$$a \sim t_\Lambda \ . \tag{4.69}$$

Using Eqs. (4.18) and (4.22), condition 1 becomes

$$\frac{V_c(\chi)}{A_c(\chi)} \gtrsim \left(\frac{t_\Lambda}{t_C}\right)^2 \left(\frac{t_C}{l_P}\right)^{1/2} \ . \tag{4.70}$$

The semiclassical regime requires that $t_C/l_P \gg 1$, and we are currently working in the regime $t_\Lambda/t_C \gtrsim 1$, so the r.h.s. is large. This conflicts with Eq. (4.68), so condition 1 cannot be satisfied.

Now consider the complementary regime, $t_\Lambda/t_C \ll 1$. The scale factor at the turnaround time is

$$a_0 \sim \sqrt{t_\Lambda t_C} \ , \tag{4.71}$$

and condition 1 becomes

$$\frac{V_c(\chi)}{A_c(\chi)} \geq \gamma \sim \left(\frac{t_\Lambda}{t_C}\right) \left(\frac{t_C}{l_P}\right)^{1/2} \ . \tag{4.72}$$

By Eq. (4.68), this condition can be satisfied only if $\gamma < 1/2$. This implies

$$\left(\frac{t_\Lambda}{t_C}\right) \lesssim \left(\frac{l_P}{t_C}\right)^{1/2} \ll 1 \ , \tag{4.73}$$

where the second inequality is required for a semiclassical solution. Solving (4.72) as an equality yields a critical value χ_3 such that condition 1 is satisfied for all $\chi > \chi_3$. Therefore, condition 1 can be satisfied for a spherical island candidate with large enough χ at the turnaround time if t_Λ is early enough.

Since it is possible to satisfy condition 1, we move on to conditions 2 and 3, equations (4.23) and (4.24). (Condition 4 only applies to subsets of closed universes.) Applying the quantum-normalcy conditions to I and its complement G yields, respectively,

$$\coth\chi \gtrsim -\gamma^{-1} \ , \quad \text{(Condition 2)} \tag{4.74}$$

$$\coth\chi \lesssim \gamma^{-1} \ . \quad \text{(Condition 3)} \tag{4.75}$$

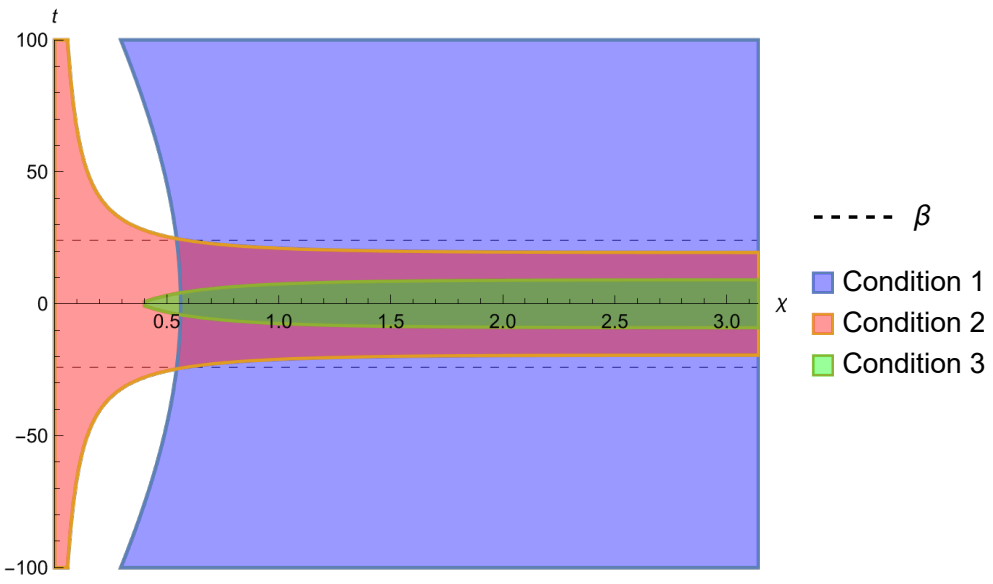

Figure 4.5: Island conditions in an open universe with $\Lambda < 0$, $t_C \gg t_\Lambda$. Chosen for display is $t_C = 77500 t_P$, $t_\Lambda = 200 t_P$. All conditions overlap only in a region with temporal width of order β around the turnaround time for large enough χ. We verify explicitly that any region at $t = 0$ whose only boundary lies in this overlap is an island.

Condition 2 is satisfied for any χ. Condition 3 can only be satisfied if $\gamma < 1$, but we already obtained the stronger restriction $\gamma < 1/2$ from condition 1.

Solving (4.75) as an equality yields a critical radius χ_4, such that all $\chi > \chi_4$ satisfy condition 3. Thus, to be an island, the region must satisfy

$$\chi^* < \chi < \pi - \chi^* \,, \tag{4.76}$$

where

$$\chi^* \equiv \max\{\chi_3, \chi_4\} \,. \tag{4.77}$$

As in Section 4.2, a careful analysis keeping $O(1)$ factors indicates that $\chi_3 > \chi_4$ for all $\gamma < 1/2$ at turnaround. Thus, condition 1 is always more stringent that condition 3 at the turnaround time.

Having completed our analysis of the time-symmetric slice, we check the full spacetime.

The forms of the scale factor are

$$(\Lambda = 0) \qquad a(\eta) = t_C \sinh \eta \tag{4.78}$$

$$(\Lambda > 0) \qquad a(t) = t_\Lambda \sqrt{\sinh\left(\frac{t}{t_\Lambda}\right)\left(\frac{2t_C}{t_\Lambda}\cosh\left(\frac{t}{t_\Lambda}\right) + \sinh\left(\frac{t}{t_\Lambda}\right)\right)} \tag{4.79}$$

$$(\Lambda < 0) \qquad a(t) = t_\Lambda \sqrt{\frac{1}{2}\left(\sqrt{1 + \frac{4t_C^2}{t_\Lambda^2}}\cos\left(\frac{2t}{t_\Lambda}\right) + 1\right)} \,. \tag{4.80}$$

Eqs. (4.78) and (4.79) describe universes that expand eternally and thus have no time symmetric slice. As expected, these two cases disallow islands. Universes described by Eq. (4.80) do recollapse, and in the regime $t_C \gg t_\Lambda$ all three conditions overlap only for large enough χ in a region with width of order β around the turnaround time (Figure 4.5). Checking the regime $t_\Lambda \gtrsim t_C$ confirms that no islands are possible in that case.

To summarize, in an open universe with $\Lambda < 0$, spherical regions with $\chi > \chi_3$ satisfy all necessary island conditions if $\gamma < 1/2$, where γ is given in Eq. (4.72). This corresponds to a universe in which curvature never dominates since $t_\Lambda/t_C \ll 1$; in fact, curvature cannot dominate even on the scale of the minimum island size. It is easy to verify that these candidates are in fact islands at $t = 0$, if R is chosen to be the matching region on Σ_R.

4.4 Chapter Summary and Conclusion

In this chapter, we searched for islands in cosmologies with nonzero spatial curvature. In Section 4.1 we stated again the QES prescription and its special case, the island formula. We discussed three necessary conditions that an island I must satisfy [95] regardless of the reference system R: $S(I) > A(\partial I)/4G_N$; I is quantum normal; and G is quantum normal, where G is the complement of I on a Cauchy slice Σ_M of M. We derived a fourth necessary condition that applies only if M is closed and G is nonempty: $S(G) > A(\partial I)/4G_N$. Next, we introduced the specific setting we aimed to study: a spatially closed or open FRW universes with a cosmological constant and radiation. The radiation is entangled with and purified by radiation in an analogous reference spacetime, in a TFD-like state. Finally, we discussed the mode in which our results will be presented: for each class of universe, a physically intuitive analysis of island candidates on the time-reflection symmetric Cauchy slice of M (if present) is followed by a graphical presentation of the validity of the four conditions in the full spacetime solution.

In Section 4.2, we searched for islands in closed FRW solutions (positive spatial curvature). We first considered the simplest case where the cosmological constant Λ vanishes. We found that the conditions 1 and 4 discussed in Section 4.1 are mutually exclusive at the turnaround time, so no proper subset of a time-symmetric slice of M is a viable island candidate. This conclusion persisted when we analyzed the full spacetime. However, we found that M itself is an island, if R contains more than half of Σ_R.

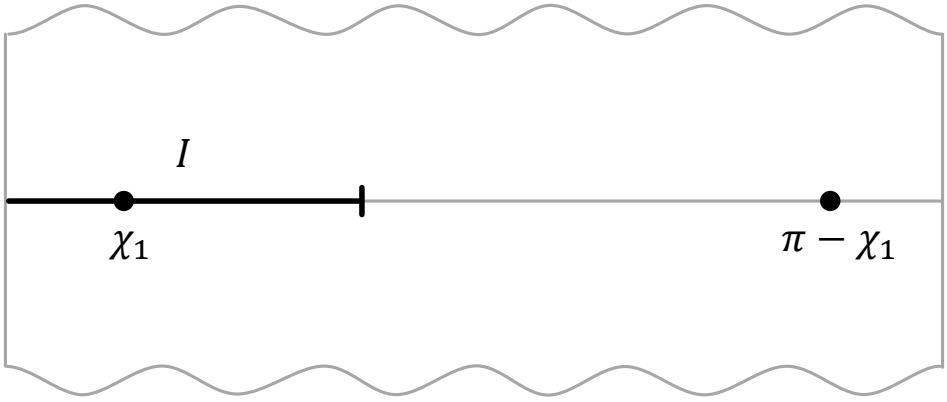

Figure 4.6: Penrose diagram of a closed recollapsing universe. The entire universe can always be an island. For a proper subset I to be an island, it must lie near the turnaround slice, with boundary within a certain angular range. This range is nonvanishing only if the cosmological constant is negative and sufficiently large.

Next, we considered closed universes with negative cosmological constant. The entire universe M was again found to be an island for sufficiently large R. For a proper subset of a time-symmetric slice of M, we found that the four conditions can be simultaneously satisfied only if the spatial curvature is sufficiently weak (and dynamically irrelevant) at the turnaround time. A check of the full solution indicated that islands only appear near the turnaround time. In this case we found explicit examples of islands that are a proper subset of the time-symmetric slice of M, with R being the analogous region on Σ_R; see Figure 4.6. We also found examples of regions that satisfy all three necessary conditions of Ref. [95] but which are not islands for any choice of R, because they fail to satisfy the condition 4.

We then examined closed universes with positive cosmological constant. M itself is again an island if R contains more than half of Σ_R. We found that no proper subset of the time-symmetric Cauchy slice of M can be an island, as conditions 1 and 4 are mutually incompatible. A check of the full solution confirmed that no proper subset of any other Cauchy slice can be an island.

In Section 4.3, we turned to solutions with negative spatial curvature (open FRW). If $\Lambda \geq 0$, there are no islands. If $\Lambda < 0$, we found islands exist if the spatial curvature radius is at least comparable to the minimum island size in the spatially flat case; see Figure 4.7. This is easy to understand geometrically: for I to be an island, one must have $S(I) > A(\partial I)/4G_N$. The entropy is extensive. In flat space, volume grows faster than area, so this condition becomes satisfied at large radius. But in a hyperbolic geometry, volume and area approach a fixed ratio for radii greater than the curvature radius. Therefore, the condition does not

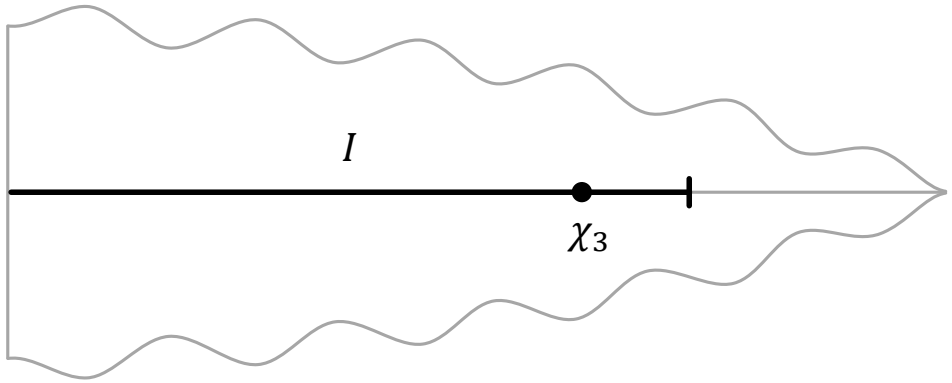

Figure 4.7: Penrose diagram of an open universe. A sufficiently large region I at the turnaround time is an island, if the cosmological constant is negative and large enough for curvature not to dominate below the critical radius χ_3.

become automatically satisfied for sufficiently large radius.

This concludes the search for islands in FRW universes containing radiation and with non-zero spatial curvature. In the next chapter, we will extend this analysis to universes with a general fluid in place of radiation.

Chapter 5

Islands in Cosmologies with General Fluids

In the previous chapter, we sought to investigate whether the newly-recognized feature of the QES prescription, namely, the involvement of islands, could teach us anything about cosmology, where we have a poor understanding of quantum gravity. Toward this end, we extended the analysis of Ref. [95], which explored when it was possible for a region in a flat FRW cosmology to be an island for a region in a nongravitating auxiliary system. Ref. [95] derived three necessary conditions for a region to be an island and found that all conditions could be satisfied in flat universes with a negative cosmological constant. The focus of the previous chapter was to expand this analysis to FRW cosmologies with nonzero curvature. We derived an additional necessary condition for subsets of closed universes to be islands. We found that the entire Cauchy slice of a closed universe was always found to satisfy all necessary conditions. Subsets of closed and open universes with negative cosmological constants were also found to satisfy the conditions in certain parameter regimes. These viable island candidates were found on or near time-symmetric slices (where the scale factor a satisfies $\dot{a} = 0$).

This analysis can be generalized further still, however. Ref. [95] and the previous chapter assumed the matter entropy in the cosmology is generated by radiation. There are, however, interesting cosmological models that involve more general fluids [124], including simple cosmologies without singularities [86]. In this chapter, we therefore extend the search for islands in cosmology by relaxing the assumption that the contents of the cosmology is radiation. We search for islands in FRW cosmologies with a general fluid with a constant equation of state fulfilling the Null Energy Condition $w \geq -1$.

5.1 Preliminaries

In this section, we restate the necessary conditions for islands. We also review FRW cosmologies and the relevant thermodynamics for a general perfect fluid, repeating and expanding

upon some of the material in Chapter 4.

Necessary Conditions for Islands

Refs. [95] combined with the previous chapter derived a set of four conditions necessary for the existence of a nonempty island in a spacetime M entangled with a reference system M_R. We will refer to a region that satisfies these four conditions as a "viable island candidate," while a region for which we consider the four conditions but have not yet checked them is an "island candidate." Assuming the global quantum state on Cauchy slices $\Sigma_M \cup \Sigma_R$ is pure, the four conditions are:

1. $S(I) > \frac{A(\partial I)}{4G_N}$.
2. I is quantum normal.
3. G is quantum normal.
4. For spatially closed M and $I \neq\subset \Sigma_M$, $S(G) > \frac{A(\partial I)}{4G_N}$.

Here G is the complement of I, namely $G \equiv \Sigma_M \backslash I$, and Q is the complement of R: $Q \equiv \Sigma_R \backslash R$. Condition 1 comes from the requirement that an island must be "worth" its cost in area, given that the QES prescriptions requires minimization of the generalized entropy. Conditions 2 and 3 are consequences of the fact that $I \cup R$ and $G \cup Q$ are quantum extremal. Island candidates that are subsets of a spatially closed universe must satisfy condition 4 in order to win out over the entire Cauchy slice, which is always a viable island candidate. See Ref. [95] and the previous chapter for a full derivation.

Ref. [95] used these conditions to search for islands in flat FRW spacetimes containing radiation entangled with a purifying reference system. The previous chapter generalized this analysis to FRW spacetimes with non-zero curvature. In this chapter, we dispense with the assumption that the contents of the universe are radiation, instead considering an arbitrary perfect fluid.

FRW and General Perfect Fluids

The cosmological models we will consider are FRW universes filled with general perfect fluid(s) with an equation of state $w \geq -1$. Recall the metric for an FRW universe is

$$ds^2 = -dt^2 + a(t)^2 \left[d\chi^2 + f^2(\chi) d\Omega^2\right] = a^2(\eta) \left[-d\eta^2 + d\chi^2 + f^2(\chi) d\Omega^2\right] \ , \qquad (5.1)$$

where t denotes cosmic time and η conformal time, which are related by $dt = a(\eta) d\eta$. We shall use both of them throughout the chapter depending on convenience. The factor $f(\chi)$ is $\sinh(\chi)$, χ, $\sin(\chi)$ for open, flat, and closed universe respectively. Notice that in contrast to some conventions, χ and η are dimensionless while the scale factor a has dimensions of

length or time. For a general constant equation of state, w_i, the scale factor, and the energy density of fluid i behave as

$$\rho_i = \rho_{0i} \left(\frac{a}{a_0} \right)^{-3(1+w_i)} , \tag{5.2}$$

where the subscript "0" denotes some time of normalization. Throughout its evolution, the universe is dominated by a single fluid except for transient periods. In this parametrization, the Big Bang singularity is at $a = 0$.[1] We are interested in islands away from the singularity where semiclassical analysis can be trusted. The governing equations of motion are given by the first Friedmann equation and the continuity equations that hold separately for each fluid:

$$H^2 = \sum_i \frac{8\pi G_N}{3} \rho_i - \frac{k}{a^2} \pm \frac{1}{t_\Lambda^2} , \tag{5.3}$$

$$\frac{d\rho_i}{dt} = -3H(\rho_i + p_i) , \tag{5.4}$$

where $t_\Lambda = \sqrt{3/|\Lambda|}$ and $k = \pm 1, 0$ is the usual spatial curvature. The entropy density of a fluid i is given by

$$s_i = \frac{\rho_i + p_i - \mu_i n_i}{T_i} , \tag{5.5}$$

where ρ_i is the energy density, p_i the pressure, n_i the number density, μ_i the chemical potential, and T_i the temperature. Neglecting the chemical potential μ_i, we have

$$s_i = \frac{(1 + w_i)\rho_{0i}}{T_i} \left(\frac{a}{a_0} \right)^{-3(1+w_i)} , \tag{5.6}$$

where we have used the equation of state of the i-th fluid $p_i = w_i \rho_i$. In local thermal, equilibrium the total comoving entropy is conserved:

$$s_c = s\, a^3 = const. \tag{5.7}$$

If the fluids are decoupled such a conservation occurs for every fluid separately assuming it is in thermal equilibrium with itself. The proof of this (taken from [124]) is as follows. Applying the laws of thermodynamics to a comoving volume element yields

$$TdS = d(\rho V) + pdV = d[(\rho + p)V] - Vdp , \tag{5.8}$$

where V is the physical volume $(a^3 \mathcal{V}(\chi))$, ρ is the equilibrium energy density, p is the equilibrium pressure, and S is the entropy per comoving volume. The energy density and pressure are related via

$$\frac{\partial^2 S}{\partial T \partial V} = \frac{\partial^2 S}{\partial V \partial T} , \tag{5.9}$$

[1] An exception is if the NEC is violated with temporary $w < -1$, which occur for example in some quintessence models or bouncing models, e.g. [32, 34, 19, 20].

which implies,

$$dp = \frac{\rho + p}{T} dT \ . \tag{5.10}$$

Substituting into Eq. 5.8, implies that

$$dS = \frac{1}{T} d[(\rho + p)V] - (\rho + p)V \frac{dT}{T^2} = d\left[\frac{(\rho + p)V}{T} + \text{const}\right] \tag{5.11}$$

and thus that

$$S = \frac{a^3(\rho + p)}{T} \tag{5.12}$$

up to a constant. The first law of thermodynamics can be expressed as

$$d[(\rho + p)V] = V dp \ , \tag{5.13}$$

which when substituted into Eq. 5.10 yields

$$d\left[\frac{(\rho + p)V}{T}\right] = 0 \ . \tag{5.14}$$

Therefore, the comoving entropy is conserved in local thermal equilibrium.

In this chapter we will consider a single fluid, deferring more realistic analysis to future work. Because the total s_c is constant, and assuming a single fluid in thermal equilibrium, the temperature of the fluid will redshift as $T \sim a^{-3w}$, which imposes the relation $s_{th} \sim \rho^{1/(1+w)}$. Using (5.10), (5.12), and $p = w\rho$, one gets

$$\rho = \rho_0 \left(\frac{T}{T_0}\right)^{(1+w)/w} \ , \tag{5.15}$$

$$s_{th} = (1 + w)\frac{\rho_0}{T_0} \left(\frac{T}{T_0}\right)^{1/w} \ . \tag{5.16}$$

Hence, at the time of normalization t_0,

$$s_c = (1 + w)\frac{\rho_0}{T_0} a_0^3 \ . \tag{5.17}$$

The constancy of the comoving entropy is essential for the conclusions we shall derive here. We are always considering the semi-classical regime so $\rho_0 \ll (8\pi G_N)^{-2}$ and $T_0 \ll (8\pi G_N)^{-1/2}$.

The QES prescription requires the calculation of the entanglement entropy of region R. Only few such controlled examples are known without heavy use of symmetries, which the FRW universe does not possess. We shall therefore use the thermal entropy density of the fluid as a proxy for the entanglement entropy as was also done in [95, 76] and the previous chapter. At least in high temperatures the entanglement entropy should converge to the thermal entropy [52]. Therefore, our analysis is certainly valid for high enough temperatures, and it remains to be seen how far can one extrapolate it to lower temperatures.

Energy Conditions General Relativity does not specify which energy momentum tensor should appear in the RHS of Einstein's equations. Therefore, energy conditions are commonly used to avoid certain solutions that may be mathematically correct but not sensible physically. In generality they are specified by the energy momentum tensor and its contraction with certain four-vectors. Since we only deal with perfect fluids, we will use the more simplified version pertaining to a perfect fluid with energy density ρ, pressure p and an equation of state w that relates the two $p = w\rho$. The Null Energy Condition (NEC) is $\rho + p = (1+w)\rho \geq 0$, so if $\rho > 0$ it means $w \geq -1$. The Dominant Energy Condition (DEC) is $\rho \geq |p|$, i.e. $1 \geq |w|$.

5.2 General Island Conditions in FRW Spacetimes

Given our choice to work with FRW spacetimes, we can rearrange the necessary conditions for islands in a simpler way. Recall that we choose to consider spherically symmetrical island candidates centered at $\chi = 0$. We denote such an island candidate as $I(\chi)$ and its complement on its Cauchy slice as G. The generalized entropy of $I(\chi)$ and G are as follows:

$$S_{\text{gen}}(I) = S(\eta, \chi) + \frac{A(\eta, \chi)}{4G_N} \ , \tag{5.18}$$

$$S_{\text{gen}}(G) = const. - S(\eta, \chi) + \frac{A(\eta, \chi)}{4G_N} \ . \tag{5.19}$$

The constant in $S_{\text{gen}}(G)$ is the matter entropy of the entire slice containing I and G, but this constant will drop out of the conditions. From these, the four conditions can be written as

$$\textbf{Condition 1:} \quad S(\eta, \chi) > \frac{A(\eta, \chi)}{4G_N} \ , \tag{5.20}$$

$$\textbf{Condition 2:} \quad S'(\eta, \chi) + \frac{A'(\eta, \chi)}{4G_N} \geq \mp \left(\dot{S}(\eta, \chi) + \frac{\dot{A}(\eta, \chi)}{4G_N} \right) \ , \tag{5.21}$$

$$\textbf{Condition 3:} \quad S'(\eta, \chi) - \frac{A'(\eta, \chi)}{4G_N} \geq \mp \left(-\dot{S}(\eta, \chi) + \frac{\dot{A}(\eta, \chi)}{4G_N} \right) \ , \tag{5.22}$$

$$\textbf{Condition 4:} \quad S^{tot}(\eta) - S(\eta, \chi) \geq \frac{A(\eta, \chi)}{4G_N} \ , \tag{5.23}$$

where dot denotes differentiation with respect to conformal time η, prime denotes differentiation with respect to the radial coordinate χ, and condition 4 applies only to subsets of closed universes.

We can use properties of FRW spacetimes and the laws of thermodynamics to manipulate the conditions into a more transparent form. In FRW we have a factorization of the different terms into space and time dependence, $A(\eta, \chi) = a^2(\eta)\mathcal{A}(\chi)$, $S(\eta, \chi) = s_{th}(\eta)V(\eta, \chi) \equiv$

$s_c\mathcal{V}(\chi)$. Here $\mathcal{A}$ and $\mathcal{V}$ refer to comoving quantities, while A and V signify physical area and volume. As we have reviewed in Section 5.1, the entropy per comoving volume is conserved. Hence, s_c is constant in time and so $S(\eta,\chi)\equiv S(\chi)$. Therefore, the time derivative vanishes $\dot{S}=0$. Finally, it is convenient to rewrite the fourth condition in terms of S_{tot} by adding to it the first condition. Thus the conditions simplify as follows. The first becomes

$$\textbf{Condition 1:} \qquad s_c > \frac{a^2(\eta)}{4G_N}\frac{\mathcal{A}(\chi)}{\mathcal{V}(\chi)} \ . \tag{5.24}$$

Consider conditions (2) and (3). Since $\dot{S}=0$, we can rewrite them as

$$S'(\eta,\chi) \geq \frac{(\mp\dot{A}\pm A')}{4G_N} \ , \tag{5.25}$$

where contrary to common notation, here we mean all possible combinations of signs. This can be rearranged into

$$S'(\eta,\chi) \geq \frac{(|\dot{A}|+|A'|)}{4G_N} \ , \tag{5.26}$$

and hence conditions 2 and 3 are simply[2]

$$\textbf{Conditions 2 and 3:} \qquad s_c \geq \frac{a^2(\eta)}{4G_N}\left(2|\mathcal{H}|+\frac{|\mathcal{A}'|}{\mathcal{A}}\right) = \frac{a^2(t)}{4G_N}\left(2a(t)|H|+\frac{|\mathcal{A}'|}{\mathcal{A}}\right) \ . \tag{5.27}$$

Adding conditions 1 and 4 (for proper subsets of closed universes) yields

$$S^{tot}(\eta) = 2\pi^2 s_c \geq 2\frac{a^2(\eta)\mathcal{A}(\chi)}{4G_N} \ , \tag{5.28}$$

and thus condition 1 + 4 is

$$\textbf{Condition 1 + 4:} \qquad s_c \geq \frac{a^2(\eta)}{4G_N}\frac{\mathcal{A}(\chi)}{\pi^2} \ . \tag{5.29}$$

Before going into specific examples we can see what conditions are more likely to be satisfied and where we may find potential obstacles. We have managed to phrase all conditions in terms of a inequalities on the comoving entropy density, $s_c > a^2/4G_N f$ where f is the fudge factor that is different between the different conditions. From this general expression, we can understand why time-symmetric slices are good candidates for islands. This is because the existence of such a slice means that a is bounded, and given a concentration of enough entropy, the conditions will be fulfilled. Moreover, given that the difference between the conditions is the fudge factor f, we expect that in various cases a single condition to encompass all others.[3]

[2] $\mathcal{H}\equiv\frac{\dot{a}}{a}$ where dot is a differentiation w.r.t conformal time η and $H\equiv\frac{\partial_t a}{a}$ where t is the so called cosmic time.

[3] One would usually call this condition a sufficient condition, as its fulfillment implies that all others are fulfilled as well. However, this is not a sufficient condition for the existence of islands, that requires further checks (see below). It is only a sufficient condition for a viable island candidate. To avoid confusion, we use the name encompassing condition, meaning that it captures all other necessary conditions.

5.3 Islands on Time-Symmetric Slices

In this section, we begin to investigate where the necessary conditions can be satisfied in a more general cosmology. First, we do not restrict ourselves to models with perfect fluids, allowing more general contents in an FRW universe. Because this complicates the question, we start by restricting to time-symmetric slices, *i.e.* slices in which the scale factor has a minimum or maximum. The QES prescription relies on extremization of surfaces. Time-symmetric slices are an extremum in the time coordinate. Therefore, these slices are natural places to look for islands. Indeed, with the exception of an entire closed universe, the viable island candidates found in Refs. [95, 76] and in the previous chapter were on or near time-symmetric slices.

Consider a time-symmetric slice and its vicinity, where $\mathcal{H} = 0$ or extremely small. Hence,

$$\textbf{Condition 1:} \qquad s_c \geq \frac{a_{ts}^2}{4G_N}\frac{\mathcal{A}(\chi)}{\mathcal{V}(\chi)} \ , \tag{5.30}$$

$$\textbf{Conditions 2 and 3:} \qquad s_c \geq \frac{a_{ts}^2}{4G_N}\frac{|\mathcal{A}'|}{\mathcal{A}} \ , \tag{5.31}$$

where a_{ts} denotes the scale factor at the time-symmetric slice. For flat universes, χ can be arbitrarily large, and $\mathcal{A}/\mathcal{V}$ and $\mathcal{A}'/\mathcal{A}$ can thus be arbitrarily small by taking large enough χ. Therefore, for flat universes, an arbitrary small amount of entropy s_c will still fulfill all conditions for large enough χ. Hence, time-symmetric slices in flat universes always contain viable island candidates. This is regardless of any other detail such as number of fluids, energy component etc. It is based solely on the constancy of s_c, and the existence of a time-symmetric slice. A specific example of such a universe was found in [95], where a flat universe with radiation and a negative cosmological constant was considered.

For open universes $\mathcal{A}/\mathcal{V}$ and $\mathcal{A}'/\mathcal{A}$ are bounded from below and asymptote to 2 for large χ, resulting in the encompassing condition:

$$s_c \geq \frac{a_{ts}^2}{2G_N} \ . \tag{5.32}$$

For closed universes, the whole manifold is always an island, as was shown in the previous chapter. Contrary to the flat and open case, the quantities $\mathcal{A}/\mathcal{V}$ and $\mathcal{A}'/\mathcal{A}$ are not monotonic in χ, so there is no general χ beyond which all conditions reduce to a single encompassing one. Beyond that we can consider a specific region of certain χ where the conditions are more simple to satisfy. Such a region is $\chi \simeq \pi/2$ on a time-symmetric slice, since (5.27) is trivially fulfilled. The rest of the conditions reduce to the encompassing condition

$$s_c \geq \frac{a_{ts}^2}{\pi G_N} \ . \tag{5.33}$$

From this we can see a reason why closed universes are in some sense more island-friendly. In an ever expanding universe, a grows without bound and therefore will always violate this

condition after a long enough time. Ever expanding closed universes will require $w < -1/3$ and/or a positive cosmological constant, which are not trivial. In contrast, the violation of the inequality may not happen in a universe with a bounded a_{ts}, meaning it is "easier" to fulfill this condition.

The above analysis depends on the existence of a time-symmetric slice. The matter and energy content of the universe affects whether such a slice can exist. Exotic matter or energy components can be introduced to produce such a slice, e.g. [19]. It is, however, standard to treat the matter contents of an FRW universe as a collection of perfect fluids, and possibly a cosmological constant and spatial curvature. Let us call such a universe, one that contains any number of perfect fluids, "conventional." We assume that all energy components are perfect fluids and further that all energy densities of all fluids are positive definite. We still restrict our search to time-symmetric slices, the existence of which are determined by the first Friedmann equation:

$$0 = \frac{8\pi G_N}{3} \sum_i \rho_{0,i} \left(\frac{a_{ts}}{a_0}\right)^{-3(1+w_i)} \pm \frac{1}{t_\Lambda^2} - \frac{k}{a_{ts}^2} \,, \tag{5.34}$$

where $\rho_{0,i} \geq 0$ is the energy density of various fluids at the turnaround time and $\pm$ is the sign of the cosmological constant. Hence, for flat and open conventional universes, a solution to the above equation exists only if there is a negative cosmological constant. For a closed universe a time-symmetric slice can exist with any Λ depending on the value of a_{ts}. We tabulate the islands in general and specifically in the case of conventional time-symmetric slices in Table 5.3. The islands found in [95, 76] and the previous chapter correspond to the conventional time-symmetric slices.

Table 5.1: Summary of viable island candidates on time-symmetric slices. The second column corresponds to island candidates in the vicinity of time-symmetric slices without limiting ourselves to perfect fluids with positive definite energy densities, while the third column corresponds to the inclusion of this limitation. The flat and open universe cases here include all possible spatial time-symmetric islands $\chi \gg 1$, while the closed universe is limited to the $\chi \simeq \pi/2$ case.

Case	**General Time sym.**	**Conventional Time sym.**
$k = 0$	Always	If $\Lambda < 0$ exists
$k = -1$	If $s_c > \frac{a_{ts}^2}{2G_N}$	If $s_c > \frac{a_{ts}^2}{2G_N}$ and $\Lambda < 0$ exists
$k = 1$	If $s_c > \frac{a_{ts}^2}{\pi G_N}$, $\quad \chi \simeq \pi/2$	Any Λ, if $s_c > \frac{a_{ts}^2}{\pi G_N}$, $\quad \chi \simeq \pi/2$

5.4 Beyond Time-Symmetric Slices: Flat Universes

Let us now deviate from time-symmetric slices and their vicinity. We wish to investigate where the necessary conditions for islands are satisfied in flat universes with a general perfect fluid. Consider a flat FRW universe filled with a perfect fluid with an equation of state w. We consider spherical islands candidates that exist far away from singularities, so as to stay in the semiclassical regime. Hence, we are interested in cases where $\eta \gg 1$ and $\rho \ll (8\pi G_N)^{-2}$. The comoving volume and area are the standard Euclidean expressions for a sphere, $\mathcal{V}(\chi) = \frac{4\pi}{3}\chi^3$ and $\mathcal{A}(\chi) = 4\pi\chi^2$. The scale factor and Ricci scalar may be written as, respectively,

$$a = a_0(t/t_0)^{2/(3+3w)} = a_0(\eta/\eta_0)^{2/(1+3w)} \ , \tag{5.35}$$

$$\mathcal{R} = \frac{6}{a^2}\left(\dot{\mathcal{H}} + \mathcal{H}^2\right) = 6\left(\frac{dH}{dt} + 2H^2\right) \sim t^{-2} \sim \eta^{-6(1+w)/(1+3w)} \ . \tag{5.36}$$

Hence, at $t = 0$ we will hit the Big Bang singularity. However, this is not enough. To trust our semi-classical analysis we need to be far away from Planck energy densities, which amounts to

$$\rho_0 \ll (8\pi G_N)^{-2} \Leftrightarrow t_0 \gg \sqrt{8\pi G_N} \ . \tag{5.37}$$

Here t_0 is an arbitrary time of normalization and we specify our results with respect to it. Finally, in a flat universe with a single fluid ρ_0 and t_0 are related via the Friedmann equation at t_0

$$\left(\frac{2}{3(1+w)t_0}\right)^2 = \frac{8\pi G_N}{3}\rho_0 \ . \tag{5.38}$$

Island candidates at $t = t_0$

Let us first consider the possibility of island candidates at $t = t_0$, where t_0 is an arbitrary normalization time. This possibility answers the following question: Assuming we are allowed to tune the temperature T_0 and the energy density ρ_0 at a given time t_0 in the FRW universe, and that the universe maintains thermal equilibrium, can an island exist? Substituting (5.35) into conditions (5.24), (5.27) and $t = t_0$ yields

$$\textbf{Condition 1:} \qquad s_c > \frac{3a_0^2}{4G_N\chi} \ , \tag{5.39}$$

$$\textbf{Conditions 2 and 3:} \qquad s_c \geq \frac{a_0^3}{4G_N}\left[\frac{4}{3(1+w)|t_0|} + \frac{2}{a_0\chi}\right] \ . \tag{5.40}$$

Using (5.38) and the expression for the comoving entropy density (5.17) yields the following inequalities:

$$\textbf{Condition 1:} \qquad \frac{(1+w)G_N\rho_0 a_0}{T_0} > \frac{3}{4\chi} \ , \tag{5.41}$$

$$\textbf{Conditions 2 and 3:} \qquad \frac{(1+w)G_N\rho_0 a_0}{T_0} > \frac{1}{2\chi} + a_0\sqrt{\frac{2\pi G_N\rho_0}{3}} \ . \tag{5.42}$$

We have the following dimensionful parameters G_N, ρ_0, T_0 and $\chi_{0,phys.} \equiv a_0\chi$, the spatial size of the island candidate, and some $\mathcal{O}(1)$ numbers which are not important at the moment. There are two possible regimes for island candidates: $\chi_{0,phys.}^{-1} \gg \sqrt{G_N\rho_0}$ and $\sqrt{G_N\rho_0} \gg \chi_{0,phys.}^{-1}$. If $\chi_{0,phys.}^{-1} \gg \sqrt{G_N\rho_0}$, then the first condition simplifies to

$$G_N\rho_0 > \mathcal{O}(1)\,\frac{T_0}{\chi_{0,phys.}} \ , \tag{5.43}$$

and the second term in the "2 and 3" condition is negligible, meaning it is encompassed by the first. Thus satisfaction of (5.43) will ensure a viable island candidate. The other regime is if $\sqrt{G_N\rho_0} \gg \chi_{0,phys.}^{-1}$, which implies that (5.43) is trivial and the "2 and 3" condition simplifies to

$$\frac{G_N\rho_0}{T_0} > \mathcal{O}(1)\sqrt{G_N\rho_0} \quad \Rightarrow \quad G_N\rho_0 > \mathcal{O}(1)\,T_0^2 \ . \tag{5.44}$$

Then (5.44) will ensure a viable island candidate.

Given freedom to tune ρ_0 and T_0 as independent energy scales, we see that viable island candidates will appear for practically any fluid and will be of any size as long as T_0 and ρ_0 obey

$$G_N\rho_0 > \mathcal{O}(1)\max\left\{T_0^2, \frac{T_0}{\chi_{0,phys.}}\right\} \ . \tag{5.45}$$

The statement also has a nice interpretation in terms of the Hubble parameter since $H \sim \sqrt{G_N\rho}$:

$$H_0 > \mathcal{O}(1)\max\left\{T_0, \sqrt{\frac{T_0}{\chi_{0,phys.}}}\right\}, \tag{5.46}$$

where H_0 is the Hubble parameter at the time of normalization t_0, and not today, as is usually denoted.

As an example of the relationship between T_0 and χ for a chosen ρ_0, we show in Figure 5.1 a plot of T_0 vs χ for $w = 2/3$, $\rho_0 = 2 \times 10^{-4}$. At any χ, there is a range of small enough T_0's such that the conditions are simultaneously satisfied.

Radiation is a special case where $\rho_0 = c_{th}T_0^4$, where c_{th} is roughly the number of degrees of freedom. Suppose we take χ_{phys} arbitrarily large to make (5.43) trivial. Substituting $\rho_0 = c_{th}T_0^4$ into (5.44) shows that the inequality is not fulfilled unless T_0 is Planckian or

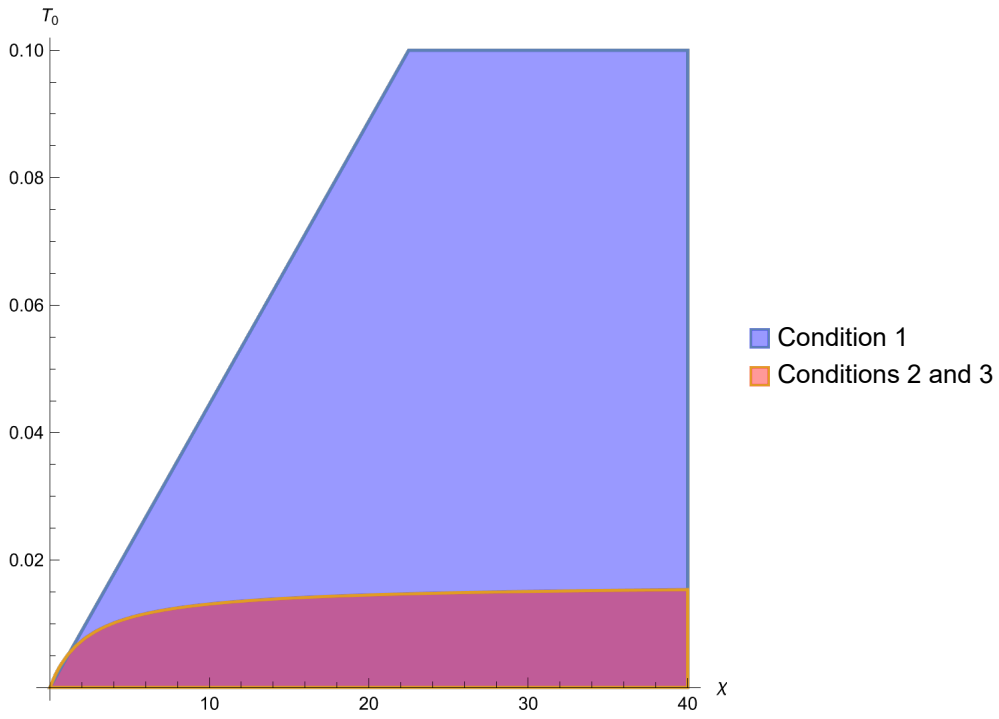

Figure 5.1: A plot of T_0 vs χ for $w = 2/3$, $\rho_0 = 2 \times 10^{-4}$ in natural units with the normalization a_0 set to 10. The conditions at a given χ are only satisfied for a small enough T_0, but for any χ there is always such a T_0 for which the conditions are all satisfied.

$c_{th} \gg 1$. In other words, for radiation ρ_0 and T_0 are not tuned appropriately to allow for viable island candidates.[4]

Islands away from $t = t_0$

We showed in the previous section that if ρ_0 and T_0 are separate free parameters, we can always tune them to create a viable island candidate on the normalization slice t_0. In the real world, however, we do not have this freedom. It is possible that ρ_0 and T_0 in our universe do not fulfill the conditions at the present time. Thus in this section we investigate whether a universe without islands at t_0 can evolve into or have evolved from one with islands.

The simpler case is to treat the normalization as the initial time, and then look for islands after this initial time $t \gg t_0$ because semiclassical regime is guaranteed: $t \gg t_0 \gg \sqrt{8\pi G_N}$, $\rho < \rho_0 \ll (8\pi G_N)^{-2}$. Assume at the normalization time t_0, the universe with

[4]Another example is degenerate fermions, which have $\mu \gg T$, $\rho_0 = \frac{c_{th}}{8\pi^2}\mu^4$, $n_0 = \frac{c_{th}}{6\pi^2}\mu^3$, $p_0 = \frac{c_{th}}{24\pi^2}\mu^4$ [124]. We therefore have to reintroduce μ into the expression of s_c. Calculating s_c from (5.5) shows that s_c vanishes, which means the conditions are not satisfied.

temperature T_0 and energy density ρ_0 did not have a viable island candidate. By considering conditions (5.24), (5.27) and (5.17) with their time dependence, we get the following conditions:

$$\textbf{Condition 1:} \qquad G_N\rho_0 > \frac{3}{4(1+w)}\frac{T_0}{\chi_{phys.}}\left(\frac{a}{a_0}\right)^3 , \tag{5.47}$$

$$\textbf{Conditions 2 and 3:} \qquad G_N\rho_0 > \frac{T_0}{2(1+w)}\left(\frac{a}{a_0}\right)^3\left[|H| + \frac{1}{\chi_{phys.}}\right] , \tag{5.48}$$

where $\chi_{phys.} \equiv a\chi$ is the physical radius of the island candidate. These expressions are valid for both contracting and expanding universes. Since $0 \leq \chi < \infty$, for any given time t, for any small amount of energy density of $G_N\rho_0$ (or equivalently comoving entropy s_c) there always exists $\chi_{phys.}$ such that (5.47) is fulfilled, and the χ dependent term in (5.48) is negligible.[5] Therefore the H-dependent part in (5.48) is our encompassing condition. Using the Friedmann equation (5.3) and (5.2), we can rewrite (5.48) as

$$\textbf{Conditions 2 and 3:} \qquad G_N\rho_0 > \frac{2\pi}{3(1+w)^2}T_0^2\left(\frac{a}{a_0}\right)^{3(1-w)} . \tag{5.49}$$

To ensure islands with $a \gg a_0$, we therefore need[6]

$$\boxed{w \geq 1} . \tag{5.50}$$

Thus for positive energy density $\rho > 0$, the necessary conditions for islands imply a violation (or saturation) of the Dominant Energy Condition (DEC), which stipulates $|w| \leq 1$. In certain cases such as radiation, one can further derive the exact relation between s_c, ρ_0, T_0 and the number of degrees of freedom, c_{th} e.g. [95], but that is unnecessary. The point is that for a finite s_c there will always be a viable island candidate for $t \gg t_0$ and a large enough χ if $w > 1$. Substituting the exact value of s_c from (5.17) and (5.35), one gets the exact time when the island may form:

$$t > t_0\left(\frac{1}{2\pi T_0 t_0}\right)^{(1+w)/(1-w)} . \tag{5.51}$$

For the special case of $w = 1$, the issue of a viable island candidate becomes a quantitative question regarding the exact values of s_c, ρ_0, etc. Considering again a large enough χ such that (5.47) is fulfilled and substituting (5.17) into (5.49) for $w = 1$, we get a condition on the temperature T_0:

$$T_0 < \sqrt{\frac{24G_N\rho_0}{\pi}} , \tag{5.52}$$

[5]Here we do not consider the case where the χ term is the dominant one because an island candidate in such a case will mean that it already existed at $t = t_0$, contrary to our initial assumption in this section. It reduces back to the question of an island at $t = t_0$, which we have already analyzed.

[6]Since in many bouncing models such as the ekpyrotic scenario we have $w \gg 1$, we get that islands in such models are ubiquitous at early stages of the contraction.

for a viable island candidate.

Let us now consider the more delicate case, where our normalization time is t_0, and we would like to investigate the possibility of islands to its past while staying in the semiclassical regime, i.e. $t_0 \gg t \gg \sqrt{8\pi G_N}$. Condition (5.24) can still be fulfilled for any time by taking large enough χ. We then need to consider (5.27). Our assumption is that at t_0 there is no island, and we wish to check whether at $t \ll t_0$ there may be one. We get the converse condition, that the DEC has to be fulfilled:

$$\frac{a_0^3}{3(1+w)G_N}\frac{|t_0|^{(1-w)/(1+w)}}{t_0^{2/(1+w)}} \geq s_c \geq \frac{a_0^3}{3(1+w)G_N}\frac{|t|^{(1-w)/(1+w)}}{t_0^{2/(1+w)}} \ , \tag{5.53}$$

$$\Rightarrow |w| < 1, \quad \frac{1}{2\pi t_0}\left(\frac{t_0}{t}\right)^{(1-w)/(1+w)} \geq T_0 \geq \frac{1}{2\pi t_0} \ . \tag{5.54}$$

The upper bound on s_c comes from requiring that there is no island at $t = t_0$, and the lower bound from requiring that there is an island at $t \ll t_0$.

On top of that we have to show that we are still in the semiclassical regime. If there is an additional energy scale, say $\rho_0 \neq T_0^4$, then it is simple to fulfill the inequalities by choosing the appropriate energy scale. An immediate example is (non-relativistic) dust with an equation of state $w = 0$ and particle mass m. Equation (5.54) gives

$$\frac{1}{2\pi t} \geq T_0 \geq \frac{1}{2\pi t_0} \ . \tag{5.55}$$

Having discussed the conditions at t_0 and before and after t_0, we now plot two examples of the regions satisfied by the conditions: one with $w = 3.2,\ \rho_0 = 10^{-6},\ T_0 = 10^{-4}$ (Figure 5.2) and the other with $w = 1,\ \rho_0 = 10^{-6},\ T_0 = 10^{-4}$ (Figure 5.3) in natural units $G_N = 1$. In these plots we substituted the exact expressions for (5.24), (5.27). They show that for the parameters chosen, a given time slice always has some minimum χ for which all the necessary conditions are fulfilled.

The conditions here are only necessary conditions for islands; satisfying all conditions does not guarantee that a particular region is an island. To check that a viable island candidate is in fact an island, we must look at the reference region of interest and confirm that application of the QES prescription forces the island candidate into that region's entanglement wedge. This is straightforward in the model discussed in Section 5.1, where M and M_R are entangled in a thermofield-double-like state. In this model, a viable island candidate $I(\chi)$ for the flat space scenarios we have so far discussed will be an island if we select the matching region R in the nongravitational spacetime M_R. This is because (i) the candidate satisfies the homology constraint of the QES prescription, (ii) satisfying the original conditions 2 and 3 implies the candidate is quantum extremal, and (iii) including the island in the entanglement wedge of R is generalized-entropy-minimizing. Regarding (iii), because of the entanglement structure in the thermofield-double-like model, decreasing the size of the island would increase the matter entropy in the entanglement wedge by an amount that goes with the volume (from the entangled pairs in R that are no longer purified by the island) while decreasing the area

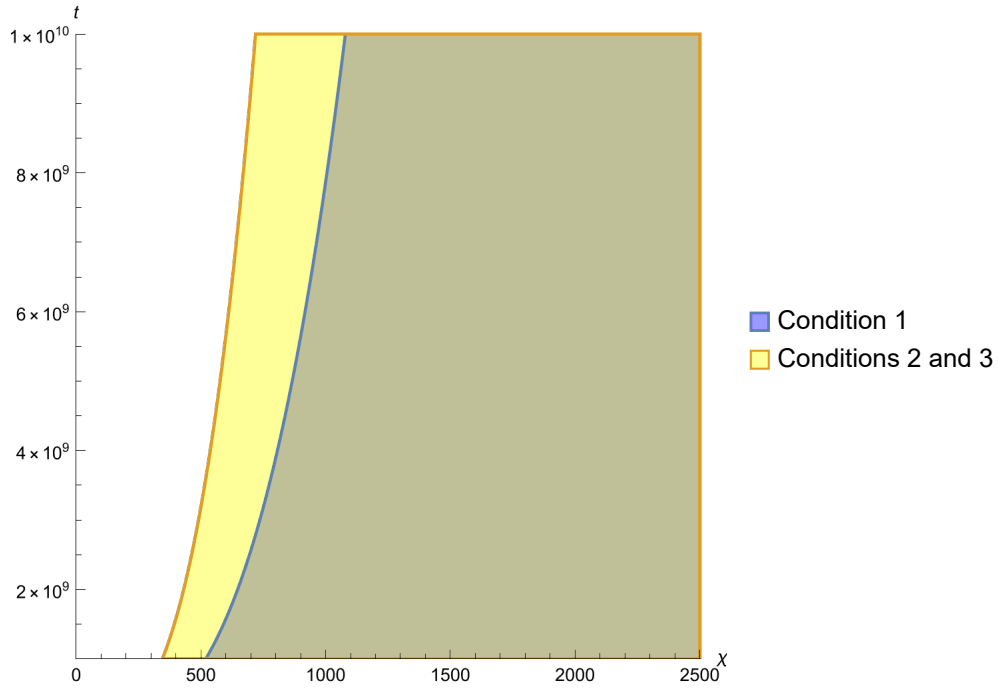

Figure 5.2: Regions satisfying the island conditions are shown for a flat universe with $w = 3.2,\ \rho_0 = 10^{-6},\ T_0 = 10^{-4}$.

contribution by an amount that, naturally, goes with the area. Increasing the size of the island would increase both the matter and area contributions. Thus the island candidate must be included in the entanglement wedge of R, and therefore $I(\chi)$ is an island. This argument holds for all the flat space scenarios we have discussed thus far.

5.5 Beyond Time-Symmetric Slices: Closed and Open Universes

In this section we rearrange the conditions in the new forms we derived in Section 5.2 for universes with nonzero curvature and a single general fluid. A drawback regarding geometries with spatial curvature is that generically we do not have an explicit time dependence and we can only give results in terms of the scale factor a.

First consider closed universes ($k = +1$) with a general perfect fluid. The comoving volume of a sphere in a closed geometry is $\mathcal{V}(\chi) = \pi(2\chi - \sin 2\chi)$, so the matter entropy of an island candidate of comoving radius χ is

$$S = s_c \pi (2\chi - \sin 2\chi) \ . \tag{5.56}$$

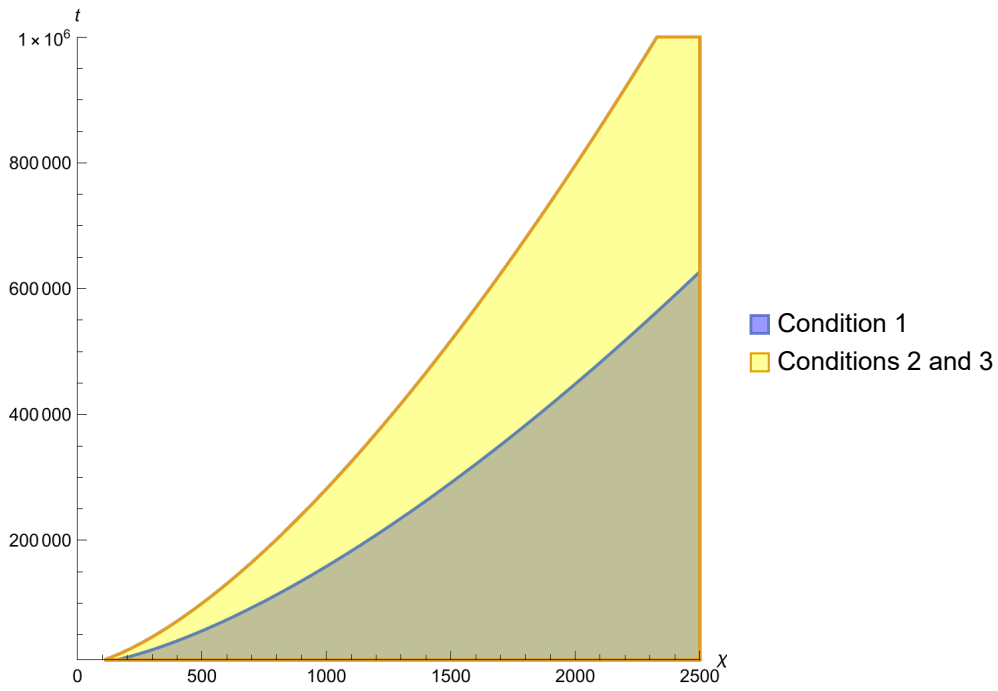

Figure 5.3: Regions satisfying the island conditions are shown for a flat universe with $w = 1,\ \rho_0 = 10^{-6},\ T_0 = 10^{-4}$.

The corresponding comoving area and its spatial derivative are $\mathcal{A} = 4\pi \sin^2\chi$ and $\mathcal{A}' = 4\pi \sin 2\chi$ respectively. We substitute the closed geometry into the simplified conditions (5.24), (5.27), (5.29) to obtain

$$\textbf{Condition 1:} \qquad s_c \geq \frac{a^2}{G_N}\frac{\sin^2\chi}{2\chi - \sin 2\chi}\ , \tag{5.57}$$

$$\textbf{Conditions 2 and 3:} \qquad s_c \geq \frac{a^2(\eta)}{2G_N}\left(|\mathcal{H}| + |\cot\chi|\right)\ , \tag{5.58}$$

$$\textbf{Condition 1 + 4:} \qquad s_c \geq \frac{a^2}{G_N}\frac{\sin^2\chi}{\pi}\ , \tag{5.59}$$

where Conditions 2 and 3 together come from Eq. (5.27). These are the general conditions for island candidates in closed universes. There are two potential obstacles for islands. First, if $|\cot\chi|$ diverges. Second, if the scale factor grows without bound. We can overcome the first difficulty by looking for islands around $\chi \simeq \pi/2$. In such a case, the conditions simplify to the encompassing condition

$$s_c \geq \frac{a^2}{\pi G_N}\ , \tag{5.60}$$

provided $\mathcal{H} < 2/\pi$, which is generally the case in an expanding universe.

Considering a closed universe with a perfect fluid and a cosmological constant, there are three possible regimes: perfect fluid domination, curvature domination, and cosmological constant domination. For the latter two, we do not expect to find anything different than the analysis carried out in the previous chapter, except that the parameters of the fluid are different from radiation. In the case of fluid domination, $G_N\rho_0/a^{3(1+w)} \gg \{t_\Lambda^2, a^{-2}\}$, the analysis resembles that of the previous section. In an expanding universe where a is monotonically growing, the only way to satisfy (5.60) is if it is satisfied at the time of normalization where $a = a_0$, when we evolve backwards and $a < a_0$, or for some finite time in the future where $a > a_0$. Once again we get a condition relating the energy density ρ_0 and the temperature T_0. Considering island candidates at the time of normalization where $a = a_0$, (5.60) reduces to

$$G_N\rho_0 > \frac{T_0}{(1+w)\pi a_0} \ , \tag{5.61}$$

while for backward time evolution we have

$$\frac{a^2}{\pi G_N} \leq s_c \leq \frac{a_0^2}{\pi G_N} \tag{5.62}$$

$$\Rightarrow \frac{T_0}{(1+w)\pi a_0}\left(\frac{a}{a_0}\right)^2 \leq G_N\rho_0 \leq \frac{T_0}{(1+w)\pi a_0} \ . \tag{5.63}$$

Notice that we did not need to use the value of Λ. Hence, islands which are subset of the closed universe manifold can exist with any type of cosmological constant, provided that the universe is dominated by the perfect fluid for long enough time.

For $\chi \neq \pi/2$, there is no simplified treatment when we move away from time-symmetric slices. The inequalities in general then become:

$$s_c \geq \frac{a^2}{G_N} \times \max\left\{\frac{\sin^2\chi}{2\chi - \sin 2\chi}, \frac{|\mathcal{H}| + |\cot\chi|}{2}, \frac{\sin^2\chi}{\pi}\right\} \ . \tag{5.64}$$

There is a particular closed universe model that warrants attention as a specific example. Notice that until now all known examples of islands contained spacetime singularities. It is interesting to consider islands in space time without singularities at least classically. We therefore apply our findings to the "Simple Harmonic Universe" scenario, [86]. This scenario consists of a perfect fluid $-1 < w \leq -1/3$, positive spatial curvature $k = +1$ and a negative Λ. It does not have a singularity at the background level and is classically stable for certain range of parameters.[7] Specifically for $w = -2/3$ there is an analytic solution for the scale factor. The scale factor is periodic, taking the form

$$a(t) = \frac{\rho_0}{2|\Lambda|} + a_0\cos(\omega t + \psi) \ , \tag{5.65}$$

[7]To be precise, it is classically stable for $a_{max}/a_{min} \sim \mathcal{O}(1)$, and for $a_{max}/a_{min} \gg 1$ it is stable for many cycles until the approximation scheme in [86] breaks down.

where $\omega \equiv \sqrt{\frac{8\pi G_N|\Lambda|}{3}}$ and $a_0 \equiv \frac{1}{2|\Lambda|}\sqrt{\frac{-3|\Lambda|}{2\pi G_N} + \rho_0^2}$.

From the thermodynamic relation, Eq. (5.6), with $w = -2/3$, the comoving entropy density obeys

$$s_c \sim \rho_0^3 \ . \tag{5.66}$$

The simple harmonic universe has two classes of time-symmetric slices: when $a(t)$ reaches a minimum or a maximum. The scale factor at these times can be found by setting $\dot{a}$ to 0 in the Friedmann equation, which yields:

$$a_{ts} = \frac{\rho_0}{2|\Lambda|}\left(1 \pm \sqrt{1 - \frac{3|\Lambda|}{2\pi G_N \rho_0^2}}\right) \ , \tag{5.67}$$

where the + or − corresponds to a_{max} or a_{min} respectively. The semi-classical regime requires $a(t) \gg l_P$, which in this case corresponds to $a_{min} \gg l_P$. For $a_{min} \gg 1$ (in natural units) we need to pick a Λ and ρ_0 such that at all times the energy density is smaller than Planckian. This can be achieved for instance with $\rho_0 = 0.01 M_P^3$ and $|\Lambda| = 10^{-4} M_P^4$, that results in $a_{min} \simeq 13/M_P$ and a ρ_0 that is always much smaller than Planckian. The complete spacetime for this parameter regime is plotted in Figure 5.4. Here $\chi = 0$ corresponds to a time at which $a(t)$ is at a maximum. There are regions of 4-way overlap around the times at which $a(t)$ reaches a minimum. Furthermore, entire Cauchy slices of this universe are always viable island candidates, which follows directly from the results of the previous chapter.

As before, we can check in the thermofield-double model whether these viable island candidates are in fact islands for some reference region R. The argument is the same, but now subsets of this universe compete the with the entire Cauchy slice, which is always a viable island candidate. A viable island candidate that is a subset of the Cauchy slice Σ_M will be an island for a region R of equal size and location on Σ_R. The entire Cauchy slice will be an island if R is more than half of Σ_R and condition 4 is violated. Hence, in our model, the time-symmetric slices at a_{min} in the Simple Harmonic Universe scenario are actually islands.

Next consider open universes ($k = -1$). For such universes, the geometric factors are $\mathcal{V} = \pi(\sinh 2\chi - 2\chi)$, $\mathcal{A} = 4\pi \sinh^2 \chi$, and $\mathcal{A}' = 4\pi \sinh 2\chi$. One can substitute these expressions and look for potential islands. The best chance is in the large χ limit, as the geometric factors asymptote to a constant value $\mathcal{A}'/\mathcal{A} \to 2$ and $\mathcal{A}/\mathcal{V} \to 2$. In the semiclassical regime $|\mathcal{H}| \ll 1$ in natural units. Hence, all conditions collapse to a single encompassing condition

$$s_c \geq \frac{a^2}{2G_N} \ . \tag{5.68}$$

Here one can again consider regimes of fluid domination, curvature domination, or Λ domination. Similar to the closed case scenario, if the perfect fluid is dominant for long enough $G_N \rho_0 / a^{3(1+w)} \gg \{t_\Lambda^2, a^{-2}\}$, the analysis will resemble the closed universe results with 2 instead of π. Considering island candidates at the time of normalization where $a = a_0$,

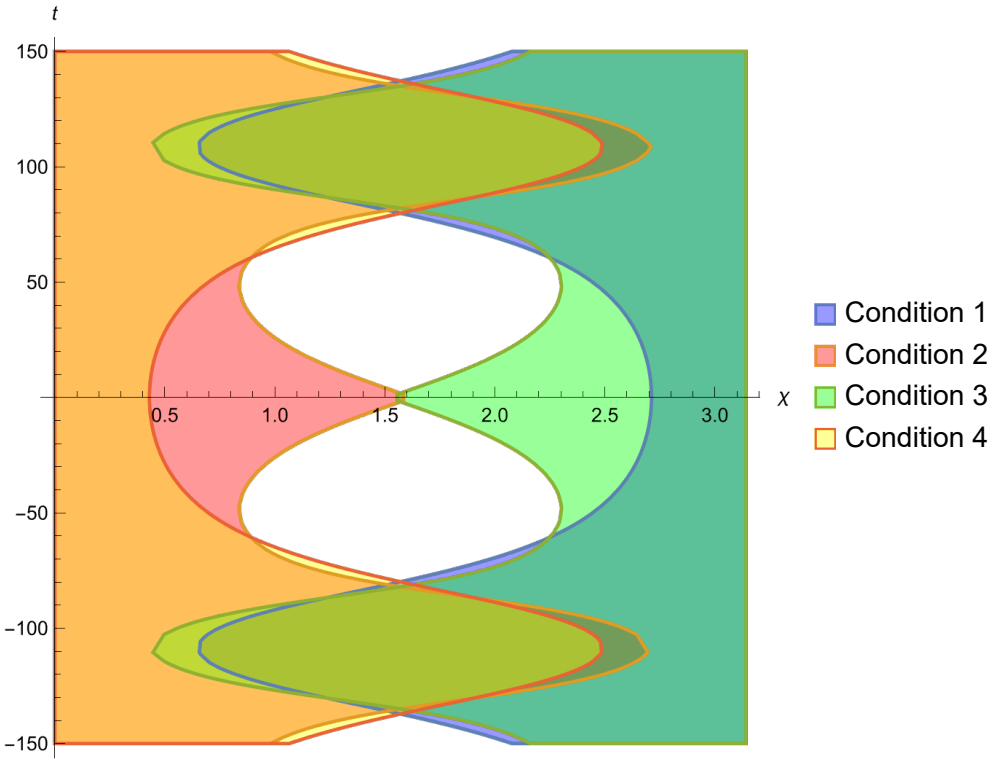

Figure 5.4: Regions satisfying the four island conditions are shown for the simple harmonic universe, with $\rho_0 = 0.01, |\Lambda| = 0.0001, T_0 = 1.6 \times 10^{-5}$. We choose to phrase the conditions here according to their original form in (5.20), (5.21), (5.22), (5.23) due to their nice symmetrical properties.

(5.68) reduces to

$$G_N \rho_0 > \frac{T_0}{(1+w)2a_0} \ , \tag{5.69}$$

while for backward time evolution we have

$$\frac{T_0}{(1+w)2a_0}\left(\frac{a}{a_0}\right)^2 \leq G_N\rho_0 \leq \frac{T_0}{(1+w)2a_0} \ . \tag{5.70}$$

Without limiting ourselves to $\chi \gg 1$ and $\mathcal{H} \ll 1$, the conditions become the following inequality:

$$s_c \geq \frac{a^2}{2G_N} \times \max\left\{\frac{2\sinh^2\chi}{\sinh 2\chi - 2\chi}, |\mathcal{H}| + |\coth\chi|\right\} \ . \tag{5.71}$$

Its fulfillment depends on the exact physical parameters such as the number of degrees of freedom, c_{th}, the energy scale ρ_0, the entropy density s_c, etc.

5.6 Chapter Summary and Conclusion

The main objective of this chapter was to generalize the analysis of [95, 76] and the previous chapter to cosmologies containing general fluids. In Section 5.1, we reviewed the Quantum Extremal Surface prescription and the necessary conditions for islands derived in [95, 76] and the previous chapter. We also described a specific model of which made use, that of a gravitating universe and a nongravitating universe entangled in a thermofield-double-like state.

As a prelude to applying the conditions to classes of spacetimes, Section 5.1 reviewed the relevant cosmological thermodynamics, including the argument from [124] that the comoving entropy density is a constant in time under the assumption of local thermal equilibrium.

In Section 5.2, we wrote out the necessary conditions for islands in full generality, with a general fluid. The crucial property of constant comoving entropy density allowed us to phrase the necessary conditions for islands for any FRW universe as inequalities regarding the comoving entropy density. This constant comoving entropy density s_c has to be larger than a time-dependent term $s_c \geq a^2/4G_N f(\eta, \chi)$, where a is the scale factor, G_N Netwon's constant, χ is a generalized radial coordinate, η is a conformal time coordinate, and $f(\eta, \chi)$ is a fudge factor that is different between the different conditions and depends on geometrical quantities such as the Hubble parameter, the comoving volume, and the comoving area. We found that in many cases, for a given choice of χ, fulfilling one inequality implies the fulfillment of all others, making it what we call an "encompassing" condition for a region to be a viable island candidate.

Since time-symmetric slices have frequently been found to contain viable island candidates, we started with considering such slices in 5.3. We arrived at the conclusion that a time-symmetric slice in a flat universe always contains an island. In open universes a time-symmetric slice contains an island if $s_c > a_{ts}^2/2G_N$, where a_{ts} is the scale factor at the turnaround time. In closed universes, one cannot combine the conditions into a single encompassing inequality. However, for $\chi \simeq \pi/2$ on a time-symmetric slice in a closed universe, one does get a single condition of $s_c > a_{ts}^2/\pi G_N$.

Time-symmetric slice could be the result of rather unconventional energy components, e.g. [19]. To make contact with models usually considered in cosmology, we distinguished a subset of universes with "conventional" components in Section 5.3. These are universes that can only include any number perfect fluids, with positive definite energy density, a cosmological constant, and spatial curvature. We elaborated on the existence of islands in this conventional subset.

Section 5.4 applied the conditions to flat universes with a general perfect fluid away from time-symmetric slices. We addressed two separate questions. **1)** Assuming that we are allowed to consider any (sub-Planckian) energy density ρ_0 and temperature T_0 of a perfect fluid w, at some normalization time t_0 is there an island? and **2)** Assuming that we start with some given ρ_0, T_0, and w at t_0, will islands form when we evolve forwards or backwards in time?

In answer to the first question, we found that all conditions can be simultaneously satisfied

if the island is large enough, and a certain inequality is fulfilled between the energy density ρ_0 and the temperature T_0 at some time of normalization t_0, $G_N\rho_0 > \mathcal{O}(1)\max\left\{T_0^2, \frac{T_0}{\chi_{0,phys.}}\right\}$. However, it does seem that for the simple case of radiation the inequalities are not fulfilled. This contrasts the results of [95, 76] and the previous chapter, in which all viable island candidates appeared on or near time-symmetric slices.

The answer to the second question is related to the Dominant Energy Condition (DEC) $|w| \leq 1$. We found that islands will always exist when we evolve forward in time if the DEC is violated $w \geq 1$ for a large enough spatial region $\chi \gg 1$. The converse is true for backward time evolution. For $\sqrt{8\pi G_N} \ll t \ll t_0$ islands form away from the Planck regime, if the DEC, $|w| \leq 1$, $\chi \gg 1$, and a certain inequality regarding the temperature T_0 are fulfilled, $\frac{1}{2\pi t_0}\left(\frac{t_0}{t}\right)^{(1-w)/(1+w)} \geq T_0 \geq \frac{1}{2\pi t_0}$. We demonstrated an island explicitly with non-relativistic dust $w = 0$. Again, radiation is a very special case that does not produce an island when taking into account all the parameters.

The reason that radiation is special is due to the conformal nature of radiation. For radiation, there is only a single energy scale which is the temperature T_0, and the conditions are not satisfied. For all other fluids, there are other energy scales such as ρ_0 or the mass of the dust particle m. As a result, there is a hierarchy between these energy scales and the conditions for islands can be fulfilled. In a certain sense, this argument explains the results of [95, 76] and the previous chapter, as spatial curvature or a cosmological constant introduced another energy scale that enabled the existence of a time-symmetric slice where conditions for islands are favorable.

In Sections 5.5, we specialized the conditions to closed and open universes with a general fluid. In the regime of fluid domination for any w, if the scale factor is monotonically growing, islands can occur only at the time of normalization t_0, before that time, and up to some finite time later. In this section, we also considered a specific example of interest, which is a closed universe without singularities: the "Simple Harmonic Universe." This model which contains a fluid with $w = -2/3$, has a negative cosmological constant ($\Lambda < 0$) and positive spatial curvature ($k = +1$). Its scale factor is periodic, and we found that all island conditions can be simultaneously satisfied near slices on which the scale factor reaches a minimum. Furthermore, entire Cauchy slices of this universe are islands, which follows directly from the results of the previous chapter. This is the first example of a possible island in space-time without singularities.

In brief, islands in cosmology require either a time-symmetric slice or a condition on the temperature and energy density of the fluid, and they are not necessarily accompanied by a singularity at least at the background level.

This concludes our discussion of how to apply the insights of the Page curve calculations of Refs. [151, 16] to cosmology. There are many unanswered questions, and we hope that our analysis will lead to further work. For now, however, we move on to a problem which we shall argue that the Page curve calculations have yet to resolve: the firewall paradox.

Chapter 6

Black Hole Cannibalism

The discovery of entanglement islands [151, 16], as discussed in the preceding chapters, provides evidence for unitary black hole evaporation, independently of AdS/CFT. It marks a new era in which the Page curve can be derived from gravitational physics directly. It does not, however, resolve the critical question of how the information escapes.

If we insist that information is preserved when a black hole evaporates, then effective field theory or General Relativity must break down substantially, at or outside of the horizon, at late times but while the horizon is still weakly curved [14]. This formulation of the information paradox is called the firewall paradox.

Stated succinctly, the firewall paradox [14, 138] is a tension between four widely accepted postulates about black hole evaporation:

1. *Unitary.* There is a unitary governing the dynamics of black hole formation and evaporation.

2. *Semi-classical field theory.* Physics outside the stretched horizon of a large black hole is well approximated by semi-classical field equations of a low energy EFT with local Lorentz invariance.

3. *Black Hole Entropy/Discrete Energy Levels.* To distant observers, a black hole behaves like a quantum system with discrete energy levels, where the dimension of the subspace of states is the exponential of the Bekenstein-Hawking entropy.

4. *No Drama.* An observer who falls freely across the horizon experiences nothing unusual.

Postulates (1) and (3) imply maximal entanglement between the late and early Hawking radiation, but postulates (2) and (4) imply that a portion of the late Hawking radiation is highly entangled with modes in the black hole interior. The full set of postulates, therefore, implies a violation of monogamy of entanglement for this portion of the late Hawking modes [14].

The firewall argument suggests that Hawking's "mistake" was the perfectly reasonable assumption that the horizon of a large old black hole is smooth. The AdS/CFT correspondence can be used to strengthen this argument [138], but it has shed no light on the bulk dynamics that would produce a firewall.

The bulk path integral derivation of the Page curve has been interpreted as a resolution of the firewall paradox [151, 18, 15, 17]. This seems plausible, since the bulk geometry involved in the calculation of the Page curve (Figure 1.1) has a manifestly smooth horizon. However, this picture just trades the firewall paradox for the state paradox [47] discussed in Chapter 3, the puzzling appearance of Hawking's result that the entropy of the radiation grows monotonically.

Then the question becomes how the state paradox is resolved. We see two possibilities. Suppose that the state paradox is resolved by gravity/ensemble duality, the proposal discussed in Chapter 3 that the gravitational path integral is dual to an ensemble of theories on the boundary. The firewall argument [14] does not apply to the ensemble-averaged state, since its evolution is not unitary. Therefore it is consistent for the horizon to be smooth. However, it is counterintuitive for Nature to be described fundamentally by an ensemble of unitary theories; it seems we could just measure the couplings and then work with the one correct theory. Moreover, we do expect the unique theory describing black hole formation and evaporation—the one that applies to an experiment conducted in a lab—to preserve information. The ensemble will be useful only for computing self-averaging quantities of the correct unitary theory, since these are the same in each theory; these evidently include the entropy, but not the final state. Hence the true S-matrix must be computed from a single unitary theory, not from an ensemble. In this theory, the firewall argument still applies.

If instead there is no gravity/ensemble duality (for example, in settings where no suitable ensemble exists, or where the gravity path integral cannot be rigorously defined), then the bulk path integral (or the saddlepoint approximation to it) would have to be viewed as an uncontrolled approximation. The path integral succeeds at computing certain quantities of a single unitary boundary theory (like the entropy) but not others (like the details of the late time state). Then there is no reason to trust the smooth geometry that appears in the input to the RT calculation, any more than we should trust the large entropy of the Hawking radiation that is manifest at this step. If we believe the output of the RT calculation—the Page curve—, then the firewall paradox precludes a smooth horizon.

It seems then, that the islands calculations of the Page curve have been a fruitful line of inquiry, but there are some questions they have thus far failed to answer. It is therefore still of interest to seek an independent resolutions of the firewall paradox.

Literature on the firewall paradox is vast and proposed resolutions numerous; see Refs. [13, 91] for a critical review. These proposals remain incomplete, and they appear to necessitate an element of nonlinearity that conflicts with the principles of quantum mechanics no less than information loss would [41, 42, 43]. Proposed resolutions include (i) modifying quantum mechanics [150, 131], (ii) allowing a breakdown of no drama [14], (iii) violating unitarity [91], (iv) identifying earlier Hawking radiation with the black hole interior [133], (v) modifying the interior geometry [139, 146, 105], (vi) invoking quantum complexity theory [93, 30, 29],

(vii) allowing for remnants [57], and (viii) violating locality [84, 147].

Many of these suggestions—in particular, options (ii), (iv), (v), (vi), and (vii)—appeal to the role of the horizon in effectively hiding a portion of the spacetime. In this chapter we present a version of the paradox that results in a manifest violation of monogamy of entanglement amongst modes at asymptotic infinity, in which none of the modes are hidden behind a horizon. This implies that hiding modes behind a horizon or appealing to strong gravitational effects are not sufficient resolutions. We argue that accounting for decoherence alleviates the tension.

6.1 The Thought Experiment

In broad strokes, our thought experiment consists of throwing a small black hole into a larger one and using the Hayden-Preskill protocol to recover the state of the smaller black hole. We argue that, given the above postulates and a qubit model of black holes, this yields a violation of monogamy of entanglement in states held only by the asymptotic observer.

Consider a black hole of mass M_1 formed from the collapse of matter in a pure state. As per Hawking's calculation [100, 101], the black hole will radiate maximally entangled pairs, one of which escapes the horizon and the other of which falls into the black hole interior. We model this black hole as a collection of N_1 qubits at its formation and its evaporation as the release of individual qubits into the environment [103]. The interior qubits undergo scrambling dynamics. We can factorize the total Hilbert space as:

$$\mathcal{H}_1 = \mathcal{H}_{\mathrm{BH}_1}(t) \otimes \mathcal{H}_{\mathrm{rad}_1}(t), \tag{6.1}$$

where $\mathcal{H}_{\mathrm{BH}_1}(t)$ corresponds to the Hilbert space of the remaining black hole and $\mathcal{H}_{\mathrm{rad}_1}(t)$ denotes that of the Hawking radiation after evolution for some time t.[1] The Hilbert space factors are time-dependent because qubits are transferred from the black hole to the radiation as the black hole evaporates. According to unitarity, the total state $|\psi_1(t)\rangle$ is pure at all times. Let us denote the state of the black hole and its Hawking radiation emitted up to time t as $\rho_{\mathrm{BH}_1}(t)$ and $\rho_{\mathrm{rad}_1}(t)$ respectively, each defined via a partial trace over the neglected system. Assume that the asymptotic observer has been collecting the radiation from this black hole since its formation.

Now suppose there is another, smaller black hole in this spacetime with mass $M_2 << M_1$, again modeled as a collection of N_2 qubits at its formation, evaporating via release of qubits. Assume that the asymptotic observer collects the radiation from this black hole until, at some time t_c after its Page time, it falls into BH_1.[2] The observer can identify which modes

[1] Although this evolution is truly time evolution, the choice of time coordinate is arbitrary [29]. In addition, one can use finite dimensional quantum information theory to describe black hole dynamics [25].

[2] One may be concerned that some radiation from BH_1 may fall into BH_2, preventing it from being collected. We can avoid this by placing the black holes in separate regions connected by an initially non-traversable wormhole. We can choose the momenta of the black holes and when the wormhole is made traversable such that the black holes collide at the appropriate time. To avoid complications with emission

correspond to which black hole by measuring the temperature.[3] After BH_2 has fallen into BH_1, the asymptotic observer continues collecting radiation emitted by BH_1. See Figure 6.2 for a summary of this sequence of events.

Hayden and Preskill demonstrated that it is information-theoretically possible for an observer outside a black hole to reconstruct the state of a quantum system (the "message") thrown into the black hole [103]. The observer first collects the Hawking radiation until they possess a system maximally entangled with the black hole, which occurs at the Page time. The message is then thrown into the black hole, which evolves via a deterministic unitary transformation that thoroughly and quickly mixes the message into the black hole's state. As the black hole continues to evaporate, the observer collects the radiation. The outside observer needs to collect only a few more qubits than the length of the original message to reconstruct it.

We choose that the state of the radiation released by BH_1 is maximally entangled with BH_1 at t_c. Our asymptotic observer therefore has the ingredients to perform the Hayden-Preskill protocol to recover the state of BH_2 when it fell into BH_1, $\rho_{\mathrm{BH}_2}(t_c)$. Recall that the asymptotic observer also collected the radiation from BH_2, which we can partition into "early" and "late" radiation corresponding to emission before and after the Page time of BH_2 respectively. Therefore, the asymptotic observer possesses the following states:

1. $\rho_{\mathrm{earlyRad}_2}(t_c)$, containing $N_2/2 + \delta$ qubits and defined from $\rho_{\mathrm{rad}_2}(t_c)$ by tracing out the qubits associated with the late radiation.

2. $\rho_{\mathrm{lateRad}_2}(t_c)$, defined from $\rho_{\mathrm{rad}_2}(t_c)$ by tracing out the qubits associated with the early radiation.

3. $\rho_{\mathrm{BH}_2}(t_c)$, reconstructed via the Hayden-Preskill protocol.

See Figure 6.2 for a circuit-style diagram of this scenario.

As we shall see, these systems exhibit a violation of monogamy of entanglement. Page's theorem [148] states that if we bipartition a statistically typical[4] quantum system into A and B with Hilbert space dimensions m and n respectively, and if $1 \ll m \leq n$, then

$$S_{m,n} \approx \ln m - \frac{m}{2n}. \tag{6.2}$$

This implies that if the joint system AB is pure and if m and n are very large, then the smaller subsystem is close to maximally mixed. In our setup, the qubits of (2) and (3) are

of radiation during transit through the wormhole, we can tune the wormhole to be very short, so that the transit time is much smaller than the expected time elapsed between emission of Hawking quanta. Alternatively, we could construct large Dyson spheres surrounding the black holes, which collect the HR from each of them until their point of collision.

[3]Or, the modes can be easily distinguished because the BH's have not yet been sent through the traversable wormholes and are therefore separate. Or if using Dyson spheres, the observer can see which Dyson sphere collected which mode.

[4]With respect to the Haar measure. For a more complete discussion, see [103, 26, 175].

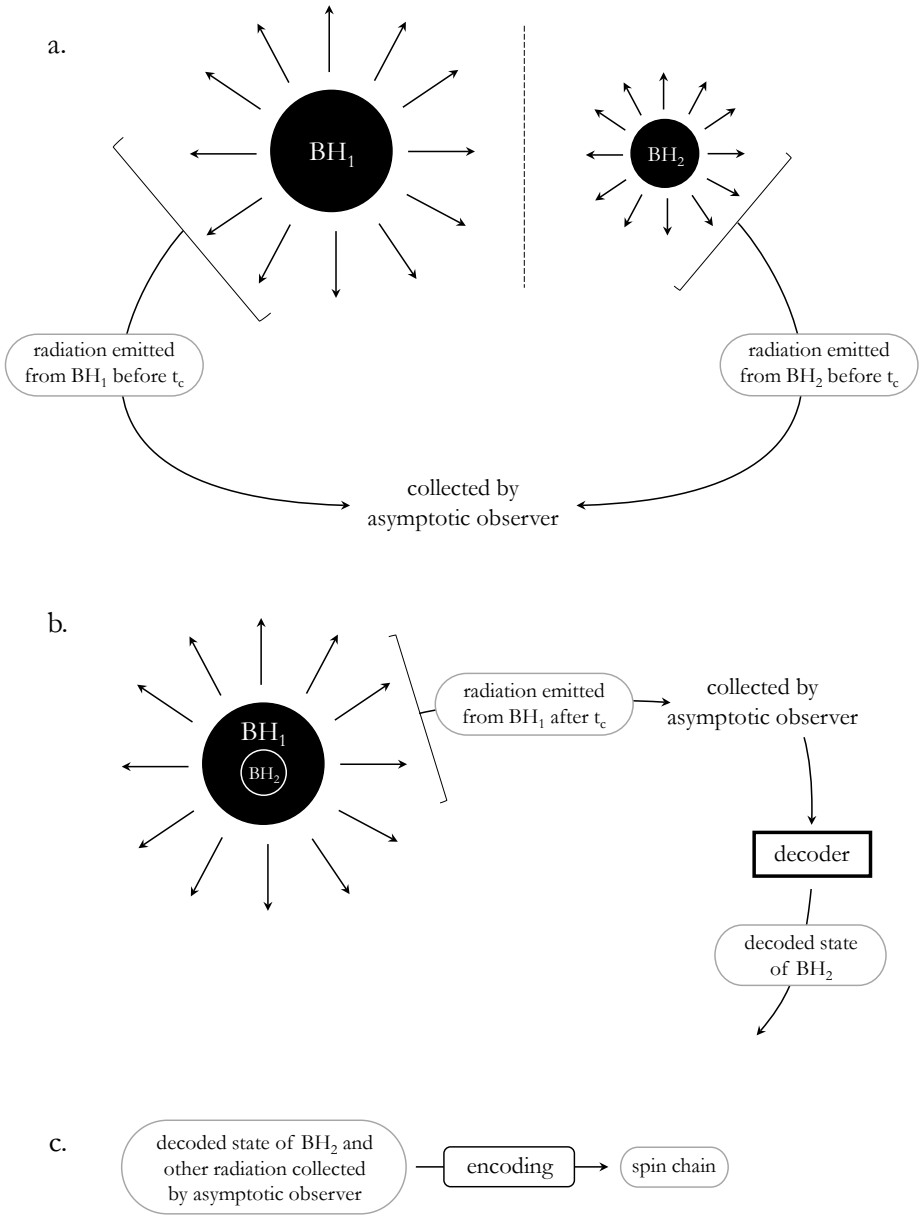

Figure 6.1: The three main steps of the thought experiment. *a.* The two black holes are initially in separate regions (see footnote 2), emitting Hawking radiation. The asymptotic observer collects the radiation emitted from both black holes. *b.* The BH_2 has fallen into BH_1. BH_1 continues to emit radiation, which is collected by the asymptotic observer. The observer runs this radiation (and the radiation previously collected from BH_1) through a decoder. *c.* Finally, all the radiation in the possession of the asymptotic observer (including the reconstructed state of BH_2) is encoded into a spin chain.

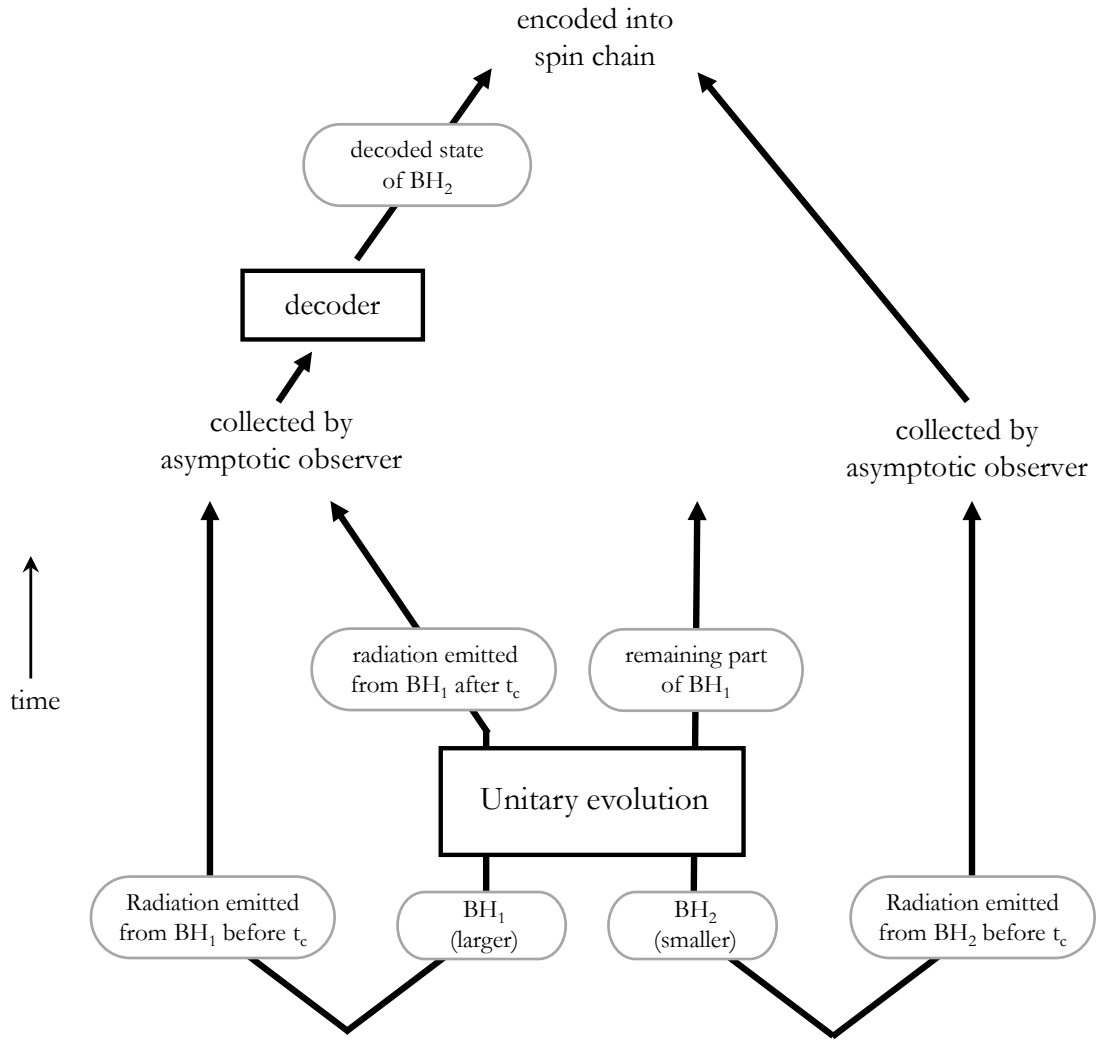

Figure 6.2: A diagram of the Hayden-Preskill protocol in which the "message" is another black hole. Black hole 1 (BH_1), the larger black hole, has been evaporating for a long time and has become maximally entangled with its previously emitted radiation. The "message" is the state of black hole 2 (BH_2), the smaller black hole, which is also maximally entangled with its previously emitted radiation. The message (BH_2) falls into BH_1 and the joint system evolves unitarily. More radiation is emitted from BH_1 and collected by the asymptotic observer. The asymptotic observer runs this radiation and the radiation previously emitted from BH_1 through a decoder to recover the state of BH_2. The asymptotic observer also collects the radiation emitted from BH_2 before it fell into BH_1.

A and the qubits of (1) are B of a pure joint system AB. We can apply Page's theorem by choosing appropriate system sizes. Therefore, the qubits making up subsystems (2) and (3) are maximally entangled with (1). A maximally mixed state has a diagonal density matrix, so $\rho_{2,3}$ is roughly diagonal. Tracing out the qubits of (3) thus yields a smaller-dimensional nearly diagonal density matrix for the qubits of (2). Therefore, (2) is nearly maximally entangled with (1).

Just before BH_1 swallows BH_2, Hawking's calculation implies a high degree of entanglement across the horizon of BH_2. Therefore, the qubits identified with the BH_2's interior and those identified with its radiation are highly entangled. Crossing the event horizon of BH_1 should not change the entanglement structure of BH_2's interior. Because the recovery procedure involves only LOCC operations (local operations and classical communication), the entanglement structure of (3) is the same as that of the original state. Therefore, subsystem (3) is highly entangled with (2). Because (2) is maximally entangled with (1), this is a violation of monogamy of entanglement. Therefore, the 3 subsystems held by the asymptotic observer exhibit a violation of monogamy of entanglement.

This thought experiment thus presents a sharp version of the firewall paradox for the *asymptotic observer*, who is free to manipulate these states, e.g. by encoding them in a spin chain, and has no time constraint on doing so. Therefore, no resolution to this paradox can rely on strong gravitational effects or on hiding something behind the black hole horizon.

6.2 A Proposed Resolution via Decoherence

In the spirit of [29, 28], we argue that accounting for decoherence resolves this paradox. Decoherence is the observation that quantum systems interacting with an environment become entangled with or, equivalently, leak information into said environment [195, 196, 87, 113]. Decoherence causes the system's density matrix to become nearly diagonal in a special basis, which is determined by details of the interaction. Frequently paired with decoherence is the Everettian view of quantum mechanics, which holds that measurement restricts the observer to a particular "branch" of the wavefunction corresponding to a measurement outcome.[5] The Everettian picture may seem to privilege an arbitrary basis for the decomposition of the global wavefunction into branches, but decoherence provides a particular basis in which the density matrix becomes essentially diagonal, corresponding to a superposition of classical macroscopic states.

For evaporating black holes, wavefunction branching occurs when something interacts with its released Hawking quanta, which have, for example, a range of possible outgoing

[5]The distinction between this view and wavefunction collapse is philosophical—the Everettian view asserts that the global wavefunction continues to exist post-measurement, while collapse-based interpretations deny this. Thus in the Everettian view, all measurement possibilities are realized within the global wavefunction as separate branches, hence the alternative name "Many Worlds interpretation." There is actually a family of related views, many of which are called the Everettian interpretation or the Many Worlds interpretation. Sometimes these terms refer to distinct views in this family, and other times they are conflated. The subtleties involved are not critical for our discussion.

momenta. A "definite geometry" requires a choice of momentum for each emitted Hawking mode and, by extension, a definite position and momentum for the black hole. The total state at non-asymptotic values of t describes an ensemble of these possible geometries [29]. A classical (definite) geometry exists only on a branch of the wavefunction. As the Hawking modes experience interactions, the state of the black hole decoheres into some preferred basis.

Fully defining the process by which BH_2 falls into BH_1 requires a definite point and time at which BH_2 crosses the event horizon of BH_1, thus requiring a definite geometry, or perhaps a projection to a subset of geometries. Therefore, an instance of this process must occur on a branch (or subset of branches) rather than on the global wavefunction. The asymptotic observer in our setup, however, sees the global wavefunction, which is a superposition of geometries. Therefore, the global observer cannot possess a definite reconstructed state $\rho_{BH_2}(t_c)$, meaning the global observer does not possess definite states in violation of monogamy of entanglement. Thus, accounting for decoherence resolves the paradox we have outlined in this work.

6.3 Chapter Summary and Conclusion

In this chapter, we have argued that the Page curve calculations of Refs. [151, 16] do not resolve the firewall paradox. We have outlined a thought experiment that puts a new perspective on the firewall paradox: an application of the Hayden-Preskill recovery protocol when the message is itself a smaller black hole. We showed that this thought yields a violation in monogamy of entanglement in the state held by the asymptotic observer. We have argued that properly accounting for decoherence resolves the paradox, because the global observer cannot hold a definite reconstruction of all the subsystems that together violate monogamy of entanglement.

This thought experiment involved the application of ideas from quantum information to shed light on understanding black holes. In the next chapter, we shall examine another concept from quantum information, Grover's search algorithm, and show how it connects to a conjecture relevant for black holes: the Eigenstate Thermalization Hypothesis.

Chapter 7

The Eigenstate Thermalization Hypothesis and Grover Search

Hayden and Preskill's protocol for recovering messages from a black hole via a quantum circuit and our discussion of decoherence in the previous chapter are not the only examples of the relevance of quantum information to black holes. Tensor networks [187, 96, 104, 157], quantum error correction [10, 92, 102, 8, 69, 77, 71, 94, 7], complexity [183, 186, 178, 165, 51, 40, 185], and other entropy measures [6, 7, 192] are just a few other examples of concepts from quantum information that have proven surprisingly pertinent for understanding gravity.

Another feature of black holes that we have yet to touch upon in this work is their connection to the Eigenstate Thermalizataion Hypthesis (ETH) [177, 68, 64, 67]. ETH is the conjecture that under certain conditions, nearby energy eigenstates behave like states drawn from the microcanonical ensemble with respect to certain "simple" observables. Because random microcanonical fluctuations are suppressed by system size, we can interpret ETH as a conjecture about state indistinguishability: each state in an ETH ensemble is hard to distinguish from the ensemble average using simple observables.

ETH is connected to black holes through holography: holographic CFTs are expected to be chaotic and thus satisfy ETH [27]. For example, Ref. [128] shows that the entropy of a black hole dual to a holographic CFT agrees with the entropy of the universal ETH density matrix in the low temperature/high energy limit. See Refs. [106, 50, 65] for further evidence along these lines and Ref. [27] for further discussion of the connection between black holes and ETH.

ETH is generally treated as a semi-empirical condition for state indistinguishability via measurement. As a rule of thumb, an ensemble with a density matrix that satisfies the ETH conditions (for some specification of simple observables) will behave like the microcanonical ensemble upon restriction to measurable observables, and its ensemble members will be indistinguishable via measurement. From the viewpoint of quantum information, however, these energy eigenstates are trivially distinguishable due to their orthogonality by the Holevo argument [107]. This might therefore seem to be a point of tension between the two approaches.

In this chapter, we show how this tension may be resolved by making two main points that draw upon the tools of quantum information. The first is that there is no conflict between the *in-principle* perfect distinguishability of energy eigenstates and the *in-practice* indistinguishability of eigenstates suggested by the ETH. As we will show, this difference can be simply understood using the information-theoretic language of quantum channels. Roughly, a macroscopic observer can be viewed as accessing the system only via a quantum channel which traces out fine-grained data about the system. We will demonstrate that for ETH ensembles this dramatically reduces the observed trace distance between states, realizing the operational constraints on the low-energy observer in terms of quantum information. Further, we partially invert this logic and deduce that exponential contraction of the trace distance between states implies ETH-like matrix elements. In our setup, a system where the ETH holds is thus roughly equivalent to a system where low-energy observers have difficulty telling things apart.

Our second main point is that ETH can be promoted from a semi-empirical belief to a formal complexity-theoretic statement about the difficulty of operationally distinguishing states after data restriction. We will show that the sharp lower bound on the complexity of Grover search given by BBBV [35] necessitates that distinguishing states in an ETH ensemble post-channel application takes exponentially many queries. Effective indistinguishability can therefore be understood precisely in the language of quantum complexity theory.

An outline of our argument is as follows:

1. Restriction to an algebra of simple operators (representing coarse-grained or IR observables) is uniquely equivalent to a partial trace channel [Eq. (7.5)].

2. For an ETH ensemble, the partial trace channel exponentially suppresses the trace distance between ensemble members [Eq. (7.20)]. Conversely, exponential suppression implies ETH-like matrix elements [Eq. (7.24)].

3. Grover search distinguishes states by increasing their trace distance, thereby prying them apart. The procedure takes exponentially many queries to pry apart exponentially close states [Eq. (7.34)] and is provably optimal for this task. The ETH is therefore itself lower-bounded (in our simple setup) to be exponentially hard by the lower complexity bound of distinguishing near-identical states implied by Grover search.

In Section 7.1, we review the relevant aspects of ETH and its connection to distinguishability. In Section 7.2, we describe our proposed coarse-graining quantum channel, discuss its connection to thermodynamics, and show that the channel exponentially suppresses the trace distance for an ensemble obeying the ETH. We also show the converse, namely that exponential suppression of trace distance implies ETH-like matrix elements. In Section 7.3, we review Grover search and its complexity bound, map it to the problem of state distinguishability, and show that Grover search requires exponentially many queries to distinguish exponentially suppressed states. This implies that restricting to coarse-grained observables in an ETH ensemble yields exponentially hard distinguishability, as well as the converse result that exponential hardness implies a simple form of the ETH.

7.1 A Review of the Eigenstate Thermalization Hypothesis

Statement of the Eigenstate Thermalization Hypothesis

The Eigenstate Thermalization Hypothesis (ETH) was originally introduced as a conjecture about the conditions required for a quantum system to thermalize (i.e. exhibit expectation values that agree with the microcanonical ensemble) [177]. The ETH states that the expectation values of observables for a quantum system with eigenstates $|E_i\rangle$ will evolve to those predicted by the microcanonical ensemble if the following two conditions on the observables are met: (i) the diagonal matrix elements $\langle E_i|\hat{\mathcal{O}}|E_i\rangle$ vary slowly with the state; and (ii) the off-diagonal matrix elements $\langle E_i|\hat{\mathcal{O}}|E_j\rangle,\ i \neq j$, are exponentially small in N, the number of degrees of freedom in the system [164].

In other words, the ETH is an ansatz for matrix elements of observables in the basis of the Hamiltonian's eigenstates. More formally, said ansatz is [164, 68, 64]:

$$\mathcal{O}_{ij} = \mathcal{O}(\bar{E})\delta_{ij} + e^{-S(\bar{E})/2} f_{\mathcal{O}}(\bar{E}, \omega) R_{ij} \ , \tag{7.1}$$

where $\bar{E} \equiv (E_i + E_j)/2$, $\omega \equiv E_i - E_j$, $S(E)$ is the thermodynamic entropy, and $\mathcal{O}(\bar{E})$ signifies the expectation value for the operator $\hat{\mathcal{O}}$ in the microcanonical ensemble at energy $\bar{E}$. Further, the ETH requires that $\mathcal{O}(\bar{E})$ and $f_{\mathcal{O}}(\bar{E}, \omega)$ are smooth functions of $\bar{E}$ and ω, and that R_{ij} behaves as a random variable with zero mean and unit variance (i.e. $\overline{|R_{ij}|^2} = 1$).

For an ensemble to satisfy the ETH, at least the vast majority of eigenstates must obey the above conditions. The "weak ETH" allows an exponentially small fraction of the eigenstates to violate the ETH, having significantly different expectation values from that of the microcanonical ensemble. On the other hand, the "strong ETH" states that $\mathcal{O}_{ii}$ is very close to that of the microcanonical ensemble for *all* the eigenstates. Because some models which do not thermalize (more precisely, some integrable models) satisfy the weak ETH, it is generally accepted that the strong ETH is required to characterize thermalization [68]. For our purposes, however, it will not matter whether we use the strong or weak version of ETH.

ETH and Distinguishability

The ETH condition on diagonal matrix elements is of the form [164, 68, 64]:

$$\mathcal{O}_{ii} = \mathcal{O}(\bar{E}) + R_{ii}, \tag{7.2}$$

where R_{ii} is small (i.e., suppressed by the system size). Because this fluctuation of the expectation value from that of the microcanonical ensemble is very small for each eigenstate $|E_i\rangle$, each eigenstate is essentially indistinguishable from the ensemble average (and, by extension, from the other eigenstates).

Although ETH is not expected to hold for all operators, the general belief is that ETH applies to operators confined to a local region, which contain only a few degrees of freedom,

and to low-point functions constructed from these operators, for most non-integrable systems [68]. This claim is supported by semi-empirical evidence, such as numerical simulations of lattice systems [64, 163, 173, 174, 118, 161, 162, 180, 36, 121, 181, 120, 37, 39, 166, 176, 143, 119, 82, 141], but the connection to low-energy restrictions on measurement and distinguishability has remained imprecise. In this work, we will provide a simple operator-algebraic interpretation of these low-energy operators, which formalizes and clarifies the expected loss of distinguishability.

7.2 Coarse-Graining the ETH

In this section, we introduce the coarse-graining quantum channel for a low-energy "algebraic" observer, and prove this channel is the unique coarse-graining compatible with our assumptions. We also motivate our choice from the perspective of entropy maximization in thermodynamics. Finally, we discuss the effect of applying our partial trace channel to an ETH ensemble, showing that trace distance is exponentially suppressed, and derive a partial converse statement: that exponential contraction leads to an ETH-like expansion for matrix elements.[1]

Coarse-Graining with Quantum Channels

A macroscopic observer interacting with a finite-dimensional quantum system $\mathcal{H}$ typically has access to some limited palette of coarse-grained observables, such as pressure and temperature in thermodynamics. We will assume the simple observables form an (operator or von Neumann) *algebra*, $\mathcal{A} \subseteq \mathcal{L}(\mathcal{H})$, containing the identity and closed under products and sums. Thus, we have an "algebraic" low-energy observer.

The *Wedderburn decomposition* [193] shows that such an algebra decomposes the full (assumed finite-dimensional) Hilbert space into irreducible representations of $\mathcal{A}$ as follows:

$$\mathcal{H} \simeq \left[\bigoplus_{\alpha} \mathcal{H}_{1,\alpha} \otimes \mathcal{H}_{2,\alpha}\right] \oplus \mathcal{H}_0 \tag{7.3}$$

$$M = \left[\bigoplus_{\alpha} M_{1,\alpha} \otimes I_{2,\alpha}\right] \oplus 0 \,, \tag{7.4}$$

for every $M \in \mathcal{A}$. Here, $I_{2,\alpha}$ is the identity on $\mathcal{H}_{2,\alpha}$, and $M_{1,\alpha} \in \mathcal{L}(\mathcal{H}_{1,\alpha})$. The zero terms are present to handle the case in which none of the operators in $\mathcal{A}$ are supported (i.e., act nontrivially) on some portion of the Hilbert space. We also write $\mathcal{H}_\alpha \equiv \mathcal{H}_{1,\alpha} \otimes \mathcal{H}_{2,\alpha}$, with dimensions $d_{1,\alpha}, d_{2,\alpha}$, and decompose arbitrary states as $\rho \equiv \bigoplus_\alpha p_\alpha \rho_\alpha \oplus p_0 \rho_0$. The bracketed term in the Wedderburn decomposition was named a *generalized bipartition* by [115]. The

[1] Our argument is similar in spirit to [72], and for a single superselection sector, follows as a special case, where the subsystem A is the low-energy factor.

individual summands (labelled by α) are analogous to superselection sectors [115] of commuting observables, whose associated projectors Π_α, along with the zero projection, form a partition of unity, $I = \Pi_0 + \sum_\alpha \Pi_\alpha$.

Here we will interpret each factor $H_{1,\alpha}$ as a macroscopic "IR" Hilbert space, and each $H_{2,\alpha}$ as a space of fine-grained, macroscopically unobservable "UV" data. Given this split, a natural quantum channel onto the IR is simply given by tracing out the UV Hilbert space $\mathcal{H}_{2,\alpha}$ in each summand:

$$\mathcal{C}_{\text{IR}} : \rho \mapsto \overline{\rho} \equiv \bigoplus_\alpha p_\alpha \operatorname{tr}_2[\rho_\alpha] \oplus p_0 \rho_0 \ . \tag{7.5}$$

It is easily confirmed that $\mathcal{C}_{\text{IR}}$ is indeed a quantum channel: $\mathcal{C}_{\text{IR}}$ is clearly linear and completely positive (it maps to a positive linear combination of densities), and we can check it is trace-preserving:

$$\operatorname{tr}[\overline{\rho}] = p_0 + \sum_\alpha p_\alpha = 1 \ ,$$

since the coefficients p_α, p_0 are normalized. Thus, $\mathcal{C}_{\text{IR}}$ is a linear CPTP map and hence a quantum channel. We will focus for simplicity on states with nontrivial support in a single sector α, but our results easily generalize. We will also largely ignore $\mathcal{H}_0$, since no operator in $\mathcal{A}$ has access to it. We picture the action of the partial trace on such a single sector in Figure 7.1.

We note that our partial trace is equivalent[2] to the restriction to the subalgebra $\mathcal{A}$ [22]. Among quantum channels, the partial trace is therefore singled out as the *minimal* way of discarding information about non-simple operators. Coarse-graining could perform additional unitaries on the UV factors, but these are not constrained by the low-energy algebra and hence non-minimal. We will give a thermodynamic justification for minimality in the next section. One could consider something more complicated than a quantum channel, but the *quantum Church-Turing thesis* [66] conjectures that Nature is only as powerful as a quantum computer. A quantum channel is the only way such a computer has to discard everything but a subalgebra.

Entropy Maximization and Tomographic Completeness

We can equivalently view $\mathcal{C}_{\text{IR}}$ as acting on the full Hilbert space. Denote $\rho_{1,\alpha} \equiv \operatorname{tr}_{2,\alpha}[\Pi_\alpha \rho]$ and $\rho_{2,\alpha} \equiv \operatorname{tr}_{1,\alpha}[\Pi_\alpha \rho]$. Then $\mathcal{C}_{\text{IR}}$ simply replaces each $\rho_{2,\alpha}$ with the maximally mixed state $I_{2,\alpha}/d_{2,\alpha}$. This relates our quantum channel interpretation of the ETH to the emergence of statistical mechanics from pure states, since the channel $\mathcal{C}_{\text{IR}}$ is closely related to *Jaynes' maximum entropy principle* [112], which Katz formulated more intuitively in terms "the truth, and nothing but the truth," as we review here [117]. Suppose a quantum-mechanical system can be prepared in state ρ, and the observer measures some set $\hat{\mathcal{O}} \in A$. Making measurements many times, they obtain a set of expectations ("the truth"):

$$\rho \mapsto \{R_{\mathcal{O}}(\rho) \equiv \operatorname{tr}[\hat{\mathcal{O}}\rho]\}_{\hat{\mathcal{O}} \in A} \ . \tag{7.6}$$

[2] Up to subtleties due to identical particles that are irrelevant here [22].

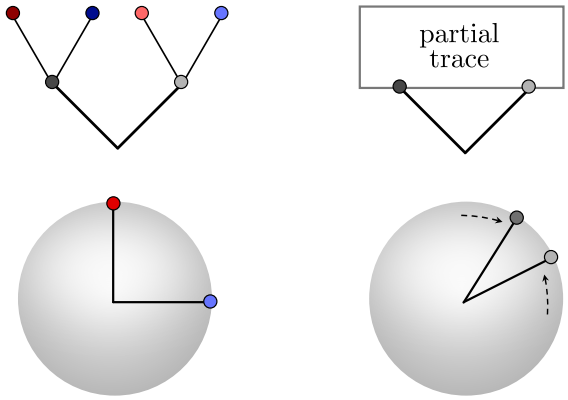

Figure 7.1: The coarse-graining in action, with shade representing the IR and hue the UV. Trace distance (Section 7.2) between two states is also shown. *Left:* Orthogonal states in the full tensor product. *Right:* After hue is traced out, states are less distinguishable.

Jaynes' principle states that the observer has most reason to believe the system is in the *maximum entropy state* ("nothing but the truth"):

$$\rho_{\text{MES}} = \text{argmax}_{R_{\mathcal{O}}(\hat{\rho})=R_{\mathcal{O}}(\rho)} S(\hat{\rho}) \ , \tag{7.7}$$

where $S(\rho)$ is the *von Neumann entropy*:

$$S(\rho) \equiv -\operatorname{tr}[\rho \log \rho] \ . \tag{7.8}$$

This can be maximized using Lagrange multipliers $\lambda_{\mathcal{O}}$ and an auxiliary Gibbs ensemble [117], yielding

$$\rho_{\text{MES}} \equiv \exp\left(\Omega - \sum_{\hat{\mathcal{O}} \in A} \lambda_{\mathcal{O}} \hat{\mathcal{O}}\right) \ ,$$

for a normalization constant Ω obeying

$$\Omega = -\log \operatorname{tr} \exp\left(-\sum_{\hat{\mathcal{O}} \in A} \lambda_{\mathcal{O}} \hat{\mathcal{O}}\right) \ , \quad \frac{\partial \Omega}{\partial \lambda_{\mathcal{O}}} = R_{\mathcal{O}} \ .$$

A derivation can be found in [117].

In general, the map $\rho \mapsto \rho_{\text{MES}}$ is not linear. But consider the set of observables A consisting of all those of the form

$$(\hat{\mathcal{O}} \otimes I_{2,\alpha}) \oplus I_0 \bigoplus_{\beta \neq \alpha} I_\beta \tag{7.9}$$

for some α and arbitrary $\hat{\mathcal{O}} \in \mathcal{L}H_{1,\alpha}$. We will abbreviate these operators as $\hat{\mathcal{O}} \otimes I_{2,\alpha}$. This is *tomographically complete* for $\mathcal{H}_{1,\alpha}$ in the sense that we uniquely recover $\rho_{1,\alpha}$ from the expectation values of the operators in A_α. In particular, we can use any orthonormal basis under the Hilbert-Schmidt inner product $\langle M_1, M_2 \rangle \equiv \mathrm{tr}[M_1 M_2^\dagger]$ to directly reconstruct the density matrix. To cap off Katz's phrase, tomographically complete sets capture "the whole truth". In this case, the Lagrange multiplier sum satisfies

$$\sum_A \lambda_{\mathcal{O}} (\hat{\mathcal{O}} \otimes I_{2,\alpha}) = \left(\sum_A \lambda_{\mathcal{O}} \hat{\mathcal{O}} \right) \otimes I_{2,\alpha} \ ,$$

and the normalization factor

$$\Omega_\alpha = \Omega_{1,\alpha} - \log d_{2,\alpha} \ .$$

Hence, the maximum entropy state is

$$\begin{aligned} \Pi_\alpha \rho_{\mathrm{MES}} &= \exp \left[\Omega_\alpha - \left(\sum_A \lambda_{\mathcal{O}} \hat{\mathcal{O}} \right) \otimes I_{2,\alpha} \right] \\ &= \exp \left(\Omega_{1,\alpha} - \sum_A \lambda_{\mathcal{O}} \hat{\mathcal{O}} \right) \otimes \frac{I_{2,\alpha}}{d_{2,\alpha}} \\ &= \rho_{1,\alpha} \otimes \frac{I_{2,\alpha}}{d_{2,\alpha}} \ , \end{aligned} \tag{7.10}$$

using tomographic completeness on the first factor.

The first term captures "the truth, the whole truth" (tomography on $\mathcal{H}_{1,\alpha}$) while the second factor captures "nothing but the truth" (entropy maximization on $\mathcal{H}_{2,\alpha}$). This result can be extended to the full sum over α, since tomographic completeness with respect to an orthonormal basis allows us to reconstruct both the densities ρ_α on each α but also their coefficients p_α, and entropy maximization proceeds on the second factor as before. Thus, our partial trace is entropy-maximizing in the sense of Jaynes, and can therefore be interpreted as a simple thermodynamic coarse-graining.

Contracting on Ensembles

Next we wish to demonstrate the effect of the coarse-graining channel on the distinguishability of states in an ETH ensemble. A natural measure of the distinguishability of quantum states is the *trace distance*, defined for densities ρ, σ by

$$D(\rho, \sigma) \equiv \frac{1}{2} \mathrm{tr} \, |\rho - \sigma| \ , \tag{7.11}$$

where $|M| \equiv \sqrt{M^\dagger M}$. In general, quantum channels $\mathcal{E}$ contract with respect to trace distance [144]:

$$D(\mathcal{E}(\rho), \mathcal{E}(\sigma)) \leq D(\rho, \sigma) \ . \tag{7.12}$$

Suppose we select ρ, σ from some ensemble of states $\mathbf{E}^{(\alpha)}$ in sector α, and apply $\mathcal{C}_{\text{IR}}$. Physically, we will interpret $\mathbf{E}^{(\alpha)}$ as the set of energy eigenstates spanning $\mathcal{H}_\alpha$.

If the $\mathbf{E}^{(\alpha)}$ are exact eigenstates of the full Hamiltonian H, then H must take diagonal form

$$H = H_0 + \sum_\alpha H_\alpha \ , \tag{7.13}$$

where each H_α acts on $\mathcal{H}_\alpha$. This means that projectors Π_α commute with time evolution, and matrix elements vanish for eigenstates in different sectors.

We consider ensembles obeying the ETH, meaning that "simple" operators $\hat{\mathcal{O}} \otimes I_{2,\alpha}$, for $|E_i\rangle, |E_j\rangle \in \mathbf{E}^{(\alpha)}$, have matrix elements of the form

$$\langle E_i | \hat{\mathcal{O}} \otimes I_{2,\alpha} | E_j \rangle = \mathcal{O}(\bar{E})\delta_{ij} + f_{\mathcal{O}}^{(\alpha)} e^{-S/2} R_{ij} \ . \tag{7.14}$$

Again, we will focus on a single sector α, with $S = \log d = \log d_{1,\alpha} d_{2,\alpha}$. We will take the size of the low-energy Hilbert space $d_{1,\alpha}$ to be small and fixed, and $d_{2,\alpha}$ to be large, so that asymptotic growth with respect to system size implies fixed $d_{1,\alpha}$ and increasing $d_{2,\alpha}$, so that $d_{2,\alpha} = \Omega(e^S)$ and $d_{1,\alpha} = \Omega(1)$.

As a warm-up, suppose the energy eigenstates $\mathbf{E}^{(\alpha)}$ are Haar-random, i.e. obtained from a reference state $|\psi^{(\alpha)}\rangle$ by applying k independent unitaries $U_i \in \mathrm{U}(\mathcal{H}_\alpha)$ chosen with Haar measure. Page's theorem [148] states that Haar-random states $\rho_{1,\alpha}(U) \equiv \mathcal{C}_{\text{IR}}(U\,|\psi^{(\alpha)}\rangle)$ are close to maximally mixed:

$$\begin{aligned} \int \mathrm{d}U \, D\left(\rho_{1,\alpha}(U), \frac{I_{1,\alpha}}{d_{1,\alpha}}\right) &\leq \frac{1}{2}\sqrt{\frac{d_{1,\alpha}^2 - 1}{d_{1,\alpha} d_{2,\alpha} + 1}} \\ &\leq \frac{1}{2}\sqrt{\frac{d_{1,\alpha}}{d_{2,\alpha}}} \ . \end{aligned} \tag{7.15}$$

From the triangle inequality for D, we find a bound on the Haar-averaged trace distance for $\rho, \sigma \in \mathbf{E}^{(\alpha)}$, after applying $\mathcal{C}_{\text{IR}}$:

$$\overline{D\left(\mathcal{C}_{\text{IR}}(\rho), \mathcal{C}_{\text{IR}}(\sigma)\right)} \leq \frac{1}{2}\sqrt{\frac{d_{1,\alpha}}{d_{2,\alpha}}} \ . \tag{7.16}$$

From our assumptions $d_{2,\alpha} = \Omega(e^S)$ and $d_{1,\alpha} = \Omega(1)$ in system size, we see that typical random states have their trace distance suppressed on the order of $e^{-S/2}$.

Subject to our assumptions about the dimension of the IR and UV factors, we will find a similar suppression from the perspective of the low-energy algebra in a moment. However, we note that for a generic set of IR observables, these assumptions are tantamount to taking an exponentially thin energy shell.[3]

[3]We thank Anatoly Dymarsky for discussion of this point.

This is not, in general, a realistic assumption for thermal systems, and more work is required to understand if (and whether) the algebraic decomposition can be used to make the sorts of constraints we are considering here. However, subject to these assumptions, the smoothness of the microcanonical average $\mathcal{O}(E)$ implies that differences in the leading-order variation of the diagonal terms in (7.14),

$$\mathcal{O}(E_i) - \mathcal{O}(E_j) \approx \mathcal{O}'(E)\,\omega \ ,$$

is also exponentially suppressed. Thus, fluctuations of the microcanonical average contribute at subleading order in (7.14), and we can restrict to matrix elements of the form

$$\langle E_i|\hat{\mathcal{O}} \otimes I_{2,\alpha}|E_j\rangle = \overline{\mathcal{O}}^{(\alpha)}\delta_{ij} + f_{\mathcal{O}}^{(\alpha)} e^{-S/2} R_{ij} \ . \tag{7.17}$$

This is analogous to the exponentially thin ETH ensemble considered in [72]. We call such superselection sectors *flat*. We will comment briefly on the more general case below.

By restricting to observables of the form $\hat{\mathcal{O}} \otimes I_{2,\alpha}$ and considering expectations, we implicitly apply our channel. Defining $\overline{\rho} \equiv \mathcal{C}_{\rm IR}(\rho)$, and $\rho_i \equiv |E_i\rangle\langle E_i|$, note that

$$\langle E_i|\mathcal{O} \otimes I_{2,\alpha}|E_i\rangle = \mathrm{tr}[\rho_i(\hat{\mathcal{O}} \otimes I_{2,\alpha})] = \mathrm{tr}[\overline{\rho}_i \hat{\mathcal{O}}] \ ,$$

since expectations on a tensor factor are given by expectations with respect to the reduced density. This is easily verified using the Schmidt decomposition. Thus, we have

$$\begin{aligned} \mathrm{tr}[(\overline{\rho}_i - \overline{\rho}_j)\hat{\mathcal{O}}] &= \langle E_i|\hat{\mathcal{O}} \otimes I_{2,\alpha}|E_i\rangle - \langle E_j|\hat{\mathcal{O}} \otimes I_{2,\alpha}|E_j\rangle \\ &= f_{\mathcal{O}}^{(\alpha)} e^{-S/2}(R_{ii} - R_{jj}) \ . \end{aligned} \tag{7.18}$$

To relate this to trace distance, we need to recall its variational form [144],

$$D(\rho,\sigma) = \frac{1}{2} \max_{-I \le \hat{\mathcal{O}} \le I} \mathrm{tr}[(\rho - \sigma)\hat{\mathcal{O}}] \ , \tag{7.19}$$

where $A \le B$ means $B - A$ is positive semidefinite, or equivalently, the eigenvalues of $\hat{\mathcal{O}}$ lie between -1 and 1. If we unit normalize the operators $\hat{\mathcal{O}} \in \mathcal{A}$, and assume the variance $f_{\mathcal{O}}^{(\alpha)} = \Omega(1)$ in the system size, then the trace distance is controlled by the maximum of random diagonal matrix elements in (7.18). (Note that the maximum is attained by an observable of the form $\hat{\mathcal{O}} \otimes I_{2,\alpha}$ since the operators are of this form by (7.4).)

Although R_{ij} has mean zero and unit variance by assumption, we are making $d = e^S$ independent draws, and the maximum will depend on S. We can define the expected maximum value x_d as the point where the tail of the cumulative distribution function (cdf) equals $1/d$:

$$1 - F(x_d) = \frac{1}{2}\left[1 - \frac{1}{\sqrt{2}}\mathrm{erf}(x_d)\right] = \frac{1}{d} \ ,$$

where $F(x)$ is the cdf of R_{ii}, presumed Gaussian. Taking d and hence x_d large, the standard large argument asymptotics for $\mathrm{erf}(x)$ give

$$x_d \sim \sqrt{\log d} = \sqrt{S} \ .$$

There are subleading corrections we can ignore. In the large sample limit, the Fisher-Tippett theorem [159] shows this estimate is asymptotically sharp, and independent of the nature of the identically distributed zero mean, unit variance draws.[4] Combining with (7.18), we find

$$D(\overline{\rho}_i, \overline{\rho}_j) = \Omega(\sqrt{S} e^{-S/2}) \ . \tag{7.20}$$

One can set a pair of constants k and k' in the exponent such that $e^{-kS} \leq \sqrt{S} e^{-S/2} \leq e^{-k'S}$ as S becomes asymptotically large. Thus, passing the flat ETH ensemble through our quantum channel results in exponential contraction.

For the more general, i.e non-flat, condition (7.14), a similar calculation gives the trace distance for $\overline{\rho}_i, \overline{\rho}_j$ in terms of the size of the energy window ΔE and the system size:

$$D(\overline{\rho}_i, \overline{\rho}_j) = \Omega(\omega) + \Omega(e^{-S/2}) \ ,$$

Thus, in general, the suppression of trace distance will depend width of the energy windows corresponding to a superselection sector. For an $O(1)$ energy window, we generically expect *polynomial* suppression of trace distance

$$D(\overline{\rho}_i, \overline{\rho}_{\mathrm{micro}}) = O\left(\frac{1}{p(S)}\right) \ ,$$

for some polynomial in S [72].

A Partial Converse

We can ask whether the converse holds, i.e. that exponential suppression of trace distance implies an ETH-like form for the matrix elements.

It is clear from (7.19) and (7.20) that diagonal matrix elements for energy eigenstates can only *differ* by terms suppressed by $e^{-S/2}$. This means we have the flat diagonal expectations, as per (7.17). To fix the leading order behaviour, we simply note that these diagonal elements are close to each other, and hence the ensemble average $\overline{\mathcal{O}}^{(\alpha)}$. More carefully, we can define a microcanonical density

$$\rho_{\mathrm{micro}} = e^{-S} \sum_i |E_i\rangle\langle E_i| = e^{-S} \sum_i \rho_i \ .$$

[4] This is analogous to the central limit theorem, so it is sometimes called the *max central limit theorem*. There are various technical niceness conditions on the distributions, but we will not belabor them here.

Then, by linearity of the channel, $\overline{\rho}_{\text{micro}} = e^{-S}\sum_j \overline{\rho}_j$ and hence

$$\begin{aligned} D(\overline{\rho}_i, \overline{\rho}_{\text{micro}}) &= \frac{1}{2}\sup_{\hat{\mathcal{O}}} \text{tr}[(\overline{\rho}_i - \overline{\rho}_{\text{micro}})\hat{\mathcal{O}}] \\ &= \frac{1}{2}\sup_{\hat{\mathcal{O}}} \sum_j e^{-S}\,\text{tr}[(\overline{\rho}_i - \overline{\rho}_j)\hat{\mathcal{O}}] = \Omega(e^{-S/2}) \ . \end{aligned}$$

Thus, for any eigenstate i, $\langle\hat{\mathcal{O}}\rangle_i \approx \overline{\mathcal{O}}$ up to corrections of order $e^{-S/2}$.

We still need to constrain off-diagonal elements. Let us first consider the implications of the ETH assumption. Define the "rotated" states $|E_{i\pm j}\rangle \equiv (|E_i\rangle \pm |E_j\rangle)/\sqrt{2}$, with densities

$$\rho^{\pm}_{ij} \equiv |E_{i\pm j}\rangle\langle E_{i\pm j}| \ . \tag{7.21}$$

Then the difference of these densities gives the off-diagonal elements:

$$\rho^{+}_{ij} - \rho^{-}_{ij} = |i\rangle\langle j| + |j\rangle\langle i| \ . \tag{7.22}$$

The ETH assumption implies

$$\text{tr}[(\rho^{+}_{ij} - \rho^{-}_{ij})(\hat{\mathcal{O}} \otimes I_{2,\alpha})] = \text{tr}[(\overline{\rho}^{+}_{ij} - \overline{\rho}^{-}_{ij})\hat{\mathcal{O}}] = f^{(\alpha)}_{\mathcal{O}} e^{-S/2}(R_{ij} + R_{ji}) \ ,$$

which by similar arguments is $\Omega(e^{-S/2})$. Going in the reverse direction, we learn that if the trace distance between $\rho^{\pm}_{ij}$ is exponentially contracted, then

$$\langle i|\hat{\mathcal{O}}|j\rangle + \langle i|\hat{\mathcal{O}}^{\dagger}|j\rangle = O(e^{-S/2}) \ . \tag{7.23}$$

For Hermitian $\hat{\mathcal{O}}$, this is precisely the scaling we expect for off-diagonal ETH elements.

Thus, combining the trace distance constraints on the reduced densities for $|E_i\rangle, |E_j\rangle \in \mathbf{E}^{(\alpha)}$, we have the ETH-like matrix elements for Hermitian operators[5]

$$\langle i|\hat{\mathcal{O}}|j\rangle = \overline{\mathcal{O}}^{(\alpha)}\delta_{ij} + e^{-S/2}A_{ij} \ , \tag{7.24}$$

for $A_{ij} = O(1)$ in system size. For a general, i.e. non-flat superselection sector, leading-order variations in the micronical average $\mathcal{O}(E)$ prevent this clear-cut identification of terms in an e^{-S} expansion.

7.3 Distinguishing Exponentially Close States

The results of the previous section show that application of our coarse-graining channel to an ETH ensemble yields exponentially-suppressed trace distance among the members

[5]This resembles the Knill-Laflamme-like [122] condition for approximate quantum error correcting codes (AQECC) given in [49]. However, in our case, the natural code subspace $\mathcal{H}_\alpha$ also controls the ETH suppression (rather than the full Hilbert space), so we do not obtain a good AQECC.

of the resulting ensemble. We were further able to establish a partial converse result: a coarse-graining map that yields exponential suppression implies ETH-like matrix elements for simple operators.

In this section, we move from information-theoretic to complexity-theoretic considerations. We connect the query complexity lower bound of Grover search to the hardness of distinguishing ETH ensemble states after coarse-graining. The Grover search algorithm [88] is a quantum search algorithm for a marked item in an unstructured data set. As will be discussed in the review below, it is quadratically faster than the fastest known classical algorithm (which runs in $O(N)$ time), running in $O(\sqrt{N})$ time.

While this modest but important speedup would usually not be considered significant in quantum algorithms, its importance lies in the fact that it is provably tight: both the query complexity—the number of queries an algorithm must make before reaching an answer—and the gate complexity—the number of required gates—of Grover search are the most efficient theoretically possible for the unstructured search problem, even up to the leading pre-factor [35]. As such, if something requires violating the query complexity or gate complexity lower bound for Grover search, it is often tantamount to a significant modification of quantum mechanics, as discussed for example in [24].

In particular, we note that because distinguishability of the pure states is easier than mixed state distinguishability for mixed states, we restrict our attention in searching for a lower bound on ETH distinguishability by focusing on hypothetical pure states that are outputs of the coarse graining quantum channel. This is not to ascribe any physical significance to the Grover search algorithm used or the existence of the reflection operator therein, but rather to use this method to provide a conservative but still substantial lower bound to the complexity of ETH distinguishability.

Review of Grover's Search Algorithm

We begin with a review of Grover search in the context of the simple search problem it was originally designed to solve [88, 144]. Suppose one aims to find a particular element in an unsorted set of size N. Given that the set has no structure, the most efficient classical method is to cycle through all the elements in the set one-by-one. Therefore, the classical solution to this search problem runs in $O(N)$ time.

Grover search is a quantum algorithm that solves the same search problem with only $O(\sqrt{N})$ operations. An outline of the algorithm is as follows [144]:

a. Start with the state $|0\rangle^{\otimes n}$.

b. Apply the Hadamard transform, which produces the superposition state $|\psi\rangle = \frac{1}{N^{1/2}} \sum_{x=0}^{N-1} |x\rangle$.

c. Repeatedly apply Grover iteration.

Grover iteration consists of the following steps:

1. Apply the "oracle" operator O, which marks the desired item by shifting its phase. The oracle takes the state $|x\rangle$ to $(-1)^{f(x)}|x\rangle$, where $f(x) = 1$ if x is a solution to the problem and $f(x) = 0$ otherwise.

2. Apply the Hadamard transform.

3. Perform a phase shift of -1 on all states except $|0\rangle$. One can achieve this by acting on the state with the operator $2|0\rangle\langle 0| - I$.

4. Apply the Hadamard transform again.

In summary, Grover iteration is an application of the operator

$$G = (2|\psi\rangle\langle\psi| - I)\,O\ . \tag{7.25}$$

If one visualizes quantum states as vectors on the Bloch sphere, Grover iteration has an intuitive geometric visualization (see Figure 7.2) [144]. We can re-express the starting quantum state $|\psi\rangle$ in terms of (i) a state $|\beta\rangle$ that is the normalized sum of solutions to the search problem and (ii) a state $|\alpha\rangle$ that is the normalized sum of states that are *not* solutions to the search problem. Defining an angle θ in terms of the total number of states (N), and the number of solutions to the search problem (M) via $\cos(\theta/2) = \sqrt{(N-M)/N}$, the initial state is:

$$|\psi\rangle = \cos\frac{3\theta}{2}|\alpha\rangle + \sin\frac{3\theta}{2}|\beta\rangle\ . \tag{7.26}$$

Each application of the Grover iteration operator (G) effects a rotation in the space spanned by $|\alpha\rangle$ and $|\beta\rangle$ by the angle θ. After k Grover iterations, the rotated state is

$$|\psi'\rangle = \cos\left(\frac{2k+1}{2}\theta\right)|\alpha\rangle + \sin\left(\frac{2k+1}{2}\theta\right)|\beta\rangle\ . \tag{7.27}$$

Thus, repeated Grover iterations rotate the state closer and closer to $|\beta\rangle$, the sum of solutions to the search problem.

Once the component parallel to $|\beta\rangle$ is greater than the component parallel to $|\alpha\rangle$, a measurement is more likely to produce a solution to the search problem than not. Expressing the nearest integer to some real number x as the function $\mathrm{CI}(x)$, the number of Grover iterations required to achieve this is

$$R = \mathrm{CI}\left(\frac{\arccos\sqrt{M/N}}{\theta}\right) \leq \left\lceil\frac{\pi}{4}\sqrt{N/M}\right\rceil\ . \tag{7.28}$$

Grover search therefore requires $O(\sqrt{N/M})$ iterations (or $O(\sqrt{N})$ iterations if there is only one solution to the search problem), making it more efficient than the classical algorithm [88, 144].

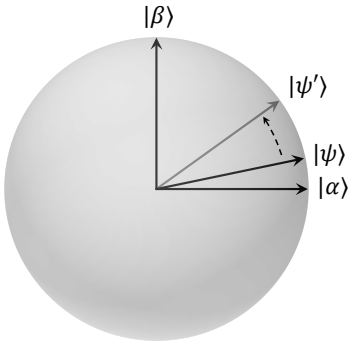

Figure 7.2: Geometric visualization of Grover iteration. States are represented as vectors on the Bloch sphere. Each application of Grover iteration rotates the initial state $|\psi\rangle$ toward the normalized sum of solutions to the search problem, $|\beta\rangle$.

What makes Grover search of particular interest is that the complexity bound of $O(\sqrt{N})$ is provably optimal; no other search algorithm can complete the task in fewer operations, nor with fewer queries [35, 144]. A sketch of the proof is as follows. Suppose we have some quantum algorithm that applies the oracle for a given search solution x and some set of unitary operations U_i such that, after k applications of the oracle, it produces the state

$$|\psi_k^x\rangle \equiv U_k O_x U_{k-1} O_x ... U_1 O_x |\psi\rangle \ . \tag{7.29}$$

One can prove that Grover search is optimal by examining the magnitude of the effect of the oracle, or, more precisely, the deviation from the state that would have evolved in the absence of the oracle. Defining the state evolved without the oracle as

$$|\psi_k\rangle \equiv U_k U_{k-1} ... U_1 |\psi\rangle \ , \tag{7.30}$$

the deviation after k steps is defined as

$$D_k \equiv \sum_x \left|\left|\psi_k^x - \psi_k\right|\right|^2 . \tag{7.31}$$

If this deviation is small, then the component parallel to $|\beta\rangle$ is not yet larger than the component parallel to $|\alpha\rangle$. Therefore, a small deviation implies that a solution to the search problem is not yet identifiable. The proof of optimality requires showing that (i) the deviation after k steps (D_k) obeys $D_k \leq 4k^2$ and (ii) the probability of identifying the search solution is greater than $1/2$ only if D_k is $\Omega(N)$. Taken together, (i) and (ii) imply that the requisite number of oracle calls obeys $k \geq \sqrt{cN/4}$. Therefore, solving the search problem requires calling the oracle $\Omega(\sqrt{N})$ times. As this is the complexity lower bound of Grover search, Grover search is an optimal solution to the search problem [35, 144].

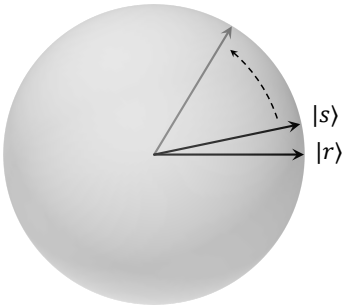

Figure 7.3: Geometric visualization of distinguishing states $|s\rangle$ and $|r\rangle$ via Grover search. States are represented as vectors on the Bloch sphere. Grover iteration rotates $|s\rangle$ away from $|r\rangle$.

Grover Search for Distinguishing States with Exponentially Suppressed Trace Distance

Although the above review of the Grover algorithm is framed in terms of a search problem, the method translates to the problem of distinguishing two quantum states. In the latter case, the two states to be distinguished, $|r\rangle$ and $|s\rangle$, play the roles of $|\alpha\rangle$ and $|\psi\rangle$ respectively. The function of Grover iteration is to rotate state $|s\rangle$ away from $|r\rangle$ until a measurement produces a state that is not $|r\rangle$ with probability greater than $1/2$. See Figure 7.3 for a visualization on the Bloch sphere.

The number of Grover iterations required to pry apart the states depends on how similar the states were originally. As mentioned previously, a measure of the similarity between (or distinguishability of) two quantum states is the trace distance, defined for two states with density matrices ρ and σ as

$$D(\rho, \sigma) \equiv \frac{1}{2} \operatorname{tr} |\rho - \sigma| \ , \tag{7.32}$$

where $|M| \equiv \sqrt{M^\dagger M}$ [144]. If the two states are single qubits, one can express the trace distance in terms of their Bloch vectors $\overrightarrow{r}$ and $\overrightarrow{s}$ as:

$$D(\rho, \sigma) = \frac{|\overrightarrow{r} - \overrightarrow{s}|}{2} \ . \tag{7.33}$$

Thus the trace distance for qubits is the Euclidean distance between their Bloch vectors up to a multiplicative factor. In other words, smaller trace distance between two states means they are closer together on the Bloch sphere.

Our aim is to find a lower bound on the hardness of distinguishing states after application of the channel defined in Section 7.2. To do so, we must compute roughly how many Grover

iterations are required to distinguish $|s\rangle$ from $|r\rangle$ given that their trace distance is exponentially suppressed. To relate the initial trace distance between the vectors to the number of Grover iterations required to pry them apart, we note that the initial trace distance D is related to the initial angle θ_{rs} between the Bloch vectors $\overrightarrow{r}$ and $\overrightarrow{s}$ via

$$D^2 = \frac{1}{4}|\overrightarrow{r} - \overrightarrow{s}|^2 = \frac{1}{2}(1 - \cos\theta_{rs}) \ , \tag{7.34}$$

assuming $\overrightarrow{r}$ and $\overrightarrow{s}$ are normalized. We are interested in the case where the states $|r\rangle$ and $|s\rangle$ are very similar, so we can expand $\cos\theta_{rs}$ to see that

$$\begin{aligned} 1 - \frac{\theta_{rs}}{2} &\approx 1 - 2D^2 \\ \implies \quad \theta_{rs} &= 2D \ . \end{aligned}$$

As defined in the previous section, the rotation angle of Grover iteration is related to the initial angle between $\overrightarrow{r}$ and $\overrightarrow{s}$ by $\theta = 2\theta_{rs}$. Successfully distinguishing the states occurs when the angle between $\overrightarrow{r}$ and the post-rotation vector $\overrightarrow{s}'$ obeys $\theta_{rs'} = \frac{\theta}{2} \geq \frac{\pi}{4}$. Assuming that the initial angular separation θ_{rs} is small, this will require rotating through approximately $\frac{\pi}{4}$ radians. Therefore, we must apply approximately $\frac{\pi}{16D}$ Grover iterations to distinguish the states. Assuming D is exponentially small, this corresponds to exponentially many Grover iterations.[6] Therefore, because Grover search is optimal, distinguishing two states with exponentially suppressed trace distance requires exponentially many queries.

Let us now consider the states that are separated from their ensemble average by an exponentially suppressed trace distance, after the partial trace channel has been implemented. Although the above discussion focused on single-qubit states, it is a straightforward extension of this result that mixed states on more than one qubit (as opposed to the single qubit described by the Bloch sphere) will similarly require an exponential number of queries to distinguish between them, as the amplitude amplification aspect of Grover search functions in an identical manner. The BBBV result [35] still applies to the mixed-state amplification problem [38], as the difficulty of distinguishing the mixed states which are the generic output of the coarse-graining channel is lower-bounded by the difficulty of distinguishing pure states in the IR Hilbert space by the data processing inequality. Recall that the ETH states that upon restricting to low point functions (e.g. applying the partial trace quantum channel) it becomes "hard" to distinguish a state in an ETH-obeying ensemble from the ensemble average. Relating this difficulty to the query complexity of Grover search is a straightforward way of quantifying this "hardness" in more precise language. As such, this is a complexity-theoretic way of seeing why states in ETH ensembles are difficult to distin-

[6] If this suppression is only inverse polynomial, this requires correspondingly polynomially many Grover iterations. For states in quantum field theories of very large numbers of qubits, this is still in practice a very long run time.

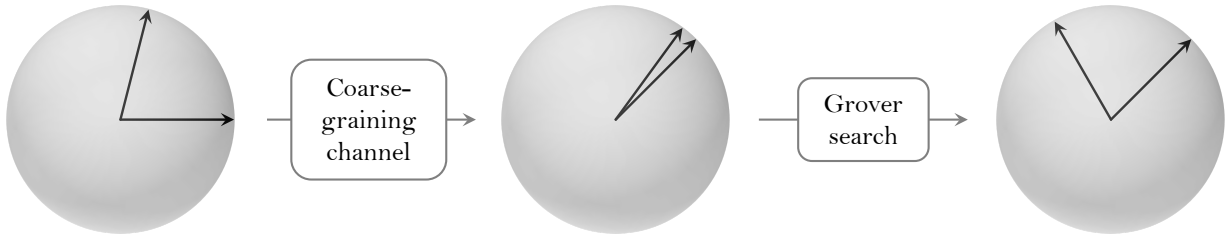

Figure 7.4: Classifying the hardness of ETH with quantum channels. A partial trace channel coarse-grains UV data and suppresses trace distance for some ensembles. Grover search pries apart states in the ensemble and makes them distinguishable.

guish from each other, especially once the additional overhead from implementing the data processing inequality is considered.[7]

Elegantly, there is also room for non-ETH states in this picture; they are simply the states that, upon the partial trace operation, are not exponentially close in trace distance from some canonical state that one is attempting to distinguish it from.

Conversely, it is immediate from the tightness of the BBBV lower bound that if density matrices take exponentially many queries to distinguish using Grover search, they must be exponentially close in trace distance. In particular, if this holds both for the reduced densities of eigenstate $\overline{\rho}_i = \mathcal{C}_{\text{IR}}(|E_i\rangle\langle E_i|)$, $|E_i\rangle \in \mathbf{E}^{(\alpha)}$, and "rotated" reduced densities $\overline{\rho}^{\pm}_{ij} = \mathcal{C}_{\text{IR}}(|E_{i\pm j}\rangle\langle E_{i\pm j}|)$, then the results of Section 7.2 immediately give the ETH-like expansion of matrix elements (7.24).

7.4 Chapter Summary and Conclusion

In this chapter, we showed that the orthogonality (and hence perfect distiguishability à la Holevo [107]) of eigenstates is compatible with near indistinguishability when passed through a quantum channel. In our model, the quantum channel is a generalized partial trace, and the algebra of observables on the remaining Hilbert space factors the set of simple operators for the purposes of ETH. This channel has a simple thermodynamic interpretation in the spirit of entropy maximization and Jaynes' principle. Furthermore, for an ensemble of eigenstates obeying the ETH, exponential suppression of energy differences in a coarse-grained window results in exponential suppression of trace distance.

[7]It is worth noting here that we do not consider the complexity of implementing the quantum channel, this result should technically only be considered an argument that the difficulty of distinguishing such states is *at least* exponentially hard.

Although closeness in trace distance already suggests hardness of distinction from a quantum information-theoretic viewpoint, we further lower bounded this hardness via a combination of the data-processing ienquality and a complexity-theoretic perspective using Grover search. The BBBV lower bound on search algorithms [35] shows the optimality of Grover search, and hence the task of telling apart our exponentially close ETH states will require at least an exponential number of queries. See Figure 7.4 for a visual summary.

Finally, we were able to reverse partially the logic of these steps. If states require an exponential number of queries to distinguish, it follows they are exponentially close in trace distance. If our coarse-graining channel exponentially suppresses the trace distance between reduced eigenstates, then they exhibit ETH-like matrix elements for simple operators. Loosely speaking, hardness of distinction is equivalent to the ETH.

This chapter concludes the main body of this work. In the final chapter, we shall discuss some implications of our results and propose future lines of inquiry.

Chapter 8

Discussion and Future Directions

In this work, we have taken steps to further the quest for quantum gravity. In light of the derivation of the Page curve for an evaporating black hole using the RT (QES) prescription [151, 16], we carefully generalized the RT prescription to the relevant unusual settings in Chapter 2. The first was the case where the reference region is part of a non-gravitating auxiliary system. Unlike in [151, 16], our derivation here did not rely on the assumption of entanglement wedge complementarity. Rather, entanglement wedge complementarity was a consequence of our results. The second case was that of double holography, where the matter in a gravitating spacetime is assumed to be holographic and thus has its own bulk dual one dimension higher. Here we clarified the three levels of holography and defined an "RT-squared" prescription that allowed one to compute von Neumann entropies in the lowest-dimension level in terms of quantities in the highest-dimensional level. Finally, we generalized the prescription to the case of double holography with a holographic bath, which is relevant for doubly-holographic derivations of the Page curve [18, 167, 55, 12, 182, 21, 56].

In Chapter 3, we used these generalizations of the RT prescription to investigate an apparent puzzle in the Page Curve calculations of [151, 16]: that the calculation makes use of Hawking's result that the entropy of the radiation grows monotonically, only to reach the final conclusion that it does not. We called this puzzle the state paradox and exhibited it in three settings. The first was an evaporating black hole surrounded by a distant detector sphere, originally introduced in [47]. The second was the setting of [151, 16]: a spacetime containing a black hole, coupled to an auxiliary system that absorbs the Hawking radiation. Finally, we exhibited the paradox in the doubly holographic setting introduced in [18].

In each case, we argued that the paradox is resolved under the conjecture that the gravitational path integral is dual to an *ensemble* of theories on the boundary. We called this proposal gravity/ensemble duality.

The mere existence of an ensemble on the boundary was sufficient to resolve the state paradox in each setting we considered. In this work, we thus did not specify more precisely what this ensemble might be. To provide further support that gravity/ensemble duality is the right solution to the state paradox, it would be desirable to define the relevant ensemble more concretely. Other works have explored the role of ensembles in holography, such in the

connection between the SYK model and JT gravity [172] and in the relationship between baby universes and wormholes [137]. A first step could be to investigate whether these ensembles are sufficient to play the role of that required to resolve the state paradox.

Furthermore, as discussed in Chapter 3, it seems that we have examples of holography that do not involve gravity/ensemble duality. A noteworthy example is type IIB supergravity on $\mathrm{AdS}_5 \times \mathbf{S}^5$, which is dual to a specific CFT [134]. Perhaps this can be explained in that the gravitational path integral computes quantities that *would* be self-averaging if an ensemble *did* exist [172], such as the entropy $S(\rho_{\mathrm{out}})$ but not the state ρ_{out}. It would be desirable, however, if something more compelling could be said about the relationship between this classic example of holography and gravity/ensemble duality. We leave this open question to future work.

Having discussed the state paradox, this work then turned to examining what could be learned from the Page curve calculations in the context of cosmology. In the spirit of [95], we searched for islands in FRW cosmologies with non-zero spatial curvature in Chapter 4. To the three necessary conditions for islands derived in [95], we added a fourth that applied only to subsets of closed universes. We then checked when regions in these cosmologies satisfied necessary conditions to be islands. We found that arbitrarily small positive curvature guarantees that the entire universe was an island. We showed that proper subsets of the time-symmetric slice of closed or open universes can be islands, but only if the cosmological constant is negative and sufficiently small.

In Chapter 5, we further extended this analysis to FRW cosmologies with a general perfect fluid, dispensing with the assumption that the universe contents were radiation. We rearranged the necessary conditions for islands derived in Refs. [95, 76] and the previous chapter as conditions on the comoving entropy density s_c, which is constant in time under the assumption of local thermal equilibrium. In flat universes, we found that time-symmetric slices always have viable island candidates for large enough χ, and these candidates will be islands in the thermofield-doubled model if the reference region is chosen to be the matching region R in M_R. For an arbitrary time slice t_0 in a flat universe, we found viable island candidates given that T_0 and ρ_0 are tuned appropriately. Treating the normalization time t_0 as an initial time and evolving forwards, we found that even under the assumption that there was no viable island candidate at t_0, a flat universe with a perfect fluid develops a viable island candidate provided that $w \geq 1$ violating the DEC. Furthermore, $w > 1$ implies that the t_0 slice will eventually evolve into a slice with a viable island candidate. Evolving backwards in time we found the opposite condition of $|w| < 1$ for a viable island candidate and again a condition on the temperature T_0 and the energy density ρ_0. Finally, we repeated the analysis on closed and open universes with a general perfect fluid. In the presence of spatial curvature, in an expanding universe with monotonically growing a, we found that viable island candidates can only exist at the time of normalization or in the past $t \leq t_0$ or up to some finite time after t_0, regardless of the equation of state w. We applied the conditions to a specific example of a closed universe with a periodic scale factor and no classical singularity, the "Simple Harmonic Universe," and found viable island candidates on slices near where the scale factor reaches a minimum. Hence, this is an example where

islands exist in a spacetime without a singularity.

Our primary motivation in Chapters 4 and 5 was to examine whether islands can exist in a larger class of cosmological models, regardless of whether they describe our own universe. But it is interesting to ask whether we could live on an island. Let us briefly discuss the extent to which our analysis constrains this question.

We considered only universes with radiation or a general fluid and a cosmological constant Λ of arbitrary sign. The visible universe has $\Lambda > 0$ [154, 160], so only the $\Lambda > 0$ case is directly relevant to the question of whether *we* live on an island. However, in a theory with multiple vacua, the universe may decay to regions with $\Lambda = 0$ or $\Lambda < 0$ in the future. Thus, results for $\Lambda \leq 0$ could still be relevant for future regions in our own universe.

The visible universe is consistent with exact spatial flatness [3]. However, observational constraints only put a lower bound on the curvature radius; they do not rule out spatial curvature on a scale somewhat larger than the visible universe. This is significant, since we showed that an arbitrarily small (hence locally unobservable) amount of positive curvature allows for islands in a universe with $\Lambda > 0$.

Indeed, exact spatial flatness requires infinite fine-tuning. Moreover, approximate spatial flatness is a dynamical repeller during matter and radiation domination. Hence, even the approximate spatial flatness of the visible universe dictated by observational constraints would require tremendous fine-tuning of initial conditions, unless it is the result of a dynamical process such as slow-roll inflation. (We are not aware of any other viable candidate process.) This is a period of accelerated expansion driven, for example, by a scalar field with a slowly varying positive potential [130]. Inflation will not make space exactly flat.

The visible universe is anisotropic and inhomogeneous at scales below 100 Mpc, whereas the FRW approximation we use assumes exact spatial homogeneity and isotropy. However, this should not affect any conclusions about cosmological islands. A necessary condition for I to be an island is that its matter entropy must exceed the Bekenstein-Hawking entropy of its boundary ∂I. This can only happen for regions much larger than the horizon scale, for which the FRW description is a good approximation. (Of course, black hole islands could exist if a small black hole forms and evaporates.)

A failure of homogeneity and isotropy at scales much larger than the visible universe is expected in plausible cosmological models [44]. This may lead to additional classes of islands. For example, if our universe descended from a metastable vacuum with larger Λ, its homogeneity and isotropy on slices of constant density is a consequence of the symmetries of the dominant instanton mediating false vacuum decay [60]. But on scales that include the parent vacuum and other baby universes, the spacetime admits no preferred slicing on which it would appear homogeneous; it is not an FRW solution. In a complex multiverse, such as the spacetime that would arise in the landscape of string theory, even the number of noncompact dimensions could change over large scales. It is interesting to ask whether there are new classes of islands in such models, especially islands associated to "hat" regions with $\Lambda = 0$ [46, 184, 4, 145]. This is an interesting possibility [126], whose general study we leave to future work.

In this work's analysis and in those of Refs. [95, 76], it is also not clear what the reference

spacetime corresponds to in the cosmological setting. It would be preferable to assign a meaningful physical significance to the reference spacetime. For example, one could consider a model involving entanglement between two gravitating universes. Certain attempts have been carried out in that direction [23]. One of the major motivations for such a development is that it may provide insight on how to apply these results to multiverse models. The multiverse consists of multiple universes originating from a parent universe in a never-ending process [33, 109, 89, 85]. Thus, entanglement between two universes seems a reasonable expectation for the multiverse.

Ref. [81] discussed entanglement wedge reconstruction in the context of islands, arguing that an island must have a coupling with its reference region for it to behave as expected for an entanglement wedge; simple entanglement between the island and the reference system is not enough. This is puzzling, because the thermofield-doubled model used here and in Refs. [95, 76] involve only entanglement, not a coupling. Understanding how to make these results consistent could lead to insight regarding the role of islands in entanglement wedge reconstruction. A first step, for example, could be to perform an analysis similar to ours here and in Refs. [95, 76] using a model with a coupling instead of the thermofield-doubled model.

Having investigated implications of the Page curve calculations of Refs. [151, 16] in the context of cosmology, in Chapter 6 we turned to a related puzzle: the firewall paradox. We argued that even given gravity/ensemble duality, the firewall paradox remains unresolved by the Page curve calculations. We presented a version of the paradox with a manifest violation of monogamy of entanglement amongst modes at asymptotic infinity, in which none of the modes are hidden behind a horizon. Our thought experiment consisted of an application of the Hayden-Preskill recovery protocol [103] in which the message was a smaller black hole. We argued that accounting for decoherence in the process implies that the asymptotic observer cannot reconstruct the subsystems in violation of monogamy of entanglement, resolving the tension.

Although we argued that the Page curve derivations of Refs. [151, 16] alone do not resolve the firewall paradox, it could be that they are connected to our resolution via decoherence. The lesson from decoherence for the firewall paradox is that if the bulk observer has access only to the system, their experiencing information loss does not conflict with unitary evolution of the system + environment. The recent works applying the RT formula to a black hole + auxiliary system have the same form: the "environment" is the auxiliary system and the black hole is the "system." Escape of Hawking radiation in [151] with absorbing boundary conditions corresponds to leakage of information into the environment, and the bulk observer has access only to the system. Again, it seems the lesson is that confusing a part (the BH) with the whole (BH + auxiliary system) leads to a contradiction. We leave further investigation of this similarity to future work.

Finally, in Chapter 7 we argued for a connection between the Eigenstate Thermalization Hypothesis (ETH) and Grover's search algorithm. We used quantum channel with the form of a generalized partial trace to argue that the orthogonality of eigenstates is compatible with near indistinguishability. We additionally showed that exponential suppression of energy

differences in a coarse-grained window yields exponential suppression of trace distance.

We further lower-bounded the hardness of distinguishability using the data-processing inequality and Grover search. This translates the BBBV lower bound on search algorithms [35] into a statement about the distinguishability of states in an ETH ensemble. More precisely, the task of telling apart our exponentially close states requires at least an exponential number of queries. Finally, we partially reversed these steps by showing that states requiring an exponential number of queries to distinguish are exponentially close in trace distance.

There is a resemblance between our coarse-graining analysis and the idea of renormalization group (RG) flow. In field-theoretic settings one often expresses ignorance of the behavior of the UV and any unknown massive fields that may live there by "integrating out" or, more formally, with arguments using RG flow. We briefly comment on the differences between this textbook approach and the coarse-graining methods we employ here. (To avoid complication, we have in mind a field theory that has been regularized, e.g. on a lattice, so that all Hilbert spaces under discussion are finite-dimensional.) When a Hilbert space describes a field theory, we can describe the field theory by a collection of 'modes' or "degrees of freedom" $\{\phi_i\}$, where the index is both a choice among the allowed positions or momenta in the (regularized) field theory and an identification of a particular field in the theory. To compute the time evolution of an initial state at time t, we use a path-integral formulation to write the overlap of the time-evolved state with states of definite field value:

$$\langle\tilde{\phi}_i\rangle\ \Psi(t) \equiv \int^{\phi_i(\tau=t)=\tilde{\phi}_i} [D\phi_i(\tau)] \exp iS\left[\phi_i(\tau)\right] . \tag{8.1}$$

Without changing this expression, we are free to partition the collection of modes $\{\phi_i\}$ into two non-overlapping sets, ϕ_1 and ϕ_2, which define a possible factorization of the (regularized) Hilbert space. We think of the first set as the system, or the modes we are interested in, and the second set as the environment, or UV modes, we do not have control over. Then we may similarly choose to do the path integral above in two steps, first integrating over one collection of degrees of freedom and then the other. This is still a computation of overlaps between states in the full Hilbert space. However, in some circumstances we may view it as a computation of overlaps in the Hilbert space of just the fields ϕ_1. To do so, we fix an initial state which has no initial entanglement between the two sectors, $|\Psi\rangle = |\Psi_1\rangle_1 |\Psi_2\rangle_2$, where we may define the states in the 1 and 2 sectors by e.g. their overlaps with the field value states $|\phi_1\rangle$, $|\phi_2\rangle$. Then, for *each* choice of initial condition $|\Psi_2\rangle$ and time-evolved state $\tilde{\phi}_2$, we have defined a possible time evolution of the initial state $|\Psi_1\rangle$. Typically, we have in mind the cases where the UV modes start and remain in their vacuum state (for example, if we are considering low-energy processes that should not excite heavy degrees of freedom), or perhaps have taken on some fixed external field value.

This formalism gives time-evolution rules on the Hilbert space describing the fields ϕ_1, but in general we do not expect to relate these rules to the evolution generated by a Hamiltonian. For special, physically-relevant partitions of the degrees of freedom, and Hamiltonians on the full Hilbert space with only perturbatively weak interactions between the two sets,

integration over the UV degrees of freedom does indeed give something close to unitary time evolution within the Hilbert space of ϕ_1 alone. It is this situation that renormalization group flow describes—for example, when the division between modes is based on a momentum cut-off Λ, and the modes with momentum greater than Λ are initialized to their vacuum state. Then, provided the time evolution has not excited the heavy modes, they only appear virtually in Feynman diagrams and may be accounted for by adding additional UV-suppressed interactions. A natural generalization, seen for example in thermal field theory, is to work with density matrices rather than states and drop the requirement that evolution neglecting the UV degrees of freedom is unitary.

In summary, RG flow, or more generally doing a portion of the path integral with specified boundary conditions, provides a (family of) maps from states in the Hilbert space of a field theory to a smaller Hilbert space describing only a subset of the original degrees of freedom. There is a sense, then, in which it might be described as coarse-graining, but it differs from the coarse-graining discussed in Chapter 7 in several respects. First, unlike the channel $\mathcal{C}_{\text{IR}}$ defined in Eq. (7.5) above, the map described here is explicitly time-dependent. (Relatedly, the Hamiltonian on the original Hilbert space appears explicitly.) Second, the channel relies not only on the state of the full system at the final time (via the choice of $\tilde{\phi}_2$), but also on an initial state at some earlier time. Changing either of these choices will change the map to the coarse-grained Hilbert space, although for non-pathological actions we expect that small changes in the boundary conditions will give small changes in the nature of the map. To reiterate: the map $\mathcal{C}_{\text{IR}}$ depends only on a choice of subalgebra $\mathcal{A}$, which *defines* a choice of simple observables, i.e., what we mean by the IR degrees of freedom. But the Hamiltonian does not appear at all, except implicitly to the extent that we expect simple observables to remain simple when evolved for short times. The cost paid in the discussion here, where time evolution plays a vital role, is the loss of a unique map given a definition of the IR. It would be very interesting to attempt to incorporate time evolution more directly into the coarse-graining prescription we have discussed in this work.

The partial-trace quantum channel discussed in Chapter 7 formalizes the intuition that the ETH keeps information about simple operators but discards information which is not accessible to a low-energy observer. This is well-motivated in the existing literature, e.g. in the study of k-designs as approximations to Haar-typical states, an approximation which is valid if one is only interested in data derived from lower moments of the distribution. This is something that is routinely done in for example the study of the information-theoretic aspects of a black hole, particularly in [103]. Another example, also in the context of black hole physics, comes from the consideration of black hole microstates. The ensemble that defines a black hole mixed state is known to obey the ETH, something which has been shown to have information-theoretic consequences [25, 27, 49] in terms of distinguishability and quantum error correction properties. In particular, in connection with the error correcting properties discussed in [27, 49], we expect that the error correcting code maps the physical Hilbert space pre-quantum channel to the logical Hilbert space post quantum channel, and thus has strong encoding properties. However, because of the difficulty of distinguishing these states, this may also demonstrate that decoding of these states is challenging.

Relatedly, the notion of trace distance for ETH ensembles has been studied in the context of chaotic CFTs [127, 128]. It would be interesting to consider whether our distinguishability arguments could be adapted to this context. In the context of holography, our algebraic setup resembles that used to discuss the notion of bulk states as an error-correcting code [10, 92]. We hope to pursue this connection in further work.

The results of this work show that, as we might expect, the choice of kept observables in a coarse-graining quantum channel defines which ensembles of density matrices obey the ETH conditions with respect to these observables. One must consider both the ensemble and the channel to determine whether the ensemble achieves the requisite compression of the trace distance. In particular, it would be interesting in future work to consider choices of ensembles and observables that have more complicated relations to the Hamiltonian than microcanonical distributions in an energy band.

Relatedly, a drawback of our simple model is that eigenstates in different sectors have strictly vanishing overlaps for simple operators. The smoothness of the ETH envelope functions $f_{\mathcal{O}}^{(\alpha)}$ then forces eigenstates at the edge of a sector $\mathcal{H}_\alpha$ to have overlap suppressed by e^{-S}, so that they are zero at order $e^{-S/2}$. This means that we cannot interpret the α as microcanonical bands, since this suppression does not agree with the results of a random microcanonical draw. The simplest modification would be weak coupling between sectors, a possibility we intend to consider in future work.

Our converse result shows that exponential difficulty of distinction implies that simple operators have $O(1)$ diagonal and $O(e^{-S/2})$ off-diagonal matrix elements, as per the ETH. However, this argument does not establish the mean or variance for these off-diagonal elements, i.e. the statistics of the A_{ij} when viewed as random draws from the energy ensemble. By considering trace distance suppression between more elaborate ensembles, it might be possible to determine these statistics from search constraints. This suggests the tantalizing possibility that ETH distinguishability is a complete problem for some quantum complexity class, perhaps QMA, when combined with the existing hardness results, provided that the scaling is not dominated by going from pure states to mixed states.

Finally, the analysis presented here is reminiscent of the discussion of Petz recovery [63, 54, 155, 114, 9, 58, 152, 15], where one considers the possibility of reconstructing a density matrix ρ_{ABC} with access only to ρ_{AB}. While Petz recovery is concerned with the ability to reconstruct the full ρ_{ABC}, the distinguishability question asked here performs a simpler task, that of distinguishing within some discrete given set ρ_{ABC_i}. It would be interesting to consider if there is an intermediate situation where full Petz recovery is not possible, but this distinguishability task is.

In this work, we have sought to further the quest for quantum gravity in a few small, but hopefully substantial, ways. It is our ambition that these steps will propel the search, and that a full theory of quantum gravity is on the horizon.

Bibliography

[1] Ian Affleck and Andreas W. W. Ludwig. "Universal noninteger 'ground state degeneracy' in critical quantum systems". In: *Phys. Rev. Lett.* 67 (1991), pp. 161–164. DOI: 10.1103/PhysRevLett.67.161.

[2] Nima Afkhami-Jeddi et al. "Free partition functions and an averaged holographic duality". In: (June 2020). arXiv: 2006.04839 [hep-th].

[3] N. Aghanim et al. "Planck 2018 results. VI. Cosmological parameters". In: *Astron. Astrophys.* 641 (2020). [Erratum: Astron.Astrophys. 652, C4 (2021)], A6. DOI: 10.1051/0004-6361/201833910. arXiv: 1807.06209 [astro-ph.CO].

[4] Anthony Aguirre, Max Tegmark, and David Layzer. "Born in an Infinite Universe: A Cosmological Interpretation of Quantum Mechanics". In: *Phys. Rev. D* 84 (2011), p. 105002. DOI: 10.1103/PhysRevD.84.105002. arXiv: 1008.1066 [quant-ph].

[5] Chris Akers, Netta Engelhardt, and Daniel Harlow. "Simple holographic models of black hole evaporation". In: (Oct. 2019). arXiv: 1910.00972 [hep-th].

[6] Chris Akers and Geoffrey Penington. "Leading order corrections to the quantum extremal surface prescription". In: *JHEP* 04 (2021), p. 062. DOI: 10.1007/JHEP04(2021)062. arXiv: 2008.03319 [hep-th].

[7] Chris Akers and Geoffrey Penington. "Quantum minimal surfaces from quantum error correction". In: (Sept. 2021). arXiv: 2109.14618 [hep-th].

[8] Chris Akers and Pratik Rath. "Holographic Renyi Entropy from Quantum Error Correction". In: *JHEP* 05 (2019), p. 052. DOI: 10.1007/JHEP05(2019)052. arXiv: 1811.05171 [hep-th].

[9] Ahmed Almheiri, Tarek Anous, and Aitor Lewkowycz. "Inside out: meet the operators inside the horizon. On bulk reconstruction behind causal horizons". In: *JHEP* 01 (2018), p. 028. DOI: 10.1007/JHEP01(2018)028.

[10] Ahmed Almheiri, Xi Dong, and Daniel Harlow. "Bulk Locality and Quantum Error Correction in AdS/CFT". In: *JHEP* 04 (2015), p. 163. DOI: 10.1007/JHEP04(2015)163. arXiv: 1411.7041 [hep-th].

[11] Ahmed Almheiri, Raghu Mahajan, and Juan Maldacena. "Islands outside the horizon". In: (Oct. 2019). arXiv: 1910.11077 [hep-th].

[12] Ahmed Almheiri, Raghu Mahajan, and Jorge E. Santos. "Entanglement islands in higher dimensions". In: (Nov. 2019). arXiv: 1911.09666 [hep-th].

[13] Ahmed Almheiri et al. "An Apologia for Firewalls". In: *JHEP* 09 (2013), p. 018. DOI: 10.1007/JHEP09(2013)018. arXiv: 1304.6483 [hep-th].

[14] Ahmed Almheiri et al. "Black Holes: Complementarity or Firewalls?" In: *JHEP* 02 (2013), p. 062. DOI: 10.1007/JHEP02(2013)062. arXiv: 1207.3123 [hep-th].

[15] Ahmed Almheiri et al. "Replica Wormholes and the Entropy of Hawking Radiation". In: *JHEP* 05 (2020), p. 013. DOI: 10.1007/JHEP05(2020)013. arXiv: 1911.12333 [hep-th].

[16] Ahmed Almheiri et al. "The entropy of bulk quantum fields and the entanglement wedge of an evaporating black hole". In: *JHEP* 12 (2019), p. 063. DOI: 10.1007/JHEP12(2019)063. arXiv: 1905.08762 [hep-th].

[17] Ahmed Almheiri et al. "The entropy of Hawking radiation". In: (June 2020). arXiv: 2006.06872 [hep-th].

[18] Ahmed Almheiri et al. "The Page curve of Hawking radiation from semiclassical geometry". In: *JHEP* 03 (2020), p. 149. DOI: 10.1007/JHEP03(2020)149. arXiv: 1908.10996 [hep-th].

[19] Michal Artymowski, Ido Ben-Dayan, and Utkarsh Kumar. "Banks-Zaks Cosmology, Inflation, and the Big Bang Singularity". In: *JCAP* 05 (2020), p. 015. DOI: 10.1088/1475-7516/2020/05/015. arXiv: 1912.10532 [hep-th].

[20] Michał Artymowski, Ido Ben-Dayan, and Udaykrishna Thattarampilly. "Sourced fluctuations in generic slow contraction". In: *JCAP* 06 (2021), p. 010. DOI: 10.1088/1475-7516/2021/06/010. arXiv: 2011.00626 [gr-qc].

[21] Dongsu Bak et al. "Unitarity of Entanglement and Islands in Two-Sided Janus Black Holes". In: (June 2020). arXiv: 2006.11717 [hep-th].

[22] A. P. Balachandran et al. "Algebraic approach to entanglement and entropy". In: *Phys. Rev. A* 88 (2 Aug. 2013), p. 022301. DOI: 10.1103/PhysRevA.88.022301. URL: https://link.aps.org/doi/10.1103/PhysRevA.88.022301.

[23] Vijay Balasubramanian, Arjun Kar, and Tomonori Ugajin. "Entanglement between two gravitating universes". In: *Class. Quant. Grav.* 39.17 (2022), p. 174001. DOI: 10.1088/1361-6382/ac3c8b. arXiv: 2104.13383 [hep-th].

[24] Ning Bao, Adam Bouland, and Stephen P. Jordan. "Grover Search and the No-Signaling Principle". In: *Phys. Rev. Lett.* 117 (12 Sept. 2016), p. 120501. DOI: 10.1103/PhysRevLett.117.120501. URL: https://link.aps.org/doi/10.1103/PhysRevLett.117.120501.

[25] Ning Bao, Sean M. Carroll, and Ashmeet Singh. "The Hilbert space of quantum gravity is locally finite-dimensional". In: *International Journal of Modern Physics D* 26.12 (Oct. 2017), p. 1743013. ISSN: 1793-6594. DOI: 10.1142/s0218271817430131. URL: http://dx.doi.org/10.1142/S0218271817430131.

[26] Ning Bao and Aidan Chatwin-Davies. "Puzzles and pitfalls involving Haar-typicality in holography". In: *SciPost Phys.* 4.6 (2018), p. 033. DOI: 10.21468/SciPostPhys.4.6.033. arXiv: 1708.08561 [hep-th].

[27] Ning Bao and Newton Cheng. "Eigenstate Thermalization Hypothesis and Approximate Quantum Error Correction". In: *JHEP* 08 (2019), p. 152. DOI: 10.1007/JHEP08(2019)152. arXiv: 1906.03669 [hep-th].

[28] Ning Bao and Yuta Kikuchi. "Hayden-Preskill decoding from noisy Hawking radiation". In: (Sept. 2020). arXiv: 2009.13493 [quant-ph].

[29] Ning Bao et al. "Branches of the Black Hole Wave Function Need Not Contain Firewalls". In: *Phys. Rev. D* 97.12 (2018), p. 126014. DOI: 10.1103/PhysRevD.97.126014. arXiv: 1712.04955 [hep-th].

[30] Ning Bao et al. "Rescuing Complementarity With Little Drama". In: *JHEP* 12 (2016), p. 026. DOI: 10.1007/JHEP12(2016)026. arXiv: 1607.05141 [hep-th].

[31] J. D. Bekenstein. "Black holes and the second law". In: *Nuovo Cim. Lett.* 4 (1972), pp. 737–740.

[32] Ido Ben-Dayan. "Gravitational Waves in Bouncing Cosmologies from Gauge Field Production". In: *JCAP* 09 (2016), p. 017. DOI: 10.1088/1475-7516/2016/09/017. arXiv: 1604.07899 [astro-ph.CO].

[33] Ido Ben-Dayan, Merav Hadad, and Amir Michaelis. "The grand canonical Multiverse and the small cosmological constant". In: *JCAP* 09 (2022), p. 052. DOI: 10.1088/1475-7516/2022/09/052. arXiv: 2110.06249 [hep-th].

[34] Ido Ben-Dayan and Judy Kupferman. "Sourced scalar fluctuations in bouncing cosmology". In: *JCAP* 07 (2019). [Erratum: JCAP 12, E01 (2020)], p. 050. DOI: 10.1088/1475-7516/2019/07/050. arXiv: 1812.06970 [gr-qc].

[35] Charles H. Bennett et al. "Strengths and weaknesses of quantum computing". In: *SIAM J. Comput.* 26 (1997), pp. 1510–1523. DOI: 10.1137/S0097539796300933.

[36] W. Beugeling, R. Moessner, and Masudul Haque. "Finite-size scaling of eigenstate thermalization". In: *Phys. Rev. E* 89 (4 Apr. 2014), p. 042112. DOI: 10.1103/PhysRevE.89.042112. URL: https://link.aps.org/doi/10.1103/PhysRevE.89.042112.

[37] Wouter Beugeling, Roderich Moessner, and Masudul Haque. "Off-diagonal matrix elements of local operators in many-body quantum systems". In: *Phys. Rev. E* 91 (1 Jan. 2015), p. 012144. DOI: 10.1103/PhysRevE.91.012144. URL: https://link.aps.org/doi/10.1103/PhysRevE.91.012144.

[38] Eli Biham and Dan Kenigsberg. "Grover's quantum search algorithm for an arbitrary initial mixed state". In: *Physical Review A* 66.6 (Dec. 2002). ISSN: 1094-1622. DOI: 10.1103/physreva.66.062301. URL: http://dx.doi.org/10.1103/PhysRevA.66.062301.

[39] Giulio Biroli, Corinna Kollath, and Andreas M. Läuchli. "Effect of Rare Fluctuations on the Thermalization of Isolated Quantum Systems". In: *Phys. Rev. Lett.* 105 (25 Dec. 2010), p. 250401. DOI: 10.1103/PhysRevLett.105.250401. URL: https://link.aps.org/doi/10.1103/PhysRevLett.105.250401.

[40] Adam Bouland, Bill Fefferman, and Umesh Vazirani. "Computational pseudorandomness, the wormhole growth paradox, and constraints on the AdS/CFT duality". In: (Oct. 2019). arXiv: 1910.14646 [quant-ph].

[41] Raphael Bousso. "Complementarity Is Not Enough". In: *Phys. Rev. D* 87.12 (2013), p. 124023. DOI: 10.1103/PhysRevD.87.124023. arXiv: 1207.5192 [hep-th].

[42] Raphael Bousso. "Firewalls from double purity". In: *Phys. Rev. D* 88.8 (2013), p. 084035. DOI: 10.1103/PhysRevD.88.084035. arXiv: 1308.2665 [hep-th].

[43] Raphael Bousso. "Violations of the Equivalence Principle by a Nonlocally Reconstructed Vacuum at the Black Hole Horizon". In: *Phys. Rev. Lett.* 112.4 (2014), p. 041102. DOI: 10.1103/PhysRevLett.112.041102. arXiv: 1308.3697 [hep-th].

[44] Raphael Bousso and Joseph Polchinski. "Quantization of four form fluxes and dynamical neutralization of the cosmological constant". In: *JHEP* 06 (2000), p. 006. DOI: 10.1088/1126-6708/2000/06/006. arXiv: hep-th/0004134.

[45] Raphael Bousso and Lisa Randall. "Holographic domains of Anti-de Sitter space". In: *JHEP* 04 (2002), p. 057. arXiv: hep-th/0112080.

[46] Raphael Bousso and Leonard Susskind. "The Multiverse Interpretation of Quantum Mechanics". In: *Phys. Rev. D* 85 (2012), p. 045007. DOI: 10.1103/PhysRevD.85.045007. arXiv: 1105.3796 [hep-th].

[47] Raphael Bousso and Marija Tomašević. "Unitarity From a Smooth Horizon?" In: *Phys. Rev. D* 102.10 (2020), p. 106019. DOI: 10.1103/PhysRevD.102.106019. arXiv: 1911.06305 [hep-th].

[48] Raphael Bousso et al. "Quantum focusing conjecture". In: *Phys. Rev. D* 93.6 (2016), p. 064044. DOI: 10.1103/PhysRevD.93.064044. arXiv: 1506.02669 [hep-th].

[49] Fernando G. S. L. Brandão et al. "Quantum Error Correcting Codes in Eigenstates of Translation-Invariant Spin Chains". In: *Physical Review Letters* 123.11 (Sept. 2019). ISSN: 1079-7114. DOI: 10.1103/physrevlett.123.110502. URL: http://dx.doi.org/10.1103/PhysRevLett.123.110502.

[50] Enrico M. Brehm, Diptarka Das, and Shouvik Datta. "Probing thermality beyond the diagonal". In: *Phys. Rev. D* 98.12 (2018), p. 126015. DOI: 10.1103/PhysRevD.98.126015. arXiv: 1804.07924 [hep-th].

[51] Adam R. Brown et al. "Complexity, action, and black holes". In: *Phys. Rev. D* 93.8 (2016), p. 086006. DOI: 10.1103/PhysRevD.93.086006. arXiv: 1512.04993 [hep-th].

[52] Pasquale Calabrese and John Cardy. "Entanglement entropy and conformal field theory". In: *J. Phys. A* 42 (2009), p. 504005. DOI: 10.1088/1751-8113/42/50/504005. arXiv: 0905.4013 [cond-mat.stat-mech].

[53] J. Cardy. "Boundary Conformal Field Theory". In: *Encyclopedia of Mathematical Physics*. Ed. by Jean-Pierre Françoise, Gregory L. Naber, and Tsou Sheung Tsun. Oxford: Academic Press, 2006, pp. 333–340. ISBN: 978-0-12-512666-3. DOI: https://doi.org/10.1016/B0-12-512666-2/00398-9. URL: http://www.sciencedirect.com/science/article/pii/B0125126662003989.

[54] Chi-Fang Chen, Geoffrey Penington, and Grant Salton. "Entanglement Wedge Reconstruction using the Petz Map". In: *JHEP* 01 (2020), p. 168. DOI: 10.1007/JHEP01(2020)168.

[55] Hong Zhe Chen et al. "Information Flow in Black Hole Evaporation". In: *JHEP* 03 (2020), p. 152. DOI: 10.1007/JHEP03(2020)152. arXiv: 1911.03402 [hep-th].

[56] Hong Zhe Chen et al. "Quantum Extremal Islands Made Easy, Part I: Entanglement on the Brane". In: (June 2020). arXiv: 2006.04851 [hep-th].

[57] Pisin Chen, Yen Chin Ong, and Dong-han Yeom. "Black Hole Remnants and the Information Loss Paradox". In: *Phys. Rept.* 603 (2015), pp. 1–45. DOI: 10.1016/j.physrep.2015.10.007. arXiv: 1412.8366 [gr-qc].

[58] Yiming Chen. "Pulling Out the Island with Modular Flow". In: *JHEP* 03 (2020), p. 033. DOI: 10.1007/JHEP03(2020)033.

[59] Sayantan Choudhury et al. "Circuit Complexity from Cosmological Islands". In: *Symmetry* 13.7 (2021), p. 1301. DOI: 10.3390/sym13071301. arXiv: 2012.10234 [hep-th].

[60] Sidney R. Coleman and Frank De Luccia. "Gravitational Effects on and of Vacuum Decay". In: *Phys. Rev. D* 21 (1980), p. 3305. DOI: 10.1103/PhysRevD.21.3305.

[61] Sean Cooper et al. "Black Hole Microstate Cosmology". In: *JHEP* 07 (2019), p. 065. DOI: 10.1007/JHEP07(2019)065. arXiv: 1810.10601 [hep-th].

[62] Jordan Cotler and Kristan Jensen. "AdS_3 gravity and random CFT". In: (June 2020). arXiv: 2006.08648 [hep-th].

[63] Jordan Cotler et al. "Entanglement Wedge Reconstruction via Universal Recovery Channels". In: *Phys. Rev. X* 9.3 (2019), p. 031011. DOI: 10.1103/PhysRevX.9.031011.

[64] Luca D'Alessio et al. "From quantum chaos and eigenstate thermalization to statistical mechanics and thermodynamics". In: *Adv. Phys.* 65.3 (2016), pp. 239–362. DOI: 10.1080/00018732.2016.1198134.

[65] Shouvik Datta, Per Kraus, and Ben Michel. "Typicality and thermality in 2d CFT". In: *JHEP* 07 (2019), p. 143. DOI: 10.1007/JHEP07(2019)143. arXiv: 1904.00668 [hep-th].

[66] D. Deutsch. "Quantum theory, the Church-Turing principle and the universal quantum computer". In: *Proceedings of the Royal Society of London Series A* 400.1818 (July 1985), pp. 97–117. DOI: 10.1098/rspa.1985.0070.

[67] J. M. Deutsch. "Quantum statistical mechanics in a closed system". In: *Phys. Rev. A* 43 (4 Feb. 1991), pp. 2046–2049. DOI: 10.1103/PhysRevA.43.2046. URL: https://link.aps.org/doi/10.1103/PhysRevA.43.2046.

[68] Joshua M Deutsch. "Eigenstate thermalization hypothesis". In: *Reports on Progress in Physics* 81 (8 July 2018). DOI: 10.1088/1361-6633/aac9f1. URL: https://iopscience.iop.org/article/10.1088/1361-6633/aac9f1.

[69] Xi Dong, Daniel Harlow, and Donald Marolf. "Flat entanglement spectra in fixed-area states of quantum gravity". In: *JHEP* 10 (2019), p. 240. DOI: 10.1007/JHEP10(2019)240. arXiv: 1811.05382 [hep-th].

[70] Xi Dong, Daniel Harlow, and Aron C. Wall. "Reconstruction of Bulk Operators within the Entanglement Wedge in Gauge-Gravity Duality". In: *Phys. Rev. Lett.* 117.2 (2016), p. 021601. DOI: 10.1103/PhysRevLett.117.021601. arXiv: 1601.05416 [hep-th].

[71] Xi Dong and Donald Marolf. "One-loop universality of holographic codes". In: *JHEP* 03 (2020), p. 191. DOI: 10.1007/JHEP03(2020)191. arXiv: 1910.06329 [hep-th].

[72] Anatoly Dymarsky, Nima Lashkari, and Hong Liu. "Subsystem ETH". In: *Phys. Rev. E* 97 (2018), p. 012140. DOI: 10.1103/PhysRevE.97.012140. arXiv: 1611.08764 [cond-mat.stat-mech].

[73] Roberto Emparan. "Black hole entropy as entanglement entropy: A Holographic derivation". In: *JHEP* 06 (2006), p. 012. DOI: 10.1088/1126-6708/2006/06/012. arXiv: hep-th/0603081.

[74] Netta Engelhardt and Aron C. Wall. "Extremal Surface Barriers". In: *JHEP* 1403 (2014), p. 068. DOI: 10.1007/JHEP03(2014)068. arXiv: 1312.3699 [hep-th].

[75] Netta Engelhardt and Aron C. Wall. "Quantum Extremal Surfaces: Holographic Entanglement Entropy beyond the Classical Regime". In: *JHEP* 01 (2015), p. 073. DOI: 10.1007/JHEP01(2015)073. arXiv: 1408.3203 [hep-th].

[76] Ricardo Espindola, Bahman Najian, and Dora Nikolakopoulou. "Islands in FRW Cosmologies". In: (Mar. 2022). arXiv: 2203.04433 [hep-th].

[77] Philippe Faist et al. "Continuous symmetries and approximate quantum error correction". In: *Phys. Rev. X* 10.4 (2020), p. 041018. DOI: 10.1103/PhysRevX.10.041018. arXiv: 1902.07714 [quant-ph].

[78] Thomas Faulkner, Aitor Lewkowycz, and Juan Maldacena. "Quantum corrections to holographic entanglement entropy". In: *JHEP* 11 (2013), p. 074. DOI: 10.1007/JHEP11(2013)074. arXiv: 1307.2892 [hep-th].

[79] Mitsutoshi Fujita, Tadashi Takayanagi, and Erik Tonni. "Aspects of AdS/BCFT". In: *JHEP* 11 (2011), p. 043. DOI: 10.1007/JHEP11(2011)043. arXiv: 1108.5152 [hep-th].

[80] Friðrik Freyr Gautason et al. "Page Curve for an Evaporating Black Hole". In: *JHEP* 05 (2020), p. 091. DOI: 10.1007/JHEP05(2020)091. arXiv: 2004.00598 [hep-th].

[81] Hao Geng et al. "Inconsistency of islands in theories with long-range gravity". In: *JHEP* 01 (2022), p. 182. DOI: 10.1007/JHEP01(2022)182. arXiv: 2107.03390 [hep-th].

[82] S. Genway, A. F. Ho, and D. K. K. Lee. "Thermalization of local observables in small Hubbard lattices". In: *Phys. Rev. A* 86 (2 Aug. 2012), p. 023609. DOI: 10.1103/PhysRevA.86.023609. URL: https://link.aps.org/doi/10.1103/PhysRevA.86.023609.

[83] G. W. Gibbons and S. W. Hawking. "Action Integrals and Partition Functions in Quantum Gravity". In: *Phys. Rev. D* 15 (1977), pp. 2752–2756.

[84] Steven B. Giddings. "Nonviolent nonlocality". In: *Phys. Rev. D* 88 (2013), p. 064023. DOI: 10.1103/PhysRevD.88.064023. arXiv: 1211.7070 [hep-th].

[85] A. S. Goncharov, Andrei D. Linde, and Viatcheslav F. Mukhanov. "The Global Structure of the Inflationary Universe". In: *Int. J. Mod. Phys. A* 2 (1987), pp. 561–591. DOI: 10.1142/S0217751X87000211.

[86] Peter W. Graham et al. "A Simple Harmonic Universe". In: *JHEP* 02 (2014), p. 029. DOI: 10.1007/JHEP02(2014)029. arXiv: 1109.0282 [hep-th].

[87] Robert B. Griffiths. "Consistent histories and the interpretation of quantum mechanics". In: *J. Statist. Phys.* 36 (1984), pp. 219–272. DOI: 10.1007/BF01015734.

[88] Lov K. Grover. "A fast quantum mechanical algorithm for database search". In: *Proceedings of the Twenty-eighth Annual ACM Symposium on Theory of Computing*. New York, NY, USA: ACM, 1996, pp. 212–219.

[89] Alan H. Guth. "Eternal inflation and its implications". In: *J. Phys. A* 40 (2007). Ed. by Joan Sola, pp. 6811–6826. DOI: 10.1088/1751-8113/40/25/S25. arXiv: hep-th/0702178.

[90] Alex Hamilton et al. "Holographic representation of local bulk operators". In: *Phys. Rev. D* 74 (2006), p. 066009. DOI: 10.1103/PhysRevD.74.066009. arXiv: hep-th/0606141.

[91] Daniel Harlow. "Jerusalem Lectures on Black Holes and Quantum Information". In: *Rev. Mod. Phys.* 88 (2016), p. 015002. DOI: 10.1103/RevModPhys.88.015002. arXiv: 1409.1231 [hep-th].

[92] Daniel Harlow. "The Ryu–Takayanagi Formula from Quantum Error Correction". In: *Commun. Math. Phys.* 354.3 (2017), pp. 865–912. DOI: 10.1007/s00220-017-2904-z. arXiv: 1607.03901 [hep-th].

[93] Daniel Harlow and Patrick Hayden. "Quantum Computation vs. Firewalls". In: *JHEP* 06 (2013), p. 085. DOI: 10.1007/JHEP06(2013)085. arXiv: 1301.4504 [hep-th].

[94] Daniel Harlow and Hirosi Ooguri. "Symmetries in quantum field theory and quantum gravity". In: *Commun. Math. Phys.* 383.3 (2021), pp. 1669–1804. DOI: 10.1007/s00220-021-04040-y. arXiv: 1810.05338 [hep-th].

[95] Thomas Hartman, Yikun Jiang, and Edgar Shaghoulian. "Islands in cosmology". In: (Aug. 2020). arXiv: 2008.01022 [hep-th].

[96] Thomas Hartman and Juan Maldacena. "Time Evolution of Entanglement Entropy from Black Hole Interiors". In: *JHEP* 05 (2013), p. 014. DOI: 10.1007/JHEP05(2013)014. arXiv: 1303.1080 [hep-th].

[97] Thomas Hartman, Edgar Shaghoulian, and Andrew Strominger. "Islands in Asymptotically Flat 2D Gravity". In: (Apr. 2020). arXiv: 2004.13857 [hep-th].

[98] S. W. Hawking. "Black Holes and Thermodynamics". In: *Phys. Rev. D* 13 (1976), pp. 191–197.

[99] S. W. Hawking. "Breakdown of Predictability in Gravitational Collapse". In: *Phys. Rev. D* 14 (1976), pp. 2460–2473. DOI: 10.1103/PhysRevD.14.2460.

[100] S.W. Hawking. "Black hole explosions". In: *Nature* 248 (1974), pp. 30–31. DOI: 10.1038/248030a0.

[101] S.W. Hawking. "Black Holes and Thermodynamics". In: *Phys. Rev. D* 13 (1976), pp. 191–197. DOI: 10.1103/PhysRevD.13.191.

[102] Patrick Hayden and Geoffrey Penington. "Learning the Alpha-bits of Black Holes". In: *JHEP* 12 (2019), p. 007. DOI: 10.1007/JHEP12(2019)007. arXiv: 1807.06041 [hep-th].

[103] Patrick Hayden and John Preskill. "Black holes as mirrors: Quantum information in random subsystems". In: *JHEP* 09 (2007), p. 120. DOI: 10.1088/1126-6708/2007/09/120. arXiv: 0708.4025 [hep-th].

[104] Patrick Hayden et al. "Holographic duality from random tensor networks". In: *JHEP* 11 (2016), p. 009. DOI: 10.1007/JHEP11(2016)009. arXiv: 1601.01694 [hep-th].

[105] Thomas Hertog and James Hartle. "Observational Implications of Fuzzball Formation". In: *Gen. Rel. Grav.* 52.7 (2020), p. 67. DOI: 10.1007/s10714-020-02720-z. arXiv: 1704.02123 [hep-th].

[106] Yasuaki Hikida, Yuya Kusuki, and Tadashi Takayanagi. "Eigenstate thermalization hypothesis and modular invariance of two-dimensional conformal field theories". In: *Phys. Rev. D* 98.2 (2018), p. 026003. DOI: 10.1103/PhysRevD.98.026003. arXiv: 1804.09658 [hep-th].

[107] Alexander S Holevo. "Bounds for the Quantity of Information Transmitted by a Quantum Communication Channel". In: *Probl. Peredachi Inf.* 9 (3 1973), pp. 3–11.

[108] Veronika E. Hubeny, Mukund Rangamani, and Tadashi Takayanagi. "A Covariant holographic entanglement entropy proposal". In: *JHEP* 0707 (2007), p. 062. DOI: 10.1088/1126-6708/2007/07/062. arXiv: 0705.0016 [hep-th].

[109] Anna Ijjas, Paul J. Steinhardt, and Abraham Loeb. "Inflationary schism". In: *Phys. Lett. B* 736 (2014), pp. 142–146. DOI: 10.1016/j.physletb.2014.07.012. arXiv: 1402.6980 [astro-ph.CO].

[110] R. Jackiw. "Lower Dimensional Gravity". In: *Nucl. Phys. B* 252 (1985). Ed. by R. Baier and H. Satz, pp. 343–356. DOI: 10.1016/0550-3213(85)90448-1.

[111] Daniel L. Jafferis et al. "Relative entropy equals bulk relative entropy". In: *JHEP* 06 (2016), p. 004. DOI: 10.1007/JHEP06(2016)004. arXiv: 1512.06431 [hep-th].

[112] E. T. Jaynes. "Information Theory and Statistical Mechanics". In: *Phys. Rev.* 106 (4 May 1957), pp. 620–630. DOI: 10.1103/PhysRev.106.620. URL: https://link.aps.org/doi/10.1103/PhysRev.106.620.

[113] E. Joos and H.D. Zeh. "The Emergence of classical properties through interaction with the environment". In: *Z. Phys. B* 59 (1985), pp. 223–243. DOI: 10.1007/BF01725541.

[114] Marius Junge et al. "Universal Recovery Maps and Approximate Sufficiency of Quantum Relative Entropy". In: *Annales Henri Poincare* 19.10 (2018), pp. 2955–2978. DOI: 10.1007/s00023-018-0716-0.

[115] Oleg Kabernik, Jason Pollack, and Ashmeet Singh. "Quantum state reduction: Generalized bipartitions from algebras of observables". In: *Phys. Rev. A* 101 (3 Mar. 2020), p. 032303. DOI: 10.1103/PhysRevA.101.032303. URL: https://link.aps.org/doi/10.1103/PhysRevA.101.032303.

[116] Andreas Karch and Lisa Randall. "Locally localized gravity". In: *JHEP* 05 (2001), p. 008. arXiv: hep-th/0011156.

[117] A. Katz. *Principles of Statistical Mechanics: The Information Theory Approach*. W. H. Freeman, 1967.

[118] Ehsan Khatami et al. "Fluctuation-Dissipation Theorem in an Isolated System of Quantum Dipolar Bosons after a Quench". In: *Phys. Rev. Lett.* 111 (5 July 2013), p. 050403. DOI: 10.1103/PhysRevLett.111.050403. URL: https://link.aps.org/doi/10.1103/PhysRevLett.111.050403.

[119] Ehsan Khatami et al. "Quantum quenches in disordered systems: Approach to thermal equilibrium without a typical relaxation time". In: *Phys. Rev. E* 85 (5 May 2012), p. 050102. DOI: 10.1103/PhysRevE.85.050102. URL: https://link.aps.org/doi/10.1103/PhysRevE.85.050102.

[120] Abdellah Khodja, Robin Steinigeweg, and Jochen Gemmer. "Relevance of the eigenstate thermalization hypothesis for thermal relaxation". In: *Phys. Rev. E* 91 (1 Jan. 2015), p. 012120. DOI: 10.1103/PhysRevE.91.012120. URL: https://link.aps.org/doi/10.1103/PhysRevE.91.012120.

[121] Hyungwon Kim, Tatsuhiko N. Ikeda, and David A. Huse. "Testing whether all eigenstates obey the eigenstate thermalization hypothesis". In: *Phys. Rev. E* 90 (5 Nov. 2014), p. 052105. DOI: 10.1103/PhysRevE.90.052105. URL: https://link.aps.org/doi/10.1103/PhysRevE.90.052105.

[122] Emanuel Knill, Raymond Laflamme, and Lorenza Viola. "Theory of Quantum Error Correction for General Noise". In: *Physical Review Letters* 84.11 (Mar. 2000), pp. 2525–2528. ISSN: 1079-7114. DOI: 10.1103/physrevlett.84.2525. URL: http://dx.doi.org/10.1103/PhysRevLett.84.2525.

[123] Jason Koeller and Stefan Leichenauer. "Holographic Proof of the Quantum Null Energy Condition". In: *Phys. Rev. D* 94.2 (2016), p. 024026. DOI: 10.1103/PhysRevD.94.024026. arXiv: 1512.06109 [hep-th].

[124] Edward W. Kolb and Michael S. Turner. *The Early Universe*. Vol. 69. 1990. ISBN: 978-0-201-62674-2. DOI: 10.1201/9780429492860.

[125] Ioanna Kourkoulou and Juan Maldacena. "Pure states in the SYK model and nearly-AdS_2 gravity". In: (July 2017). arXiv: 1707.02325 [hep-th].

[126] Kevin Langhoff, Chitraang Murdia, and Yasunori Nomura. "Multiverse in an inverted island". In: *Phys. Rev. D* 104.8 (2021), p. 086007. DOI: 10.1103/PhysRevD.104.086007. arXiv: 2106.05271 [hep-th].

[127] Nima Lashkari, Anatoly Dymarsky, and Hong Liu. "Eigenstate Thermalization Hypothesis in Conformal Field Theory". In: *J. Stat. Mech.* 1803.3 (2018), p. 033101. DOI: 10.1088/1742-5468/aab020.

[128] Nima Lashkari, Anatoly Dymarsky, and Hong Liu. "Universality of Quantum Information in Chaotic CFTs". In: *JHEP* 03 (2018), p. 070. DOI: 10.1007/JHEP03(2018)070.

[129] Aitor Lewkowycz and Juan Maldacena. "Generalized gravitational entropy". In: *JHEP* 1308 (2013), p. 090. DOI: 10.1007/JHEP08(2013)090. arXiv: 1304.4926 [hep-th].

[130] Andrei D. Linde. "Chaotic Inflation". In: *Phys. Lett. B* 129 (1983), pp. 177–181. DOI: 10.1016/0370-2693(83)90837-7.

[131] Seth Lloyd and John Preskill. "Unitarity of black hole evaporation in final-state projection models". In: *JHEP* 08 (2014), p. 126. DOI: 10.1007/JHEP08(2014)126. arXiv: 1308.4209 [hep-th].

[132] David A. Lowe et al. "Black hole complementarity versus locality". In: *Phys. Rev. D* 52 (1995), pp. 6997–7010. DOI: 10.1103/PhysRevD.52.6997. arXiv: hep-th/9506138.

[133] Juan Maldacena and Leonard Susskind. "Cool horizons for entangled black holes". In: *Fortsch. Phys.* 61 (2013), pp. 781–811. DOI: 10.1002/prop.201300020. arXiv: 1306.0533 [hep-th].

[134] Juan Martin Maldacena. "The Large N limit of superconformal field theories and supergravity". In: *Adv. Theor. Math. Phys.* 2 (1998), pp. 231–252. DOI: 10.1023/A:1026654312961. arXiv: hep-th/9711200.

[135] Alexander Maloney and Edward Witten. "Averaging Over Narain Moduli Space". In: (June 2020). arXiv: 2006.04855 [hep-th].

[136] A. Manu, K. Narayan, and Partha Paul. "Cosmological singularities, entanglement and quantum extremal surfaces". In: *JHEP* 04 (2021), p. 200. DOI: 10.1007/JHEP04(2021)200. arXiv: 2012.07351 [hep-th].

[137] Donald Marolf and Henry Maxfield. "Transcending the ensemble: baby universes, spacetime wormholes, and the order and disorder of black hole information". In: *JHEP* 08 (2020), p. 044. DOI: 10.1007/JHEP08(2020)044. arXiv: 2002.08950 [hep-th].

[138] Donald Marolf and Joseph Polchinski. "Gauge/Gravity Duality and the Black Hole Interior". In: *Phys. Rev. Lett.* 111 (2013), p. 171301. DOI: 10.1103/PhysRevLett.111.171301. arXiv: 1307.4706 [hep-th].

[139] Samir D. Mathur. "The Fuzzball proposal for black holes: An Elementary review". In: *Fortsch. Phys.* 53 (2005). Ed. by E. Kiritsis, pp. 793–827. DOI: 10.1002/prop.200410203. arXiv: hep-th/0502050.

[140] Henry Maxfield and Gustavo J. Turiaci. "The path integral of 3D gravity near extremality; or, JT gravity with defects as a matrix integral". In: (June 2020). arXiv: 2006.11317 [hep-th].

[141] Rubem Mondaini et al. "Eigenstate thermalization in the two-dimensional transverse field Ising model". In: *Phys. Rev. E* 93 (3 Mar. 2016), p. 032104. DOI: 10.1103/PhysRevE.93.032104. URL: https://link.aps.org/doi/10.1103/PhysRevE.93.032104.

[142] Robert C. Myers, Razieh Pourhasan, and Michael Smolkin. "On Spacetime Entanglement". In: *JHEP* 06 (2013), p. 013. DOI: 10.1007/JHEP06(2013)013. arXiv: 1304.2030 [hep-th].

[143] Clemens Neuenhahn and Florian Marquardt. "Thermalization of interacting fermions and delocalization in Fock space". In: *Phys. Rev. E* 85 (6 June 2012), p. 060101. DOI: 10.1103/PhysRevE.85.060101. URL: https://link.aps.org/doi/10.1103/PhysRevE.85.060101.

[144] Michael A. Nielsen and Isaac L. Chuang. *Quantum Computation and Quantum Information*. 10th. USA: Cambridge University Press, 2011. ISBN: 1107002176.

[145] Yasunori Nomura. "Physical Theories, Eternal Inflation, and Quantum Universe". In: *JHEP* 11 (2011), p. 063. DOI: 10.1007/JHEP11(2011)063. arXiv: 1104.2324 [hep-th].

[146] Yasunori Nomura, Fabio Sanches, and Sean J. Weinberg. "Black Hole Interior in Quantum Gravity". In: *Phys. Rev. Lett.* 114 (2015), p. 201301. DOI: 10.1103/PhysRevLett.114.201301. arXiv: 1412.7539 [hep-th].

[147] Kento Osuga and Don N. Page. "Qubit Transport Model for Unitary Black Hole Evaporation without Firewalls". In: *Phys. Rev. D* 97.6 (2018), p. 066023. DOI: 10.1103/PhysRevD.97.066023. arXiv: 1607.04642 [hep-th].

[148] Don N. Page. "Average entropy of a subsystem". In: *Phys. Rev. Lett.* 71 (1993), pp. 1291–1294. DOI: 10.1103/PhysRevLett.71.1291. arXiv: gr-qc/9305007.

[149] Don N. Page. "Information in black hole radiation". In: *Phys. Rev. Lett.* 71 (1993), pp. 3743–3746. DOI: 10.1103/PhysRevLett.71.3743. arXiv: hep-th/9306083.

[150] Kyriakos Papadodimas and Suvrat Raju. "An Infalling Observer in AdS/CFT". In: *JHEP* 10 (2013), p. 212. DOI: 10.1007/JHEP10(2013)212. arXiv: 1211.6767 [hep-th].

[151] Geoffrey Penington. "Entanglement Wedge Reconstruction and the Information Paradox". In: *JHEP* 09 (2020), p. 002. DOI: 10.1007/JHEP09(2020)002. arXiv: 1905.08255 [hep-th].

[152] Geoffrey Penington et al. "Replica wormholes and the black hole interior". In: (Nov. 2019). arXiv: 1911.11977 [hep-th].

[153] Alfredo Pérez and Ricardo Troncoso. "Gravitational dual of averaged free CFT's over the Narain lattice". In: (June 2020). arXiv: 2006.08216 [hep-th].

[154] S. Perlmutter et al. "Measurements of Ω and Λ from 42 high redshift supernovae". In: *Astrophys. J.* 517 (1999), pp. 565–586. DOI: 10.1086/307221. arXiv: astro-ph/9812133.

[155] Denes Petz. "Sufficient subalgebras and the relative entropy of states of a von Neumann algebra". In: *Commun. Math. Phys.* 105.1 (1986), pp. 123–131. DOI: 10.1007/BF01212345.

[156] Joseph Polchinski. "The Black Hole Information Problem". In: *New Frontiers in Fields and Strings*. World Scientific, 2017. Chap. 6, pp. 353–397. DOI: 10.1142/9789813149441_0006.

[157] Xiao-Liang Qi and Zhao Yang. "Space-time random tensor networks and holographic duality". In: (Jan. 2018). arXiv: 1801.05289 [hep-th].

[158] Lisa Randall and Raman Sundrum. "A large mass hierarchy from a small extra dimension". In: *Phys. Rev. Lett.* 83 (1999), pp. 3370–3373. arXiv: hep-ph/9905221.

[159] R.D. Reiss and M. Thomas. *Statistical Analysis of Extreme Values: With Applications to Insurance, Finance, Hydrology and Other Fields*. Birkhaeuser Verlag Basel - Boston - Berlin, 2007.

[160] A. Riess et al. "Observational Evidence from Supernovae for an Accelerating Universe and a Cosmological Constant". In: *Astron. J.* 116 (1998), pp. 1009–1038. DOI: 10.1086/300499. arXiv: astro-ph/9805201.

[161] Marcos Rigol. "Breakdown of Thermalization in Finite One-Dimensional Systems". In: *Phys. Rev. Lett.* 103 (10 Sept. 2009), p. 100403. DOI: 10.1103/PhysRevLett.103.100403. URL: https://link.aps.org/doi/10.1103/PhysRevLett.103.100403.

[162] Marcos Rigol. "Quantum quenches and thermalization in one-dimensional fermionic systems". In: *Phys. Rev. A* 80 (5 Nov. 2009), p. 053607. DOI: 10.1103/PhysRevA.80.053607. URL: https://link.aps.org/doi/10.1103/PhysRevA.80.053607.

[163] Marcos Rigol, Vanja Dunjko, and Maxim Olshanii. "Thermalization and its mechanism for generic isolated quantum systems". In: *Nature* 452 (Apr. 2008), pp. 854–858. DOI: doi.org/10.1038/nature06838. URL: https://doi.org/10.1038/nature06838.

[164] Marcos Rigol and Mark Srednicki. "Alternatives to Eigenstate Thermalization". In: *Phys. Rev. Lett.* 108 (11 Mar. 2012), p. 110601. DOI: 10.1103/PhysRevLett.108.110601. URL: https://link.aps.org/doi/10.1103/PhysRevLett.108.110601.

[165] Daniel A. Roberts, Douglas Stanford, and Leonard Susskind. "Localized shocks". In: *JHEP* 03 (2015), p. 051. DOI: 10.1007/JHEP03(2015)051. arXiv: 1409.8180 [hep-th].

[166] Guillaume Roux. "Finite-size effects in global quantum quenches: Examples from free bosons in an harmonic trap and the one-dimensional Bose-Hubbard model". In: *Phys. Rev. A* 81 (5 May 2010), p. 053604. DOI: 10.1103/PhysRevA.81.053604. URL: https://link.aps.org/doi/10.1103/PhysRevA.81.053604.

[167] Moshe Rozali et al. "Information radiation in BCFT models of black holes". In: *JHEP* 05 (2020), p. 004. DOI: 10.1007/JHEP05(2020)004. arXiv: 1910.12836 [hep-th].

[168] Shinsei Ryu and Tadashi Takayanagi. "Aspects of Holographic Entanglement Entropy". In: *JHEP* 0608 (2006), p. 045. DOI: 10.1088/1126-6708/2006/08/045. arXiv: hep-th/0605073.

[169] Shinsei Ryu and Tadashi Takayanagi. "Holographic derivation of entanglement entropy from AdS/CFT". In: *Phys.Rev.Lett.* 96 (2006), p. 181602. DOI: 10.1103/PhysRevLett.96.181602. arXiv: hep-th/0603001.

[170] Phil Saad. "Late Time Correlation Functions, Baby Universes, and ETH in JT Gravity". In: (Oct. 2019). arXiv: 1910.10311 [hep-th].

[171] Phil Saad, Stephen H. Shenker, and Doublas Stanford. "A semiclassical ramp in SYK and in gravity". In: (2018). arXiv: 1806.06840 [hep-th].

[172] Phil Saad, Stephen H. Shenker, and Doublas Stanford. "JT gravity as a matrix integral". In: (2019). arXiv: 1903.11115 [hep-th].

[173] Lea F. Santos and Marcos Rigol. "Localization and the effects of symmetries in the thermalization properties of one-dimensional quantum systems". In: *Phys. Rev. E* 82 (3 Sept. 2010), p. 031130. DOI: 10.1103/PhysRevE.82.031130. URL: https://link.aps.org/doi/10.1103/PhysRevE.82.031130.

[174] Lea F. Santos and Marcos Rigol. "Onset of quantum chaos in one-dimensional bosonic and fermionic systems and its relation to thermalization". In: *Phys. Rev. E* 81 (3 Mar. 2010), p. 036206. DOI: 10.1103/PhysRevE.81.036206. URL: https://link.aps.org/doi/10.1103/PhysRevE.81.036206.

[175] Yasuhiro Sekino and Leonard Susskind. "Fast Scramblers". In: *JHEP* 10 (2008), p. 065. DOI: 10.1088/1126-6708/2008/10/065. arXiv: 0808.2096 [hep-th].

[176] S. Sorg et al. "Relaxation and thermalization in the one-dimensional Bose-Hubbard model: A case study for the interaction quantum quench from the atomic limit". In: *Phys. Rev. A* 90 (3 Sept. 2014), p. 033606. DOI: 10.1103/PhysRevA.90.033606. URL: https://link.aps.org/doi/10.1103/PhysRevA.90.033606.

[177] Mark Srednicki. "Chaos and quantum thermalization". In: *Phys. Rev. E* 50 (2 Aug. 1994), pp. 888–901. DOI: 10.1103/PhysRevE.50.888. URL: https://link.aps.org/doi/10.1103/PhysRevE.50.888.

[178] Douglas Stanford and Leonard Susskind. "Complexity and Shock Wave Geometries". In: *Phys. Rev. D* 90.12 (2014), p. 126007. DOI: 10.1103/PhysRevD.90.126007. arXiv: 1406.2678 [hep-th].

[179] Douglas Stanford and Edward Witten. "JT Gravity and the Ensembles of Random Matrix Theory". In: (July 2019). arXiv: 1907.03363 [hep-th].

[180] R. Steinigeweg, J. Herbrych, and P. Prelov šek. "Eigenstate thermalization within isolated spin-chain systems". In: *Phys. Rev. E* 87 (1 Jan. 2013), p. 012118. DOI: 10.1103/PhysRevE.87.012118. URL: https://link.aps.org/doi/10.1103/PhysRevE.87.012118.

[181] R. Steinigeweg et al. "Pushing the Limits of the Eigenstate Thermalization Hypothesis towards Mesoscopic Quantum Systems". In: *Phys. Rev. Lett.* 112 (13 Apr. 2014), p. 130403. DOI: 10.1103/PhysRevLett.112.130403. URL: https://link.aps.org/doi/10.1103/PhysRevLett.112.130403.

[182] James Sully, Mark Van Raamsdonk, and David Wakeham. "BCFT entanglement entropy at large central charge and the black hole interior". In: (Apr. 2020). arXiv: 2004.13088 [hep-th].

[183] Leonard Susskind. "Computational Complexity and Black Hole Horizons". In: *Fortsch. Phys.* 64 (2016). [Addendum: Fortsch.Phys. 64, 44–48 (2016)], pp. 24–43. DOI: 10.1002/prop.201500092. arXiv: 1403.5695 [hep-th].

[184] Leonard Susskind. "The Census taker's hat". In: (Oct. 2007). arXiv: 0710.1129 [hep-th].

[185] Leonard Susskind and Ying Zhao. "Complexity and Momentum". In: *JHEP* 21 (2020), p. 239. DOI: 10.1007/JHEP03(2021)239. arXiv: 2006.03019 [hep-th].

[186] Leonard Susskind and Ying Zhao. "Switchbacks and the Bridge to Nowhere". In: (Aug. 2014). arXiv: 1408.2823 [hep-th].

[187] Brian Swingle. "Entanglement Renormalization and Holography". In: *Phys. Rev. D* 86 (2012), p. 065007. DOI: 10.1103/PhysRevD.86.065007. arXiv: 0905.1317 [cond-mat.str-el].

[188] Tadashi Takayanagi. "Holographic Dual of BCFT". In: *Phys. Rev. Lett.* 107 (2011), p. 101602. DOI: 10.1103/PhysRevLett.107.101602. arXiv: 1105.5165 [hep-th].

[189] C. Teitelboim. "Gravitation and Hamiltonian Structure in Two Space-Time Dimensions". In: *Phys. Lett. B* 126 (1983), pp. 41–45. DOI: 10.1016/0370-2693(83)90012-6.

[190] Robert M. Wald. *General Relativity*. Chicago: The University of Chicago Press, 1984.

[191] Aron C. Wall. "Maximin Surfaces, and the Strong Subadditivity of the Covariant Holographic Entanglement Entropy". In: *Class. Quant. Grav.* 31.22 (2014), p. 225007. DOI: 10.1088/0264-9381/31/22/225007. arXiv: 1211.3494 [hep-th].

[192] Jinzhao Wang. "The refined quantum extremal surface prescription from the asymptotic equipartition property". In: *Quantum* 6 (2022), p. 655. DOI: 10.22331/q-2022-02-16-655. arXiv: 2105.05892 [hep-th].

[193] J.H.M. Wedderburn. *Lectures on Matrices*. American mathematical society colloquium publications. Dover Publications, 1964. URL: https://books.google.ca/books?id=9ZMZAQAAIAAJ.

[194] Edward Witten. "Matrix Models and Deformations of JT Gravity". In: (June 2020). arXiv: 2006.13414 [hep-th].

[195] H.D. Zeh. "On the interpretation of measurement in quantum theory". In: *Found. Phys.* 1 (1970), pp. 69–76. DOI: 10.1007/BF00708656.

[196] W.H. Zurek. "Pointer Basis of Quantum Apparatus: Into What Mixture Does the Wave Packet Collapse?" In: *Phys. Rev. D* 24 (1981), pp. 1516–1525. DOI: 10.1103/PhysRevD.24.1516.